NTNU – Trondheim
Norwegian University of
Science and Technology

Bearing capacity failure envelopes of foundations with skirts subjected to combined loading

Qiuhong Meng

Geotechnics and Geohazards
Submission date: June 2013
Supervisor: Gudmund Reidar Eiksund, BAT

Norwegian University of Science and Technology
Department of Civil and Transport Engineering

NORWEGIAN UNIVERSITY OF SCIENCE AND TECHNOLOGY
DEPARTMENT OF CIVIL AND TRANSPORT ENGINEERING

Report Title:	Date: 10.06.2013			
Bearing capacity failure envelopes of foundations with skirts subjected to combined loading	Number of pages (incl. appendices): 85			
	Master Thesis	X	Project Work	
Name: Qiuhong Meng				
Professor in charge/supervisor: Gudmund Eiksund				
Other external professional contacts/supervisors: Corneliu Athanasiu				

Abstract:

Mudmat foundations are widely used as temporary seabed supports of manifolds, PLEM and PLET in offshore activities. To determine ultimate states of offshore mudmat foundations with skirts subjected to combined loadings, an increasing focus is put on use of the failure envelope approach.

This master thesis used the PLAXIS 3D models of a mudmat foundation, developed in the project thesis, to determine the bearing capacities envelopes(different combinations of vertical load, horizontal load and torsion moment that cause failure of the supporting soil). The affections of torsion moment on the failure envelope were specially focused on and studied.

Suitability of the simplified method accounting for torsion moments is also evaluated by comparing the results from PLAXIS 3D.

Keywords:

1. Bearing capacity
2. Failure envelope
3. PLAXIS 3D
4. Torsion moment

_____Qiuhong Meng_____

NTNU
Norwegian University of
Science and Technology

HOVEDOPPGAVE

(Master thesis)

2013

Stud. Techn. Qiuhong Meng

Bearing capacity failure envelopes of foundations with skirts subjected to combined loading

Background:

There is an increasing focus on use of the failure envelope approach to determine ultimate states of offshore mudmat foundations with skirts subjected to combined loadings. The reason for that is that this approach considers explicit the independent load components and allows graphical interpretation of the safety factor associated to different load paths.

Thesis objects and contents:

The thesis will use the PLAXIS 3D model of a mudmat foundation to determine the bearing capacity envelopes(combination of vertical load, horizontal load and moments that cause failure of the supporting soil). Special focus will be directed towards the effect of torsion moment on the failure envelope.

The main goals of master thesis are summarized as follows:

1) Parametric studies are needed to investigate the reliability of results when torsion moment is included in loading conditions and to determine the optimum element mesh (number of elements) to achieve convergence and realistic results.
2) Use of optimized model to study the shape of failure envelope.
3) Express enveloped analytically in a non-dimensional form.
4) Use the results to reveal the failure mechanism, and stress distribution between the different parts of the mud mat foundation: skirts, plates/bottom of soil compartment, skirt tip.
5) Evaluate the suitability of the simplified methods accounting for torsion moments by comparing the results from PLAXIS with the results from simplified methods.

Report

The work should be organized as a research and an emphasis is put on clear representation.

Associated partner

The thesis is designed in collaboration with Multiconsult AS. Workplace: NTNU

Date: June.10th, 2013

NTNU
Bygg anlegg og transport, faggruppe for geoteknikk

June.10th, 2013

Gudmund Eiksund
Corneliu Athanasiu

Preface

This report is a master thesis at the Institute of Geotechnical Engineering, NTNU, 2013.

The main aim of the thesis was to study the bearing capacity envelopes, with special focus on the effect of torsion moment on the failure envelope. It has been performed a numerical study of element program PLAXIS 3D. The results of the numerical studies are used to verify the hand calculation that takes into account the torsions.

The work of this thesis is performed from Jan.9th, 2013 to June.10th, 2013. Workload of this thesis had the following time distributions:

Collection of literature and literary study	20%
Studying the program PLAXIS 3D	20%
Numerical calculations and processing of data	40%
Writing and editing report	20%

At the beginning of this thesis, I spent about 1 month to collect and study literatures relevant to mudmat foundation and failure envelopes. However, the parametric studies to investigate the reliable results took more time than I planned. Plenty of problems come out during the finite element analyses with PLAXIS 3D, like: nonconvergence of the final results, inappropriate selection of drainage type, not enough load steps, etc. It was unfortunately to make some changes in the time plan, and more time was spent on PLAXIS 3D models. Fortunately, this PLAXIS 3D program equipped me with adequate experience and would be beneficial to me in later life of work.

I would like to thank my supervisors, Corneliu Athanasiu (Multiconsult AS) and Gudmund Eiksund (NTNU) for their contributions to my thesis. Due to limited literatures on this issue, I got lots of vital guidances from Corneliu and frequent assistances from Gudmund. Their contributions have been indispensable.

Finally, I would like to thank all the lecturers at NTNU, especially those at the Department of Geotechnical Engineering, for a fantastic experience in Norway. I am sure that this two-year study in NTNU would be the forever fortune in my life.

Summary

The bearing capacity of the foundation is reduced in combination with horizontal loads and moments, and can be further reduced when torsion moment is applied. Therefore, torsion moment must be taken into account when calculating the loading capacity. This is particularly relevant for offshore foundations (underwater structures), since torsion is often of considerable size.

The aim of this thesis is to make a numerical study of a rectangular mudmat foundation subjected to vertical loading, horizontal loading and torsion moment. The numerical calculations were mainly calculated by the finite element program PLAXIS 3D. Meanwhile, hand calculations of bearing capacities with Janbu and Davis & Booker methods are also carried out for comparison.

The numerical studies were limited to undrained loading condition, where the undrained shear strength increases linearly with depth for a rectangular mudmat foundation;

a) with outer skirts only
b) with both outer and inner skirts

Vertical and horizontal bearing capacities of mudmat foundation from finite element program PLAXIS 3D correspond well with the hand calculation results by Janbu method. However, the vertical bearing capacities from PLAXIS 3D are slightly higher than Janbu method, with a difference of 460kN(Model 1) and 80 kN(Model 2), corresponding to a difference of 6% and 1%, respectively. It may have several explanations:

- The results of finite element programs is dependent on network element and element type. Theoretically, the analyses of model with more fine meshes and smaller average element size would generate more accurate results.
- PLAXIS 3D builds a real 3-dimensional model, taking into consideration the 3D affections. However, Janbu method is based on the plane strain.

However, torsional bearing capacity from PLAXIS 3D is almost twice the value determined from hand calculations, which may because of the conservative calculation method or some possible parametric errors in PLAXIS 3D.

By intergrating the FEM analyses package PLAXIS 3D with the Swipe test procedure of loading, the failure envelopes of mudmat foundation and approximating expressions are investigated. Through numerical computations and comparative analyses based on FEM, the two-dimensional failure envelopes of mudmat foundation are established by using proposed method to evaluate the stability of foundation under combined loadings. These results could be utilized to provide vital reference for the design and construction of mudmat foundation.

Contents

List of figures

List of tables

APPENDIX

ANNEX OVERRIEW

Notations

Symbol	Unit	Term
A'/A_{eff}	m2	Effective area of mudmat foundation
B'/B_{eff}	m	Effective width
L'/L_{eff}	m	Effective length
C_{ref}	kN/m2	Cohesion
C_{in}	kN/m2/m	Increase of cohesion
D	m	Skirt height
d	m	Skirt thickness
EA	kN/m	Axial stiffness
EI	kN/m2	Bending stiffness
E_{ref}	kN/m2	Young's modulus
E_{in}	kN/m2/m	Increase of stiffness
F_{skirt}	kN	Force on the skirt
H	kN	Horizontal load
V	kN	Vertical load
T	kNm	Torsion moment
H_{ult}	kN	Ultimate horizontal load
V_{ult}	kN	Ultimate vertical load
T_{ult}	kNm	Ultimate torsion moment
K_a	-	Earth pressure coefficient acting on the active side of the skirt
K_p	-	Earth pressure coefficient acting on the passive side of the skirt
N_c	-	Bearing capacity factor for clay
P_a	kN	Horizontal reaction force due to active earth pressure
p_P	kN	Horizontal reaction force due to passive earth pressure
R_{inter}	-	Interface strength reduction
r	-	Roughness
ω	-	Rotation of principal plane when subjected to horizontal load
S_u	kN/m2	Static undrained shear strength
$S_{u,in}$	kN/m2/m	Increase of undrained shear strength per meter
γ	kN/m3	Unit weight of the soil
τ	kN/m2	Shear stress
τ_h	kN/m2	Avarage mobilized shear stress
τ_d	kN/m2	Avarage mobilized shear strength
σ	kN/m2	Normal stress
ν	-	Poisson's ratio
ϕ	°	Angle of internal friction
ψ	°	Dilatancy angle
p	kN	Surcharge pressure
M_{stage}	-	Factor of calculation stage
α	°	Angle between failure plane and horizontal plane
e_B	m	Eccentricity along the width
e_L	m	Eccentricity along the length
Z_r	m	Reference depth for mean shear strength
$S_{u,D/2}$	kN	Shear strength at a depth of D/2

Chapter 1 INTRODUCTION

1.1 Background of thesis

Accelerated global demand of resources has pushed the oil and gas exploration and field development continuously move into deeper water. Today, a significant part of the offshore field development takes place in the water depths of more than 500 meters, like in the North Sea, offshore Australia, and the Bay of Bengal. (Andersen, 2008)

Jacket platforms used offshore for oil extraction are generally temporarily supported by mudmat foundations during installation. Besides, Subsea mudmats are often used to provide additional support for equipment on the sea floor, like manifolds, PLEM(pipeline end manifold) and PLET(pipeline end termination) when the seabed is too soft to adequately support the equipments. See Fig.1.1.

Figure 1.1: PLET supported by mudmat foundation on seabed

The PLET is assumed to be temporarily supported by a 21m*9m rectangular mudmat foundation on seabed in this thesis. Due to an eccentric gravity load and environmental actions, the mudmats are subjected to combined vertical, horizontal, moment, and torsion(VHMT) loadings.

The bearing capacity of the foundation is reduced in combination with horizontal loads and moments, and can be further reduced when torsion moment is applied. Therefore, torsion moment must be taken into account when calculating the loading capacity. This is particularly relevant for offshore foundations (underwater structures), since torsion is often of considerable size. A typical geometry of mudmat foundation can be: length L=21m, width B=9m, and depth D=1m. See Fig.1.2.

Figure 1.2: Skirted shallow foundation for subsea facility (Detail Design Inc.)

1.2 Objective of the thesis

Classical Soil Mechanics has solutions for bearing capacity of foundations subjected to vertical loads. Combined loadings, including horizontal load and overturning moments can also be solved using classical Soil Mechanics. However, if the torsion moment is also present together with vertical and horizontal forces and with overturning moments, no theoretical approach exists and numerical (finite element) analyses must be carried to evaluate the foundation capacity.

This thesis focuses on creating a numerical model of a mudmat foundation subjected to combined loadings: vertical loading, horizontal loading, and torsion moment(HVT). Finite element analyses(PLAXIS 3D) and hand calculations are undertaken to study the effect of torsion moment on bearing capacity of mudmat. Results and analyses are finally compared, and give failure envelopes for different combinations of loadings. These failure envelopes can be used to provide vital reference for the design and construction of mudmat foundation.

Different PLAXIS 3D models of mudmat foundations are created and studied. Finally, discussions and comparisons based on the hand calculations and PLAXIS 3D results are given.

1.3 Scope and Limitations

This thesis focuses on the effects of the torsion on the bearing capacity. Therefore, it is appropriate to keep most of the other parameters constant. The task is limited to examining two cases.

i.) foundation without inner skirts;
ii.) foundation with a 1×2 inner skirts.

To calculate the ultimate bearing capacity of mudmat foundation, assumptions of the analyses are made as follows:

- Soft clay is assumed on the seabed, which behaves as a perfectly plastic material.
- Shear strength increases linearly with depth.
- Analyses are restricted to undrained condition. This is because mudmat foundation is put on soft clay as a temporary supporter for jacket platforms. When the load is applied to the foundation relatively quickly, there is little or no dissipation of excess pore pressure.
- A general shear failure occurs, i.e., there is a fully formed failure surface beneath the foundation.
- The limit theorems apply.
- Numerical analyses are performed by general element programs PLAXIS 2D and PLAXIS 3D, respectively.

1.4 Structure of thesis

Chapter 2 is an introduction to the theoretical basis for this thesis. It starts with the very basic theory by explaining definitions of what a bearing capacity is, to explain the impact of torsion on bearing capacity. The theory about torsion is referred to literatures from supervisor (Corneliu Athanasiu).

Chapter 3 deals with the various programs, and requirements for the various parameters, which are used for the numerical analyses.

The main results and comparisons are presented in Chapter 4.

Chapter 5 is a discussion section. Here are some comments on the results made in Chapter 4 and a little discussion about the assumptions of torsion in Chapter 2. In addition, a brief comparison of the results from PLAXIS and the proposed method of calculating the effect of torque.

Chapter 2 THEORETICAL BACKGROUND

Bearing capacity is the capacity of soil to support the loads applied to the ground. The bearing capacity of soil is the maximum average contact pressure between the foundation and the soil which should not produce shear failure in the soil. Ultimate bearing capacity is the theoretical maximum pressure which can be supported without failure; allowable bearing capacity is the ultimate bearing capacity divided by a factor of safety.

There are many different methods to calculate the bearing capacity of a foundation. The best known methods are possibly Terzagi, Meyerhof, Hansen and Verci. In Norway, Janbu method is the most prevalent method. In this thesis, Hansen and Janbu methods are used to compare with the results from PLAXIS 3D.

2.1 Bearing capacity of foundation

2.1.1 Ground failure modes

Shear failure is defined as when the soil divides into separate blocks or zones, which move along slip surfaces. Three principal modes of shear failure may be defined:

a) General Shear Failure

   A continuous slip surface occurs up to ground level. Soil above failure surface in state of plastic equilibrium, with heaving on either side. Failure is sudden and catastrophic and accompanied by tilting of the footing, see curve a below.

b) Local Shear Failure

   Significant compression under footing causes only a partial development of plastic equilibrium. Failure surface is not continuous. Some minor heaving at ground level but no catastrophic failure, see curve b below.

c) Punching Shear Failure

   Slip surfaces almost vertical, large vertical displacements. No heaving, tilting or catastrophic failure. Compression increases the density of the soil, see curve c.

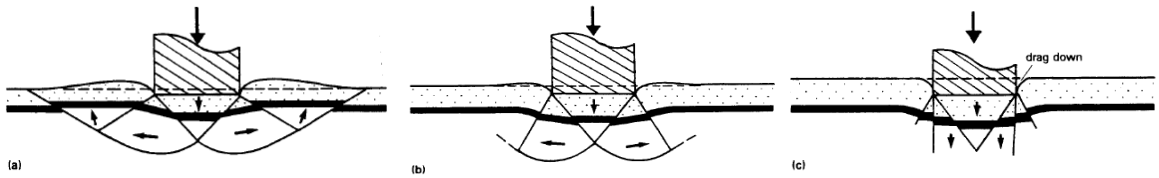

Figure 2.1: three different types of shear failure modes

The mode of failure which is likely to occur beneath any foundation depends on:

- the compressibility of the soil,
- the foundation depth to width ratio D/B

Settlement-pressure curves of these three different shear failure modes can be demonstrated as follows.

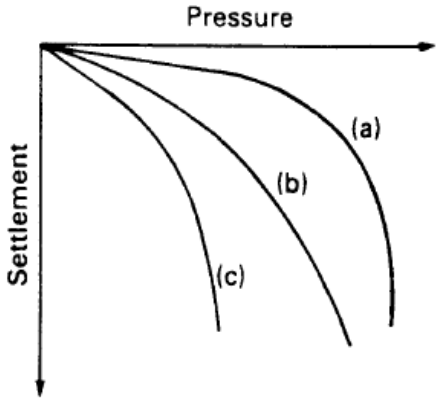

Figure 2.2: settlement-pressure curves for different modes of shear failure

2.1.2 Definitions of bearing capacity

Ultimate bearing capacity, q_{ult} is the intensity of bearing pressure at which the supporting ground is expected to fail in shear, i.e. a building will collapse. In Eurocode 7 the equivalent value is defined as the *ultimate limit state design vertical capacitance*, Q_d and is expressed as a load (force) and not as a pressure or stress.

Safe bearing capacity, q_s is maximum design load which takes into account the extent of the site investigation and the consequences of failure. The safe bearing capacity q_s can be expressed by suggested minimum factors of safety F in equation: $q_s = q_{ult}/F$.

Allowable bearing capacity, q_a is the bearing capacity that will cause acceptable settlement of the structure.

When a uniformly distributed load q is applied to a foundation, the foundation will get a settlement δ. Settlement will increase with the increase of load q. When the load q reaches the ultimate bearing capacity $q = q_{ult}$ (See Fig. 2.3), foundation will get a very large settlement increase with further increase of the load q. This is considered as a shear failure.

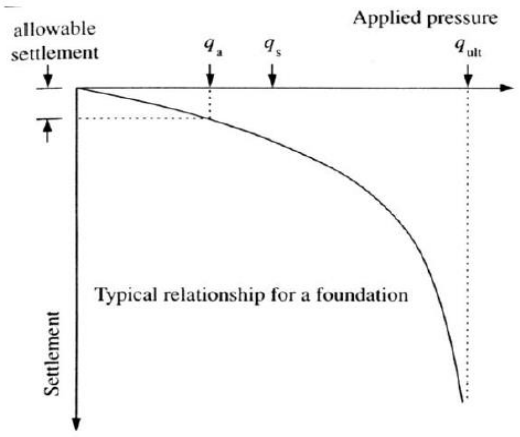

Figure 2.3: load-deformation curve

2.1.3 Effect of foundation depth D

Normally, a foundation stands a certain depth under the ground. When a foundation is subjected to vertical loadings, the soil under the foundation will be pushed away to both sides and soil at the sides will be raised. When the masses are located on the two sides of the foundation, with a depth D, it seems like a surcharge pressure which counteracts the shear stresses. The size of the surcharge pressure can be defined as p by equation (2.1)below.

$$p = \rho g D = \gamma D \qquad (2.1)$$

Where, p = surcharge pressure

$\gamma = \rho g$ = soil density above foundation level

D = foundation depth

2.1.4 Stress field under foundations

Ultimate bearing capacity is defined as the least pressure (loading) to cause shear failure in the soil beneath the foundation. As with retaining walls, failure is assumed to take place along a distinct failure surface.

- Pure vertical loading

A normal stress zone for bearing capacity subjected to pure vertical load in S_u-analysis can be seen in Fig.2.4.

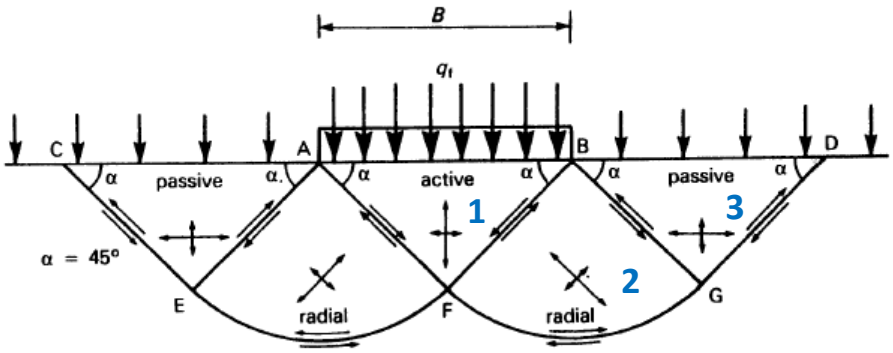

Figure 2.4: normal stress zone for bearing capacity subjected to pure vertical load in Su-analysis

The stress zone is a combination of active rankine zone, prandtl zone and passive rankine zone. By introduction of horizontal force, there will be shear stresses on the foundation interface. Therefore, the foundation plane will no longer be a principal stress plane and the principal stresses in the zone under the foundation are rotated an angle ω (Janbu, 2010).

When subjected to pure vertical load, failure path will be symmetrical as shown in Fig. 5. Also, shear stresses t_h equal zero since no horizontal forces exist. Due to the impact of vertical load on the foundation, soil wedge squeezes in zone 1, pushing the soil in Zone 2 to Zone 3. This means that the largest principal stress must be vertical, and zone 1 is an active zone (Emdal, A, Grande L, 2004).

Failure plane in soil wedge zone 1 has a angle of α with the horizontal plane in Fig.5. The degree of the angle α depends on the type of analysis, i.e. S_u-analysis or aφ-analysis. In this thesis we will only focus on S_u-analysis, thus α is always equal to 45 degrees for pure vertical load.

When Zone 2 is pressed by zone 1, it will also push zone 3 to the other side. Thus, zone 3 is considered as a passive zone where the main stresses are horizontal and failure plane in this zone will be equal to α. For S_u analysis of pure vertical load is α = 45 degrees.

- Inclined and eccentric loading

When subjected to centric inclined load, Zone 2 is a transition zone where the largest principal stresses rotate from vertical position in zone 1 to the horizontal position in zone 3. There are various shapes of the curved line between the two zones, depending on whether it is Su-analysis or aφ-analysis. In S_u-analyses the curved lines in Zone 2 are circular, while in aφ-analysis are logarithmic spiral.

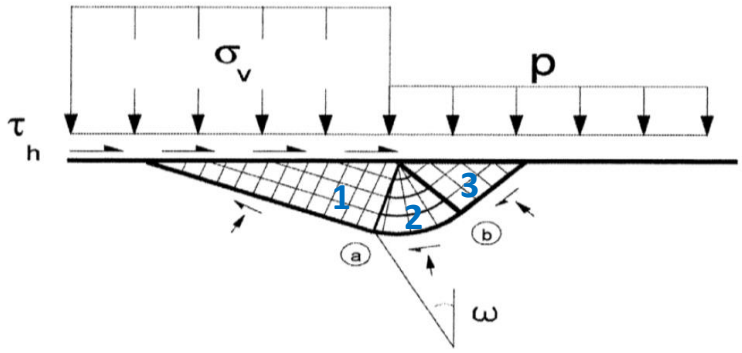

Figure 2.5: Zone combination, subjected to inclined and eccentric load in Su-analysis

When subjected to inclined and eccentric loadings, horizontal load gives a shear stress on the foundations, which makes horizontal plane no longer a principal stress plane. The largest main stress σ_1 will thus get a rotation of angle ω relative to the vertical axis, as shown in Fig.2.5.

Most methods developed for calculating capacity differs between the so-called Su-analyses and aφ-analyses. Su-analyses assume a short-term loading and undrained behavior, while aφ-analyses require a long-term loading and drained behavior. In this thesis, we only focus on S_u-analyses as mentioned before.

2.2 Effective foundation area

All forces acting on the foundation, including forces transferred from the upper structures, are transferred to the foundation base and combined into resultant forces H and V in the horizontal and vertical direction, respectively, at the foundation –soil interface.

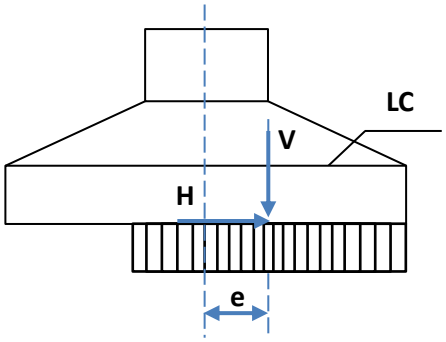

Figure 2.6: horizontal and vertical Loading under idealized conditions

The load center, denoted as LC, is the point where the resultant of H and V intersects the foundation-soil interface, and implies an eccentricity e of the vertical force V relative to the center line of the foundation. Reference is made to Fig.2.6, and the eccentricity is calculated as: e = M/V.

An effective area A_{eff} is needed for the bearing capacity analysis. The effective foundation area is constructed such that its geometrical center coincides with the load center, and such that it follows as closely as possible the nearest contour of the true area of the foundation base. (DNV A. G., 2010)

For a quadratic area of width B, the effective area A_{eff} can be defined as equation 2.2:

$$A_{eff} = B_{eff} * L_{eff} \qquad (2.2)$$

in which the effective dimensions B_{eff} and L_{eff} depend on which of the two idealized loading scenarios leads to the most critical bearing capacity for the actual foundation.(see Fig. 8)

$$e_L = M_Y/V$$

$$e_B = M_X/V$$

$$B_{eff} = B - 2e_B \qquad (2.3)$$

$$L_{eff} = L - 2e_L$$

Therefore,

$$A_{eff} = (B - 2M_X/V)(L - 2M_Y/V) \qquad (2.4)$$

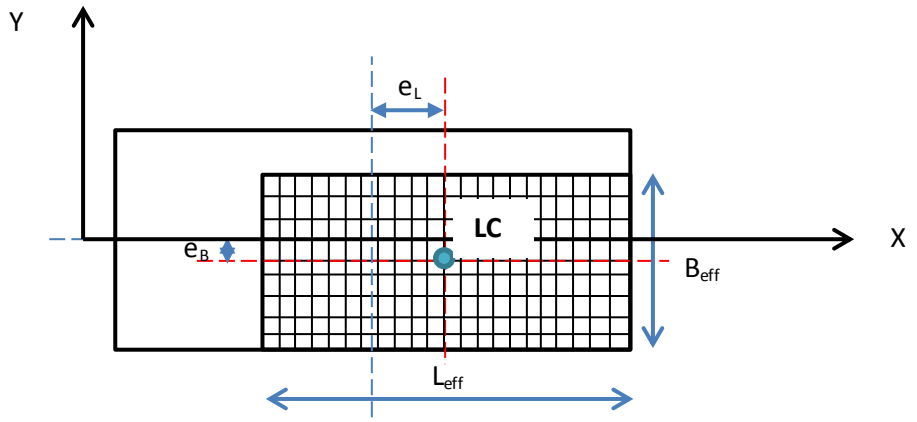

Figure 2.7: effective foundation area

Reference is made to Fig.2.7. Effective area representation that leads to the poorest or most critical result for the bearing capacity of the foundation is the effective area representation to be chosen. (DNV A. G., 2010)

2.3 Janbu method

Janbu method is currently the most widely used method in Norway. As with the other methods, Janbu method also distinguishes between S_u-analyses and aφ-analyses. The differences between Janbu method and other methods, such as Hansen method, could be that, Hansen used a correction factor, while Janbu introduces a concept called roughness. (Janbu, 2010)

For foundations that are subjected to short-term load, the bearing capacity of the soil could be determined by equations 2.5:

$$\sigma_v = N_c \tau_d + p \qquad (2.5)$$

where,

N_c = bearing capacity factor

τ_d = mobilized mean shear strength of the soil in the failure zone under the foundation

$p = \gamma D$ = surcharge pressure

2.3.1 Roughness

In Janbu method, roughness r will take the horizontal forces into consideration. Roughness r can be determined by the ratio of average mobilized shear stress τ_h to average mobilized shear strength τ_d. See equation 2.6 below.

$$r = \frac{\tau_h}{\tau_d} \qquad (2.6)$$

τ_h = mobilized shear stress = H/(BL)

H = horizontal force

Shear stress τ_h means the foundation is no longer subjected to vertical load only, but also to horizontal load. In the case of horizontal load, failure plane gets a rotation of ω, which can be expressed by the formula of r, see equation 2.7.

$$tan\omega = f_\omega = \frac{1}{r}(1 - \sqrt{1 - r^2})$$

$$\omega = 0{,}5 arcsin r \qquad (2.7)$$

2.3.2 Bearing capacity factor Nc

Bearing capacity factor N_c is a function of foundation width/length(B/L) and roughness r, and can be determined by equation 2.8.

$$N_c = 1 + \pi + \sqrt{1 - r^2} - arcsinr$$

$$N_c = 1 + \pi - 2\omega + cos2\omega \qquad (2.8)$$

r	ω	Nc
0	0,000	5,142
0,1	0,050	5,036
0,2	0,101	4,920
0,3	0,152	4,791
0,45	0,233	4,568
0,5	0,262	4,484
0,6	0,322	4,298
0,7	0,388	4,080
0,8	0,464	3,814
0,9	0,560	3,458
0,95	0,627	3,201
0,96	0,644	3,135
0,97	0,663	3,059
0,98	0,685	2,970
0,99	0,715	2,853
1	0,785	2,571

Table 2.1: Bearing capacity factor Nc

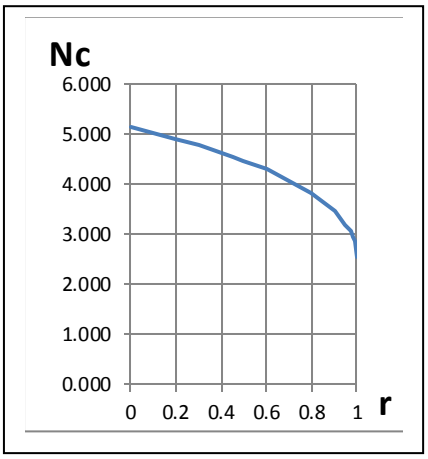

Figure 2.8: Bearing capacity factor Nc - roughness r curve

2.3.3 Mean shear strength

To calculate the undrained bearing capacity of soft clay with increasing shear strength with depth, a mean S_u value taken from a reference depth Zr is used (Emdal, 2011). Theoretical solutions of this problem indicate that such a reference depth Z_r is about half the maximum depth of an active rankine zone (zone 1). One approach to this depth is given in equation XX.

$$Z_r = \frac{B_o}{2(2-r)} \sin\left(\frac{\pi}{4} - \omega\right) + D \qquad (2.9)$$

Where, Zr is the reference depth when Su linearly increases with depth.

2.3.4 Ultimate vertical capacity by Janbu method

Therefore, the average shear strength is: $\overline{S_u} = S_{u,z=0} + \rho Z_r$ (2.10)

And the ultimate vertical capacity derived by Janbu method is : $q_{v,ult} = N_c \overline{S_u} + p$ (2.11)

2.4 Davis & Booker method

2.4.1 Davis & Booker formula for vertical bearing capacity

Davis & Booker method gives an exact solution of bearing capacity for a strip foundation where shear strength S_u increases with depth. The value of factor F is given in Fig.10 with rough and smooth cases. For this thesis, only rough case is considered, because it is believed a fragile foundation.

The bearing capacity determined by Davis & Booker method can be expressed by equation (2.10) shown below.

$$\frac{Q}{B} = F\left[(2+\pi)S_{u0} + \frac{\rho B}{4}\right] \qquad (2.12)$$

Where, Q = vertical load

B = foundation width

S_{u0} = shear stress at foundation level

ρ = shear stress increase in depth

The correction factor F is given as a function of dimensionless heterogeneity factor $\kappa = kB/S_{uo}$ as presented in Fig. 11. Values of F as a function of κ are shown in Fig.2.9. (Davis, 1973)

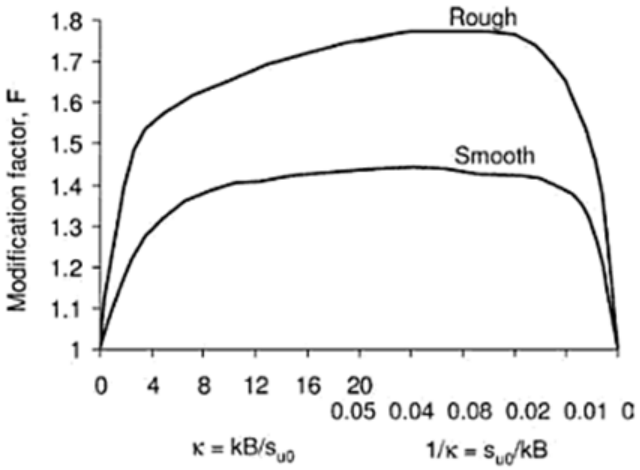

Figure 2.9: Bearing capacity modification factor for linearly increasing Su with depth (Davis, 1973)

For a mudmat foundation with a depth of D, shear stress at foundation level can be determined by $S_{u0} = S_{u,z=0} + \rho D$ as shown in Fig.2.10.

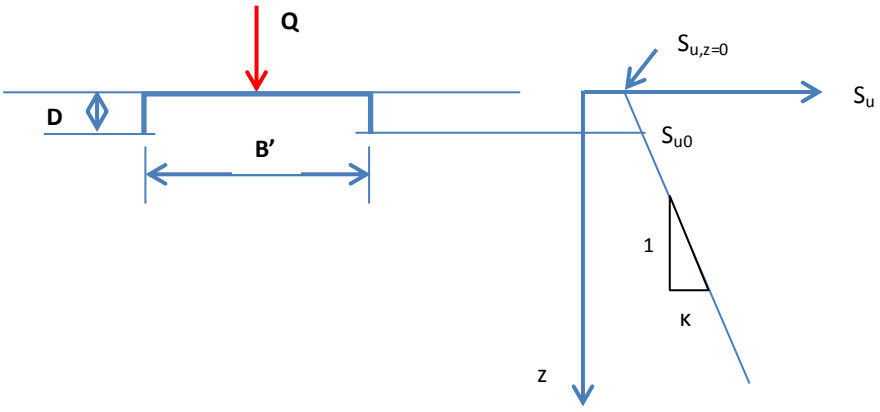

Figure 2.10: Shear strength S_{u0} of mudmat foundation with a depth of D

2.4.2 Ultimate vertical capacity by Davis & Booker method

In traditional calculations of the load capacity, it is assumed that surcharge pressures from any side of the filling with a depth D provides a restoring force p. However, in Janbu method, the masses on the foundation level are only considered as a load and cutting contributions provided by the soil are not taken into account.

When the foundation is pressed down by a vertical load, one oppositely directed shear force due to friction between foundation and ground will occur. The shear force is exerted around the circumference of the foundation base. Along the complete shear failure plane, earth is compressed up. Then it also has oppositely directed shear force due to friction between soil and soil. The shear force exerted in a zone can be approximately shown in Fig.12. A mean S_u is used for the analysis of side embankment, ie. S_u at a depth of D/2. (Athanasiu, 2006)

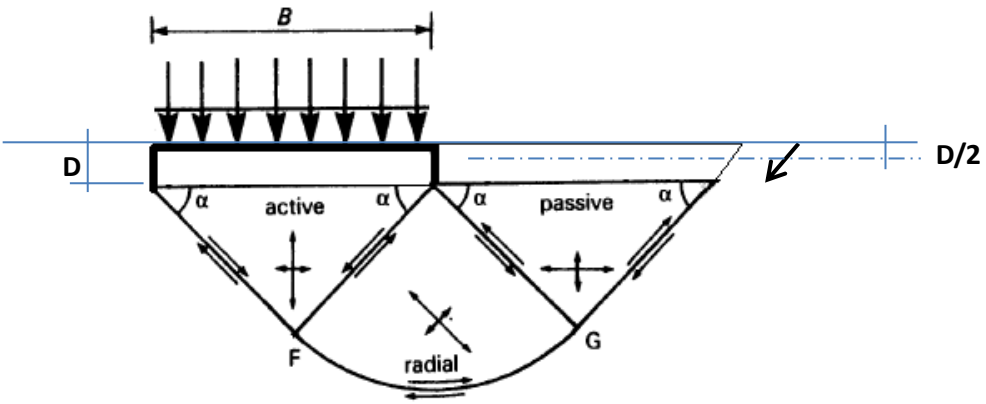

Figure 2.11: shear force that counteract the deflection of foundation

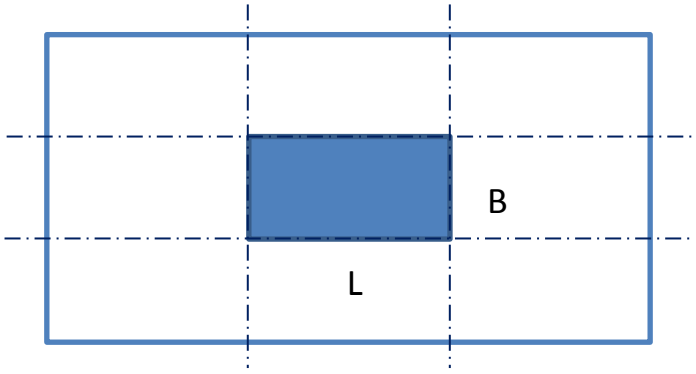

Figure 2.12: dimension of shear force that counteract the deflection of foundation

The Shear forces dimension that counteracts the deflection of foundation has a perimeter equal to C = 2(3B+3L) = 6(B+L).

For a foundation subjected to purely vertical load, the shear forces in the upper layer provide an additional capacity to the loading capacity.

Additional capacity due to shear forces can be expressed by equation (2.13).

$$q_{add} = \left[\frac{2(B+L)}{A} + \frac{2(3B+3L)}{A}\right] DS_{u,z=\frac{D}{2}} = \frac{8(B+L)}{A} DS_{u,z=\frac{D}{2}} \qquad (2.13)$$

Where,

B = foundation width

L = foundation length

A = BL = foundation area

$S_{u,z=D/2}$ = average shear strength of the masses at the foundation level

Together, for the pure vertical load case, we have the formula for ultimate vertical bearing capacity as in equation (2.14).

$$q_{v,ult} = F_{rough}\left[(2+\pi)S_{u,z=D} + \frac{\rho B}{4}\right]\left(1 + \frac{0.2B}{l}\right) + p + \frac{8(B+L)}{A} DS_{u,z=\frac{D}{2}} \qquad (2.14)$$

Equation 2.12 is not able to calculate the bearing capacity with horizontal loads. By replacing the expression of N_c in Janbu method, an equation that takes into account the horizontal forces is derived in equation (2.15).

$$q_{v,ult} = F_{rough}\left[(1+\pi+cos2\omega-2\omega)S_{u,z=D}+\frac{\rho B}{4}\right]\left(1+\frac{0.2B}{l}\right)+p+\frac{8(B+L)}{A}DS_{u,z=\frac{D}{2}} \qquad (2.15)$$

2.5 Combined loading forces with torsion moments

Sometimes a torsion moment is applied with vertical and horizontal forces as combined loading forces on the foundation. The torsion moment can be caused by horizontal load with an eccentricity, or the base plate is subjected to a torsion transferred from the overhead structure.

There is currently no good way to calculate the capacity of a foundation subjected to a torsion moment. A foundation subjected to torsion will rotate around the axis of the torsion. The torsion moment will make different displacements of the foundation depending on how far from torsion point you are. This means that the foundation will have various mobilized sizes of shear stresses caused by the torsion depending on the distance from the point of torsion. This can be illustrated in Fig.2.13, where maximum and average shearing stresses are given by equation (2.16).

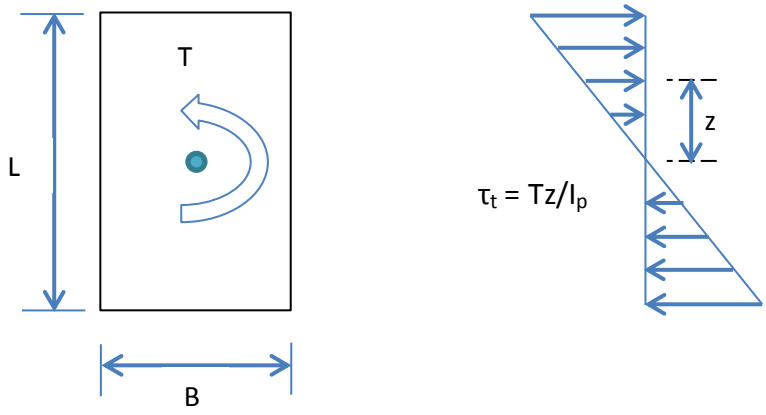

Figure 2.13: shear stress generated from torsion moment

$$\tau_t = \frac{T}{I_p} * z$$
$$\tau_{t,max} = \frac{T}{I_p} * \frac{L}{2} \qquad (2.16)$$
$$\tau_{t,ave} = \frac{T}{I_p} * \frac{L}{4}$$

Where,

I_p = polar moment of inertia
T = torsion moment
z = distance from the center of the base plate to the point where shear stress works
τ_t = shear stress generated from torsion moment at a distance of z
$\tau_{t,max}$ = maximum shear stress generated from torsion moment
$\tau_{t,ave}$ = average shear stress generated from torsion moment

Shear stress distribution for a foundation subjected to torsion can be seen in Fig.2.14, it is natural to assume that it will develop into two oppositely directed shear failure as shown in Fig.15.

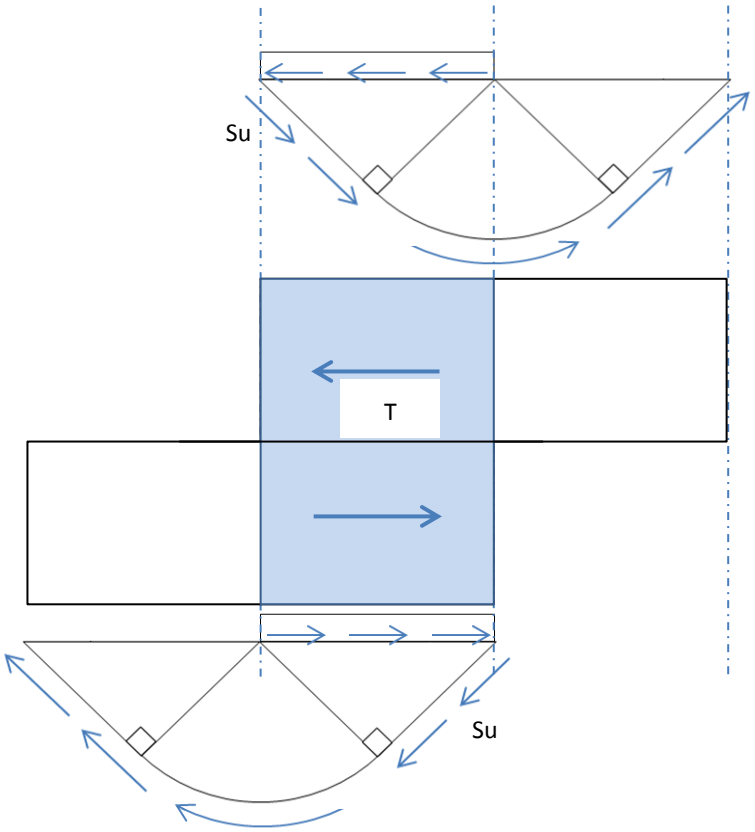

Figure 2.14: top-view of foundation subjected to torsion, with shear rupture profiles

2.5.1 Superposition method

Torsion moment often occurs due to horizontal load with an eccentricity. Therefore, it is natural to consider a load combination where the horizontal load and torsion acting simultaneously.

One possible simplified method to calculate how much shear is mobilized by torsion moment and horizontal load is to superpose them. That is, the shear stresses caused by the horizontal loads and torsion moments are calculated separately for side summing the results (Athanasiu, 2006). This can be illustrated in Fig.2.15.

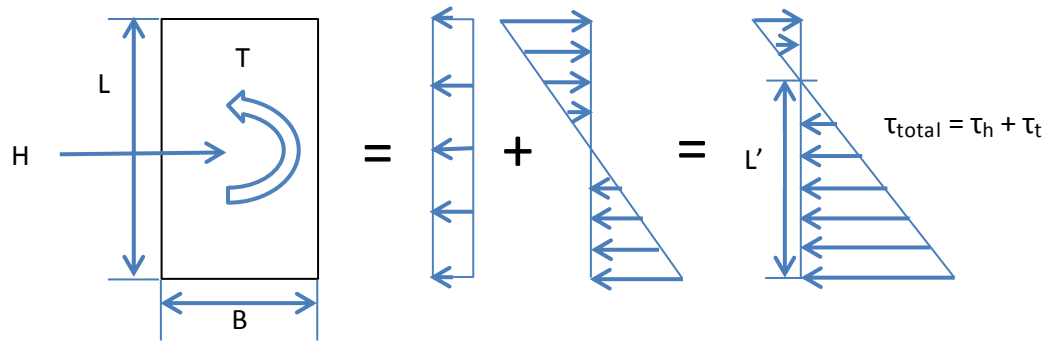

Figure 2.15: Shear stress due to torsion moment and horizontal force

Where, $\tau_h = \frac{H}{A'}$ $\tau_t = \frac{Tr}{I}$ (2.17)

Here, I is the is the torsion constant for the section, r is the distance between the rotational axis and the furthest point in the section (at the outer surface).

To calculate the shear stresses, we need the effective areas which has been determined in chapter 2.2:

$$A' = B'L'$$

Where, $L' = L - 2\Delta L,\ B' = B$ (2.18)

$$\Delta L = \frac{T}{H}$$

In Janbu method, the affections of horizontal load is taken into account by introducing roughness r, which could be represented by the ratio of mobilized shear stress τ_h to shear strength τ_d. See equation (2.19)

$$r = \frac{\tau_h + \tau_t}{\tau_d} \quad (2.19)$$

Shear stress caused by torsion moment varies in proportion to the distance to the pivot point. It is therefore expedient to make a simplification that, the resultant shear stresses generated by torsion moment and horizontal force $\tau_h + \tau_t$ is assumed to have an equal distribution over the effective length L' as shown in Fig.2.16.

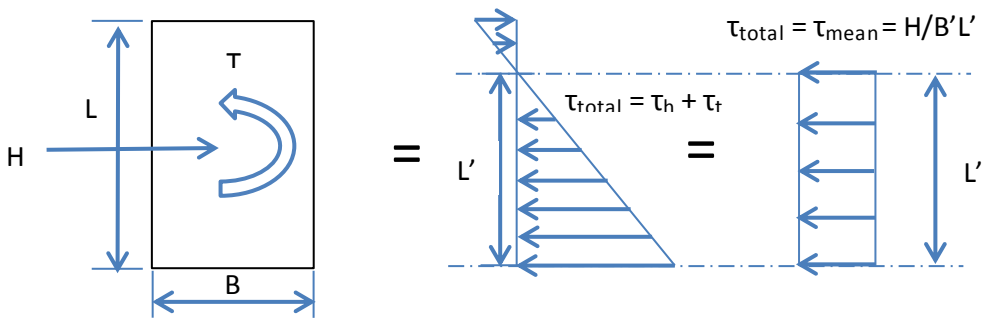

Figure 2.16: Simplified mean shear stress due to torsion moment and horizontal force

This simplification gives a mean shear stress expressed in Equation (2.20).

$$\tau_h + \tau_t = \tau_{mean} = \frac{H}{B' L'} \qquad (2.20)$$

2.5.2 Shear stress that exceeds the shear capacity

Discussions in chapter 2.2.3 are not sufficient, which do not consider the situation that the shear stresses due to torsion moment exceed the shear strength. Thus, a violation will result in redistribution of stresses. This is illustrated in Fig.2.17. There is a limit to the amount of shear stresses that can be redistributed and this limit can be defined by the roughness r.

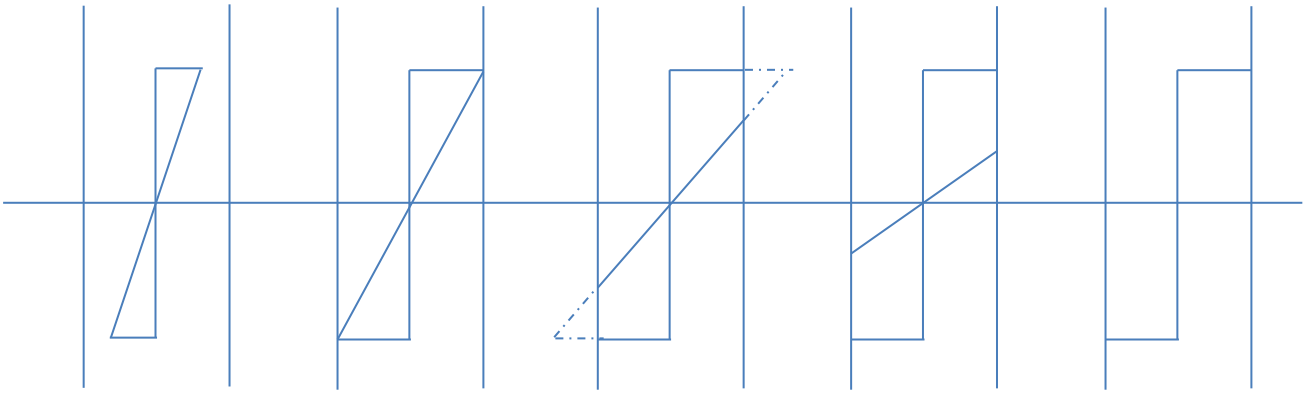

Figure 2.17: redistribution of shear stresses of a foundation

Fig. (1) and (2) are the cases of shear stresses due to torsion less than the shear strength. Then it is not necessary to redistribute the shear stress. In Fig.(3) the shear stresses partly exceed the shear strength which are then redistributed.

Soil under the foundations must take on the shear stresses which are applied to the foundation. Therefore, we allocate the same area of space in Fig. (4) where there is still available capacity as in Fig. (3). Fig.(5) shows a case where all the cutting capacity is utilized. In other words, this means roughness r = 1, since roughness shows how much of the capacity is utilized.

2.5.3 DNV offshore standard method

To calculate the ultimate horizontal capacity of mudmat foundation subjected to combined loads with torsion moment, <Offshore Standard DNV-OSD-J101,2007> can be helpful.

When a torsion moment T is applied to the foundation in addition to the forces H and V, the interaction between the torsion and these forces can be accounted for by replacing H and T with an equivalent horizontal force H'. The bearing capacity of the foundation is then to be evaluated for the force set (H',V) instead of the force set (H,V) (DNV, 2010).

The equivalent horizontal force can be calculated as equation (2.21)

$$H' = \frac{2T}{L'} + \sqrt{H^2 + (\frac{2T}{L'})^2} \qquad (2.21)$$

where L' is the length of effective area.

Therefore, the ultimate horizontal capacity can be determined by equation (2.22)

$$H = \sqrt{H'^2 - \frac{4H'T}{L'}} \qquad (2.22)$$

Chapter 3 PLAXIS 3D PROGRAM AND MODELS

3.1 Introduction of PLAXIS 3D

PLAXIS is a widely used numerically simulation tool both for 2-dimensional and 3-dimensional geotechnical analyses. PLAXIS is based on the finite element method and can use various soil models to simulate the soil behavior at different situations. For more details related to this application setup and operation, please refer to user manual and reference for PLAXIS 3D 2012.

PLAXIS 3D program is a three-dimensional finite element program widely used in geotechnical analysis to perform deformation and stability analysis. The generation of a three-dimensional finite element model in the PLAXIS 3D program is based on the creation of a geometry model, which involves a composition of volumes, surfaces, lines and points. Soil stratigraphy at different locations could be determined through the definition of vertical boreholes. Soil layers and ground surfaces could be non-horizontal as well. (PLAXIS 3D Reference, 2012)

PLAXIS 3D program computes the stresses following a Cartesian coordinate system. All of these output data, including compressive stresses and forces, pore pressures, will be taken to be negative, whereas tensile stresses and forces are taken to be positive. Cartesian coordinate system and positive stress directions are shown in Fig.3.1.

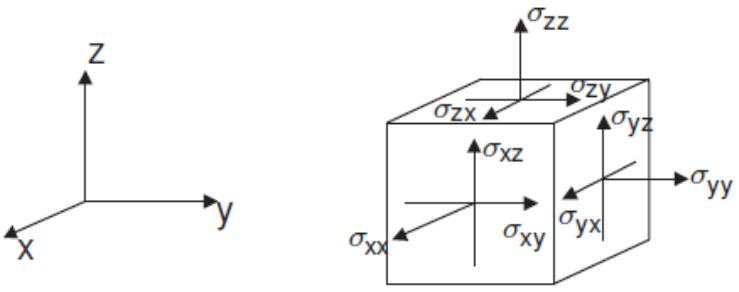

Figure 3.1: Cartesian coordinate system and positive stress directions (PLAXIS 3D Reference 2012)

3.2 Idealized soil and foundation conditions

The realistic soil conditions at the site may be complicated. For a simplification, only one layer of soft clay with shear strength linearly increasing with depth is considered.

For analysis of skirted foundations, combined loads are normally transferred to the level of the skirt tips such that the bearing capacity is related to the shear strength at skirt tip level(e.g. Tani & Craig, 1995; Watson & Randolph, 1997). Tani & Craig (1995) propose that the behavior of an embedded shallow foundation in an undrained soil with a linear increase in strength with depth can be approximated by analyzing a surface foundation, but with the soil strength profile described by equation (3.1).

$$S_u = S_{u0} + kz \qquad (3.1)$$

Where S_{u0} is the shear strength at foundation level, and k is the strength gradient with a depth of z. Centrifuge tests reported by Tani & Craig (1995) and Waton & Randolph (1997) suggest this is reasonable for embedment depths less than around 30% of the foundation width. The degree of heterogeneity can be represented by the dimensionless coefficient:

$$\kappa = \frac{kB'}{S_{u0}} \qquad (3.2)$$

For a shallow foundation with skirts of depth D, the shear strength at foundation level is:

$$S_{u0} = S_{u,z=0} + kD = 2+1.3*1 = 3.3kPa \qquad (3.3)$$

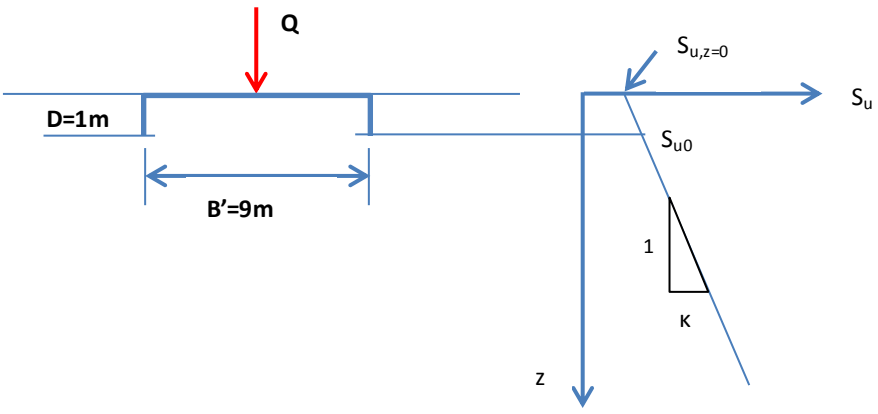

Figure 3.2: Idealised soil and foundation conditions

Where, $S_{u,z=0}$ is the shear strength at the mudline.

In this thesis, all the finite element analyses were carried out with the software PLAXIS 3D.

3.3 Material parameters of soil

The soil conditions at the site consist of a layer of very soft clay at the seabed with a linear increase of $S_{u,inc}$ = 1.3kPa/m to a depth of 18 meters.

An undrained soil condition is represented with a linear elastic perfectly plastic constitutive law defined by the undrained Young's modulus (E_u) and Poisson's ratio (υ) and failure according to Tresca criterion, defining the maximum shear stress in any plane limited to the undrained shear strength (S_u). (Gourvenec, 2007)

Relevant parameters can be determined as follows:

- Undrained shear stress profile: S_u=2 +1.3z (kPa)
- Young's modulus of the soil is assumed to vary linearly with depth, maintaining a constant modulus ratio of E_u/S_u =500
- Possion's ratio is υ=0.49
- Lateral earth pressure coefficient is $K_o' = \upsilon/(1-\upsilon)$=0.96
- A soil layer with depth of D=2B=18m was selected for models

Parameters for soil can be summarized below in table 3.1.

Parameters	Name	Soil	Unit
Material model	Model	Mohr Coloumb	-
Drainage type	Type	Undrained (C)	-
Unit weight above phreatic level	γ_{unsat}	15,5	kN/m^3
Unit weight below phreatic level	γ_{sat}	15,5	kN/m^3
Stiffness	E_u	1000	kN/m^2
	$E_{u,inc}$	650	kN/m^2
Poisson's ratio	v_u	0.49	-
Shear Strength	$S_{u,ref}$	2	kPa
	$S_{u,inc}$	1.3	kPa
Lateral earth pressure coefficient	K_o	0.96	-

Table 3.1: soil parameters for PLAXIS 3D models

Based on previous analyses in chapter 3.2, a linearly increasing shear strength profile described by $\kappa = \frac{kB'}{S_{u0}} = \frac{1.3*9}{3.3} = 3.5$ according to equations (3.2) is considered.

The choice of soil model and associated material parameters representing the behavior of clay is usually the largest challenge in terms of getting a good result.

In PLAXIS 3D, there are various models available, like Mohr Coloumb(MC), Hardning Soil(HS) and Soft Soil(SS) models. All these models are basically considered as efficient stress models with an isotropic shear strength provided by the cohesion $c = a\tan\varphi$, friction angle φ and MC failure criterion.

It is complicated to use HS and SS models to model a single isotropic undrained shear strength profile. Thus, It is not recommended to use these models to model the short-term undrained condition. (Andresen, 2004)

The MC model is also regarded as an effective stress model, but since dilatant or contractive behaviors are not modeled in the elastic range before strength limit is reached, it is possible to select c_{mod} and φ_{mod} so proper undrained shear strengths are modeled.

The MC model is used as the total stress model by setting $c(z)=S_u(z)=2+1.3z$ and $\varphi= 0$. A possion' ratio of $\upsilon= 0.49$ is used.

In MC models, it is not possible to provide anisotropic shear strength of consolidated active and passive triaxial and direct shear tests(S_{uA}, S_{uP}, S_{uD}). Therefore an average value of shear strength must be used. See equation (3.4). This simplification does not significantly affect the analyses in this thesis. This is because the amount of the active - passive and triaxial shear strength is equal in undrained analysis and the simplifications give reasonable consequences.

$$S_u \approx \frac{1}{3}(S_u^A + S_u^P + S_u^D) \qquad (3.4)$$

Basically stiffness has no impact on the bearing capacity of a foundation, except for the deformation. E-modulus is set to $E=1000kN/m^2$ at mudline, which is a relatively low value for clay (Vegvesen, 1992). Results showed that when E-modulus was assigned with values from 1000 to 5000, no significantly change occurred on the bearing capacity, but displacements became lower.

Due to numerical problems, 'tension cut off' was deselected in PLAXIS 3D models.

3.4 Material parameters of foundation

3.4.1 Base plate and skirts

In this thesis, it is assumed that a PLET is temporarily supported during installation by a 21m by 9m rectangular mudmat foundation. To simplify the calculations, a unit weight of 0kN/m^3 is assigned to base plate and skirts in order to neglect the affections of self-weight of mudmat foundation.

Skirted mudmat foundations with embedment depth to foundation breadth ratio D/B of about 0,1(D/B=1/9=0,1) are considered under conditions of plane strain with a skirt thickness of 15mm.

In addition, the mudmat foundation is assumed behaving elastically, its Young's modulus is E=1E9 kN/m^2, and Poisson's ratio is υ=0.3. Therefore, the base plate and skirts are set to be very rigid with a stiffness of E_1=E_2=1E9 kN/m^2.

Parameters of base plate and skirts are summarized in table 3.2.

Parameters	Steel baseplate	Steel skirts
d	0,2m	0,015m
γ	0kN/m^3	0kN/m^3
E_1=E_2	1E9 kN/m^2	1E9 kN/m^2
v_{12}	0,3	0,3

Table 3.2: Parameters of base plate and skirts

Mudmat foundations with and without 1*2 inner skirts are shown below in Fig.3.3.

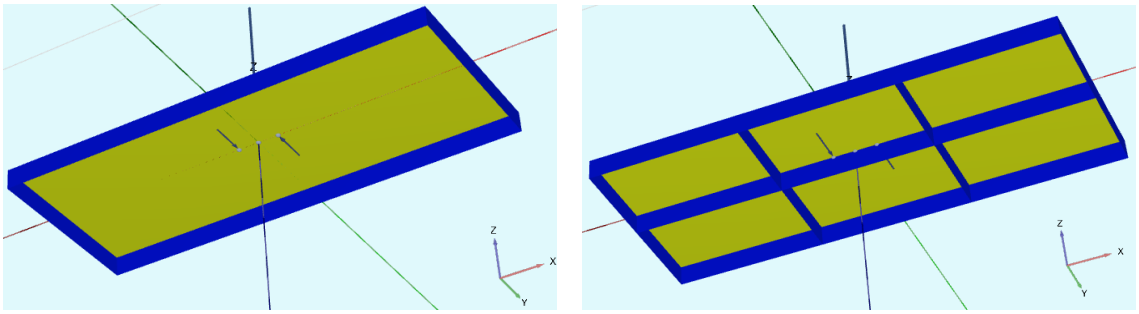

Figure 3.3: Mudmat foundations with and without inner skirts

3.4.2 Interface

In PLAXIS 3D, interface must be set along base plate and skirts to take into account the interface properties and relative displacement between structure and soil. Without an interface the structure and the soil are tied together and no relative displacement (slipping/gapping) is possible between structure and soil.

By using an interface, node pairs are created at the interface of structure and soil. From a node pair, one node belongs to the structure and the other node belongs to the soil. The interaction between these two nodes consists of two elastic-perfectly plastic springs. One elastic-perfectly plastic spring is used to model the gap displacement and the other one is to model slip displacement. Also see the connectivity plot of a soil-structure connection with and without interface. (PLAXIS, 2012)

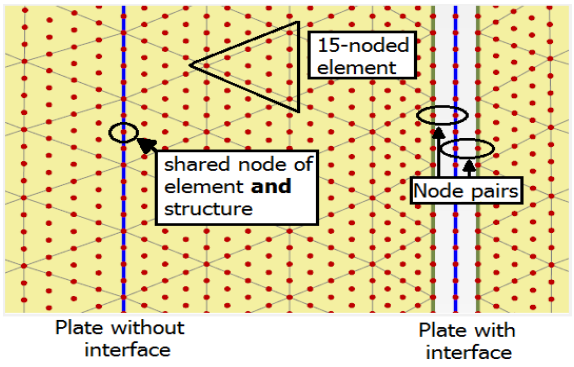

Figure 3.4: connectivity plot of a soil-structure connection (PLAXIS, 2012)

Interface under the base plate may have large affections on the horizontal capacity. The strength of the mudmat and clay interface was modeled using an interface factor R, where the maximum shear stress at the interface $\tau_{max} = RS_u$. The 'rough' and 'smooth' extremes of interface strength correspond to R=1 and R=0 respectively. An intermediate roughness of R=0.5 was assumed for PLAXIS models, which is a typical assumption for steel/soft clay interface.

Mudmat foundation with interface activated is shown below in Fig.3.5.

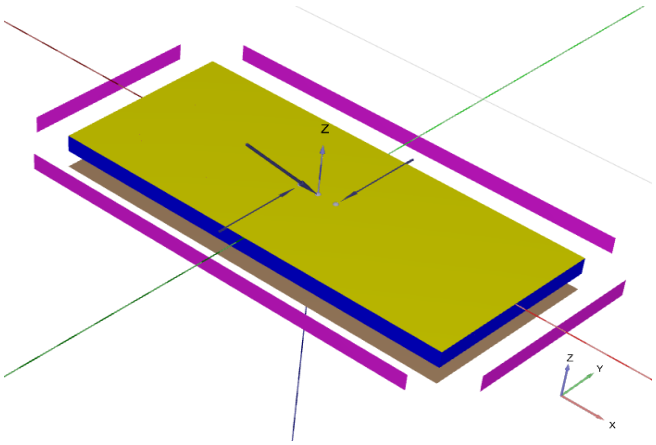

Figure 3.5: Mudmat foundation with interface activated

3.5 Descriptions of models

In order to investigate failure envelopes of mudmat foundation under combined loads(VHT), three dimensional perfect elasto-perfectly plastic finite element analysis for bearing capacity behaviors of mudmat foundation is carried out by utilizing the specialized finite element analysis software PLAXIS 3D for geotechnical engineering projects.

All together 3 models(see Table.3.3) were utilized for the analyses of the effect of torsion moment on the bearing capacity of the mudmat foundation.

#	Model 1	Model 2	Model 3
Inner skirts	NO	NO	YES
Meshes	medium	fine	fine

Table 3.3: Different models for analyses

Based on the displacement corresponding to the ultimate bearing capacity, failure envelopes in different load spaces will be plotted by the loading procedure of Swipe test which was originally suggested and applied in a small-scale model tests by Tan (Tan, 1990) and then widely applied into practice. The loading procedure includes two loading steps which are illustrated in Fig.3.6, an example of search of failure envelope in V-H loading space. (Wu Ke, 2011)

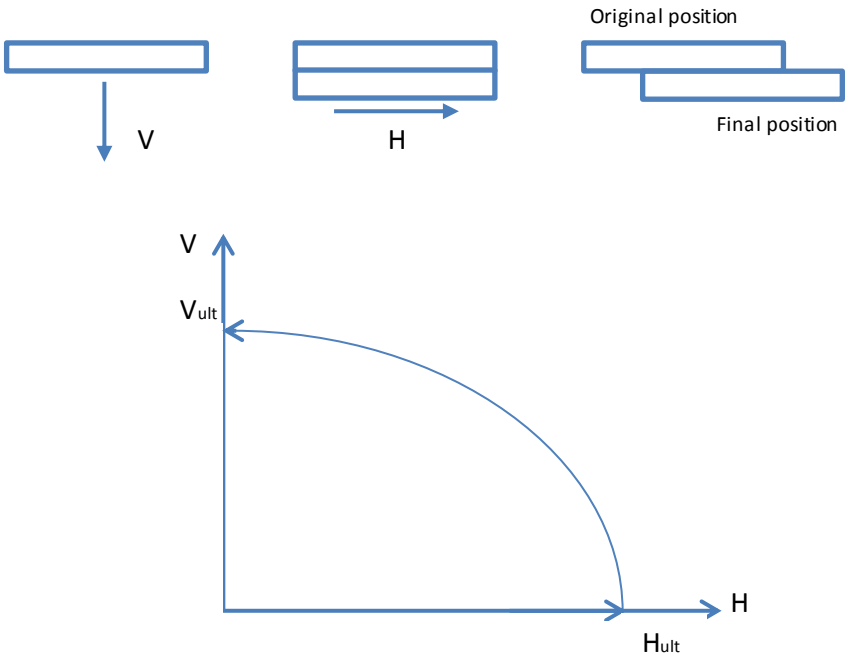

Figure 3.6: The loading procedure of Swipe test

3.6 Model geometry

The lateral dimensions of the 3D models are 40m×30m with one soil layer of 18m as described before. These dimensions were selected such that the model boundaries have negligible effects on the results. Model geometry is shown below in Fig.3.7.

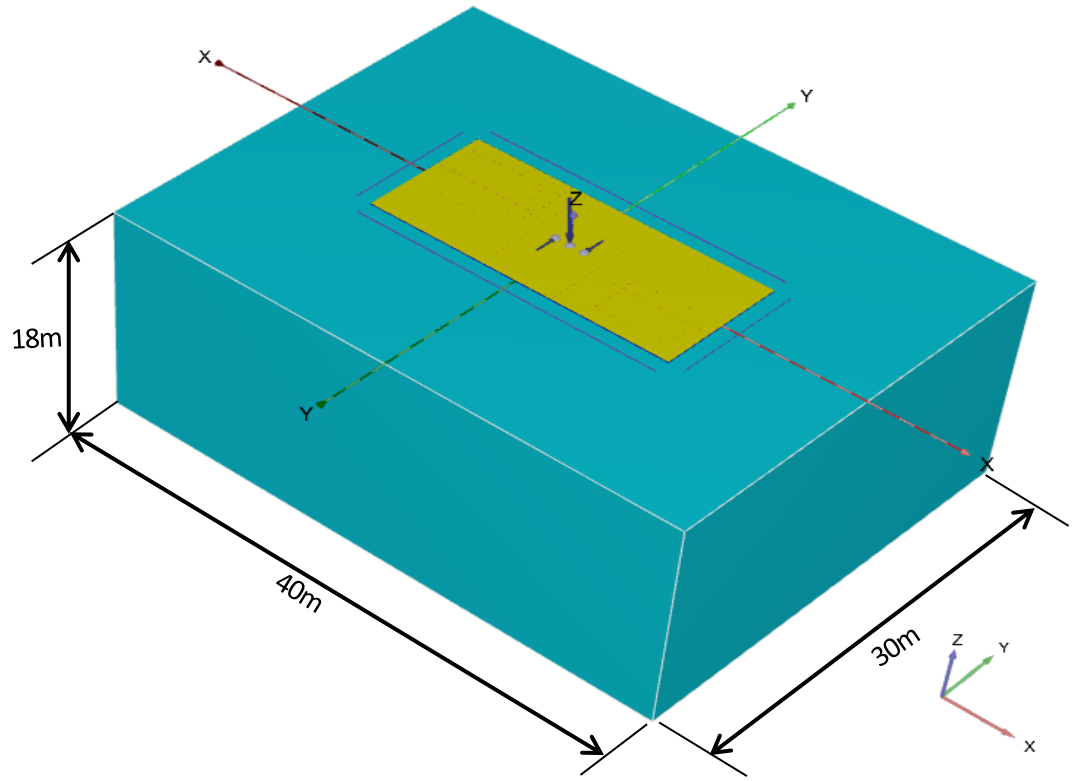

Figure 3.7: Geometry of PLAXIS 3D model

As shown in Fig. 3.7, an inner soil volume with dimensions of 40m×30m×18m is introduced. The inner soil volumes have larger affections on the foundation than outer soil volumes, thus should be studied more carefully. To achieve a more accurate results, inner soil volumes were refined several times to get more fine meshes than outer soil volumes. All of these three components have their central point placed in the origin point of the Cartesian coordinate system. Dimensions are summarized as shown in Table 3.4.

Components	Lateral soil volume	Mudmat foundation
Length/m	40	21
Width/m	30	9
Height/m	18	1

Table 3.4: Dimensions of soil volumes and mudmat foundation

3.7 Element meshes

Medium meshes and fine meshes are generated for different models to compare the results. The local refinement factors were increased to 1 and 0.5 for lateral soil volume and mudmat foundation respectively. The element distribution was set to 'medium' and 'fine' in order to get medium and fine meshes for different models.

The mesh information is shown in table 3.5.

Parameters	Model 1	Model 2	Model 3
Meshes	Medium	Fine	Fine
No. of soil elements	11351	31043	31043
No. of nodes	18151	47597	47597
Average element size	1,379m	0,8342m	0,8342m

Table 3.5: Mesh property for medium meshes and fine meshes

Medium finite element mesh of PLAXIS 3D models is shown in Fig. 3.8.

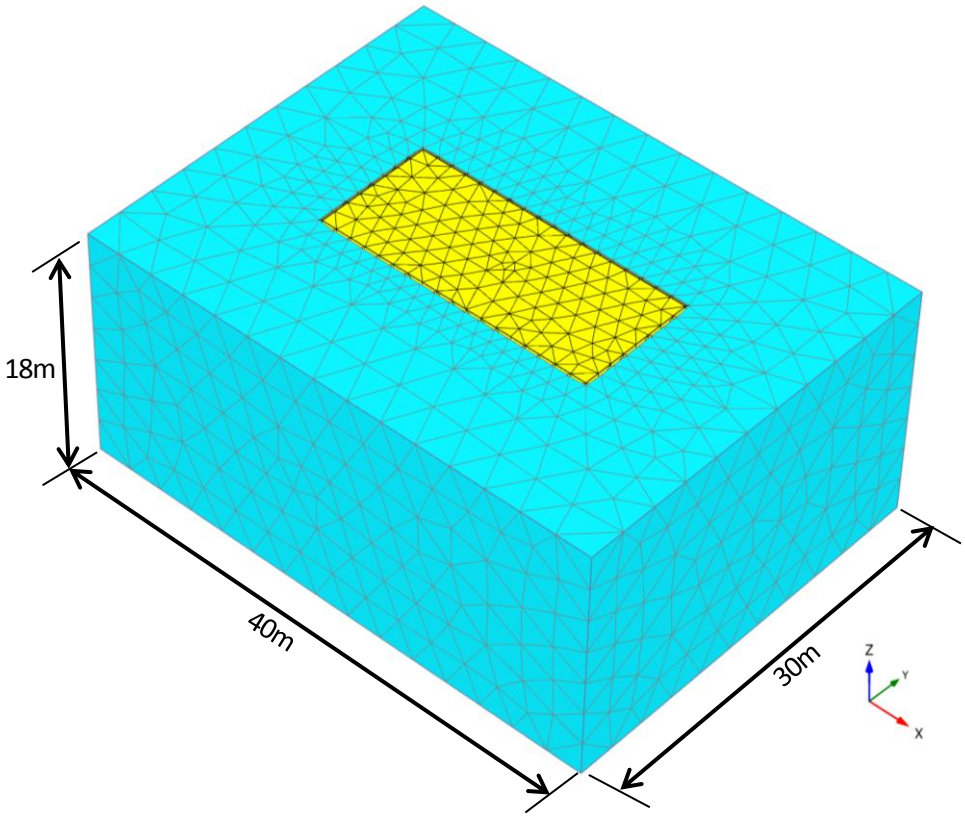

Figure 3.8: Medium meshes of PLAXIS 3D Model 1

Fine finite element mesh of PLAXIS 3D models is shown in Fig. 3.9.

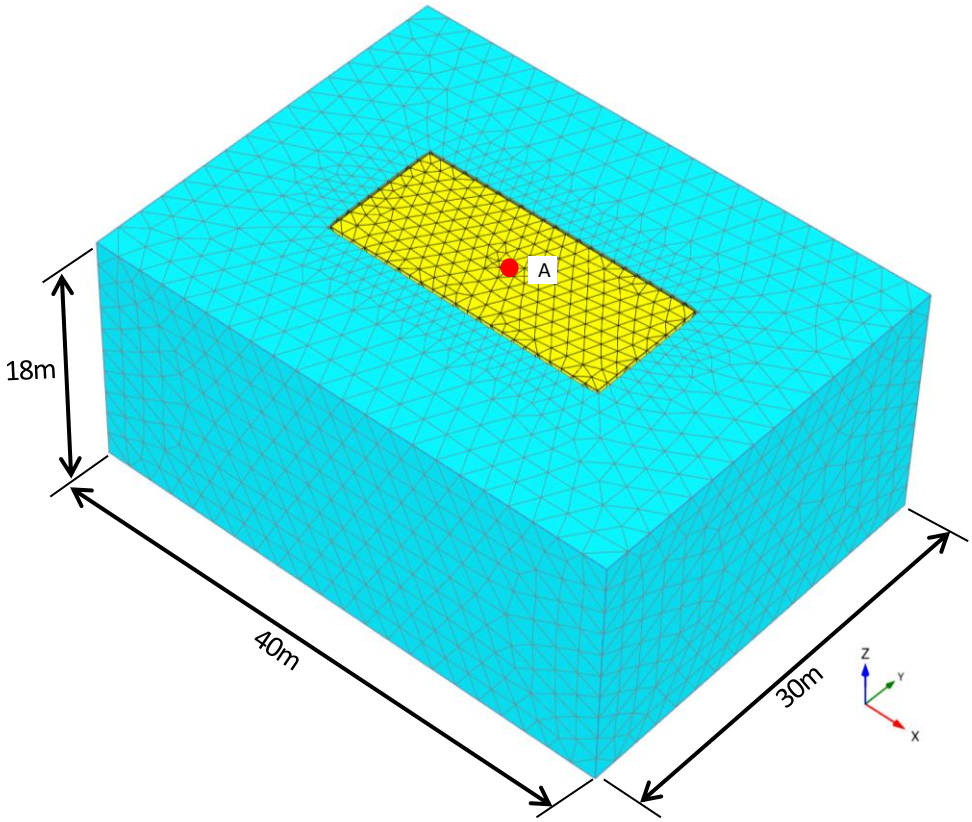

Figure 3.9: Fine meshes of PLAXIS 3D Model 2 and Model 3

Reference node A, as shown in Fig. 3.7 is defined in table 3.5 for the load-displacement curves which are used to determine the ultimate bearing capacities.

Reference node	Position (m,m,m)
A	Center of base plate, (0,0,0)

Table 3.6: Reference nodes and the positions

3.8 Load combinations

In this thesis, each analysis followed a single load path to failure in V-T, H-T and V-H-T load space, respectively. See Fig. 3.10. A constant vertical load of 20000 kN was imposed as a directed force, and the horizontal and torsion load components were applied at a different ratios seen in table 3.7.

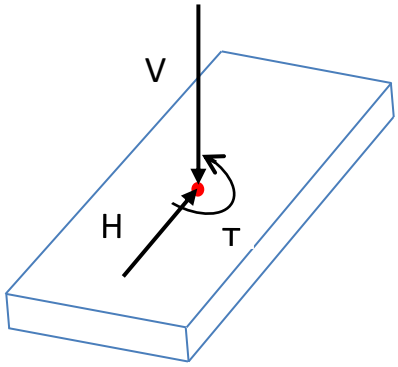

Figure 3.10: Mudmat foundation subjected to combined loads of V, H and T

Loading path	V-T		H-T		V-H-T		
#	V	T/V	H	T/H	V	H/V	T/V
	kN	kN	kN	kN	kN	kN	kNm
1	20E3	0	20E3	0	20E3	0.1	0
2	20E3	0.1	20E3	0.1		0.2	
3	20E3	0.2	20E3	0.2		0.4	
4	20E3	0.4	20E3	0.4		0.8	
5	20E3	0.8	20E3	0.8		1.6	
6	20E3	1.6	20E3	1.6	20E3	0.1	0.2
7	20E3	3.2	20E3	3.2		0.2	
8	20E3	6.4	20E3	6.4		0.4	
9	20E3	12.8	20E3	12.8		0.8	
10	20E3	25.6	20E3	25.6		1.6	
11	20E3	0	20E3	0	20E3	0.1	0.4
12	20E3	0.1	20E3	0.1		0.2	
13	20E3	0.2	20E3	0.2		0.4	
14	20E3	0.4	20E3	0.4		0.8	
15	20E3	0.8	20E3	0.8		1.6	
16	20E3	1.6	20E3	1.6	20E3	0.1	0.8
17	20E3	3.2	20E3	3.2		0.2	
18	20E3	6.4	20E3	6.4		0.4	
19	20E3	12.8	20E3	12.8		0.8	
20	20E3	25.6	20E3	25.6		1.6	
No. of paths	**10**		**10**		**20**		

Table 3.7: Loading paths on V-T, H-T and V-H-T load spaces

Representation of the interaction of horizontal load(H) and torsion(T) at a constant vertical load(V) is convenient since in reality vertical foundation load is quasi-constant, largely due to the self-weight of the super-structure and foundation system, whereas the horizontal and torsion components result from the environmental forces are variable, but may be coupled.

3.9 Failure envelopes

Many researchers have been seeking to characterize a failure envelope in loading space to describe the foundation response transformation from safe condition to failure state recently. Martin, Murff, Bransby and Randolph have analysed the failure envelope of foundation under combined loads in undrained saturated sand clay based on the limited analysis. However, a reasonable computation pattern and analysis method is still lacking for the analyses of the stability of offshore foundation subjected to torsion moment. (Wu Ke, 2011)

The applied loads gives rise to load paths that move from the origin across the failure envelope, initially at gradients determined by the elastic stiffness, but with the gradients changing owing to internal plastic yielding as the paths approach the failure envelope.

Bounding envelopes of ultimate limit states under combinations of vertical, horizontal and torsion loadings(VHT) predicted by the finite element analyses are presented as failure envelopes in Fig. XX. The envelopes are plotted in both normalized load space(H/H_{ult} against V/V_{ult}) and dimensionless load space(H/AS_{u0} against V/AS_{u0}) for each of the four torsion load cases considered: T/V=0, 0.2, 0.4, 0.8.

Three-dimensional failure surfaces normally provide a useful qualitative assessment of ultimate limit states under general loading. For quantitative comparison, two-dimensional slices through the three-dimensional surface are more useful for direct determination of ultimate limit states (Gourvenec, 2007). Example of failure envelopes plotted in dimensionless load space is illustrated in Fig.3.11.

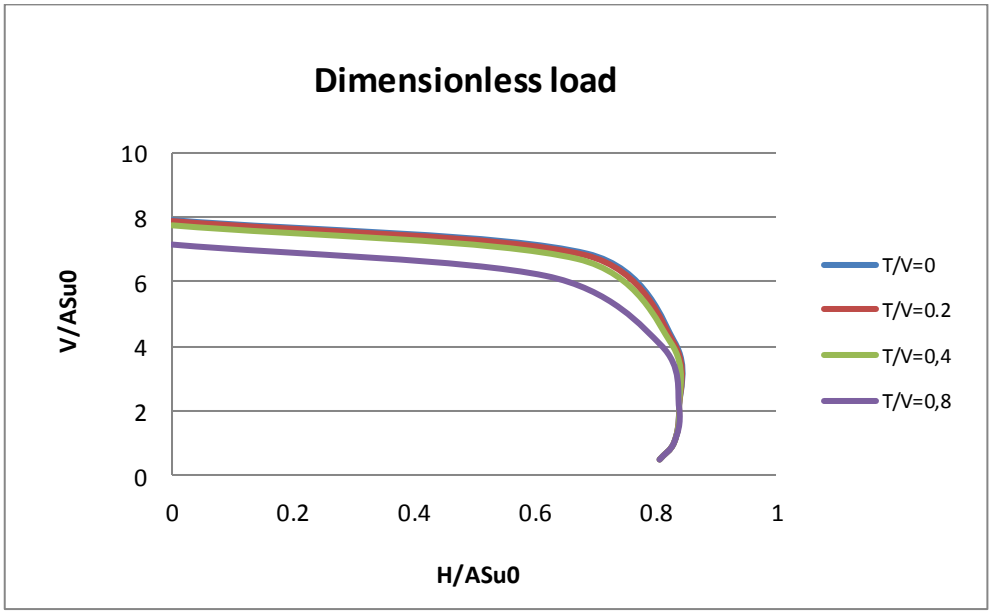

Figure 3.11: Example of failure envelope plotted in dimensionless load space

Chapter 4 RESULTS AND COMPARISONS

4.1 Interpretations of ultimate bearing capacity in PLAXIS 3D

Ultimate bearing capacity for a particular load combination can be derived from a graph shown in Fig.4.1. It shows the Mstage against deformation for a foundation subjected to vertical and horizontal loads without torsion. Ultimate bearing capacity is defined as described in Chapter 2, when the soil under the foundation has a large deformation without further increase of the load q.

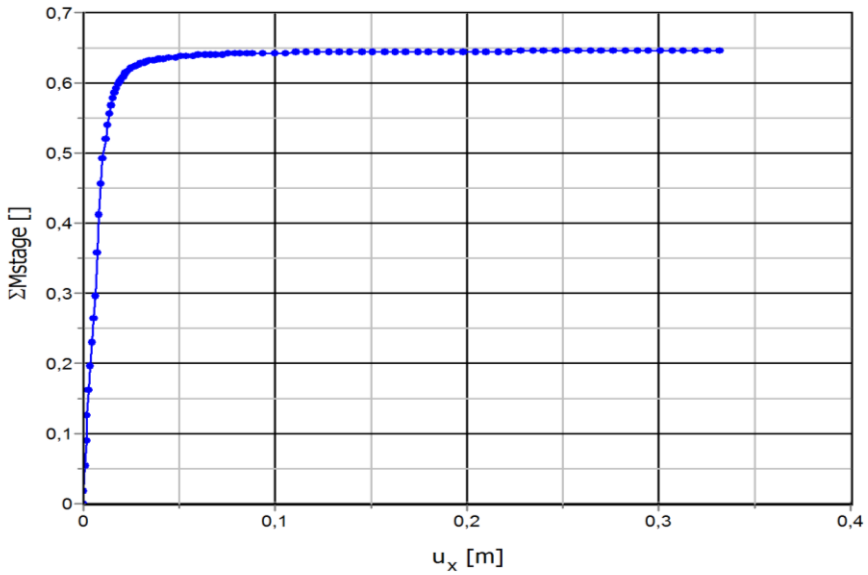

Figure 4.1: Mstage-deformation curve from the analysis of PLAXIS 3D

q is equal to M_{stage} multiplied by the constant value of 10000, since the vertical load of the model is V=10000kN/m^2. Therefore, the ultimate vertical capacity of the foundation subjected to a load combination of V =10000kN/m^2 , H/V=0,1, T/V=0 showing in Fig.4.1 is V_{ult}= M_{stage}* 10000=0,646*10000=6460kN. Similarly, ultimate horizontal capacity is H_{ult}= M_{stage}* 10000*(H/V)=0,646*10000*0,1=646kN.

The notation adopted for different loads that utilized is shown in Table 4.1 below.

Parameters	Vertical load	Horizontal load	Torsion load
Load	V	H	T
Ultimate load	V_{ult}	H_{ult}	T_{ult}
Dimensionless load	V/AS_{u0}	H/AS_{u0}	T/ABS_{u0}
Normalised load	V/V_{ult}	H/H_{ult}	T/T_{ult}

Table 4.1: Summary of notation for loads

4.2 Results of hand calculations

4.2.1 Vertical and horizontal bearing capacities when T=0

Vertical and horizontal bearing capacities of mudmat foundation calculated by Janbu method is shown in Table 4.2 and the plot is shown in Fig.4.2.

Janbu method	
V (kN)	H (kN)
8037	401
7909	469
7761	537
7487	637
7379	670
7128	734
6818	796
6420	854
5863	905
5718	914

Table 4.2: Summary of vertical and horizontal bearing capacities from hand calculations

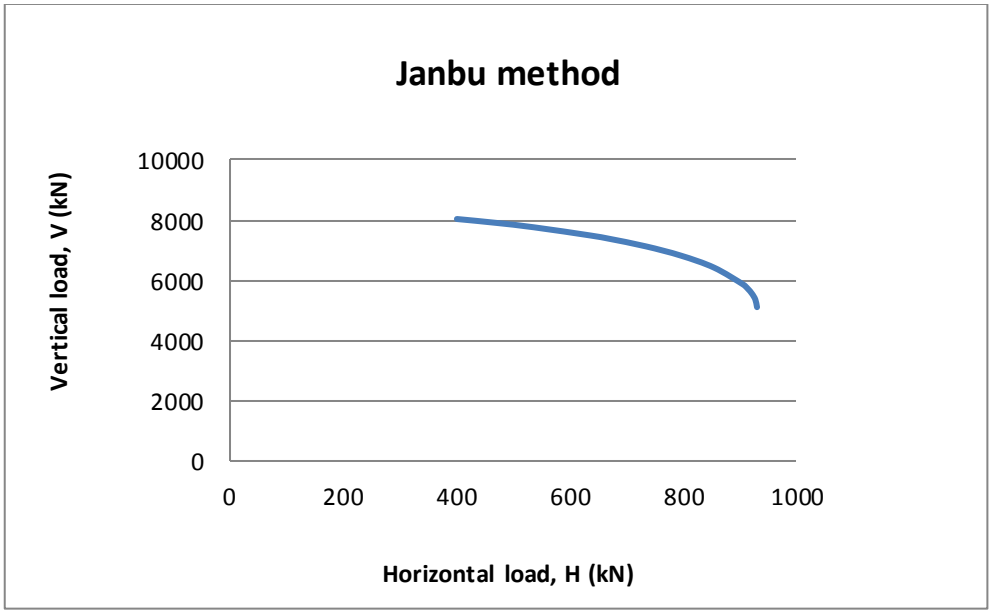

Figure 4.2: Results of Janbu method hand calculations illustrated in V-H load space

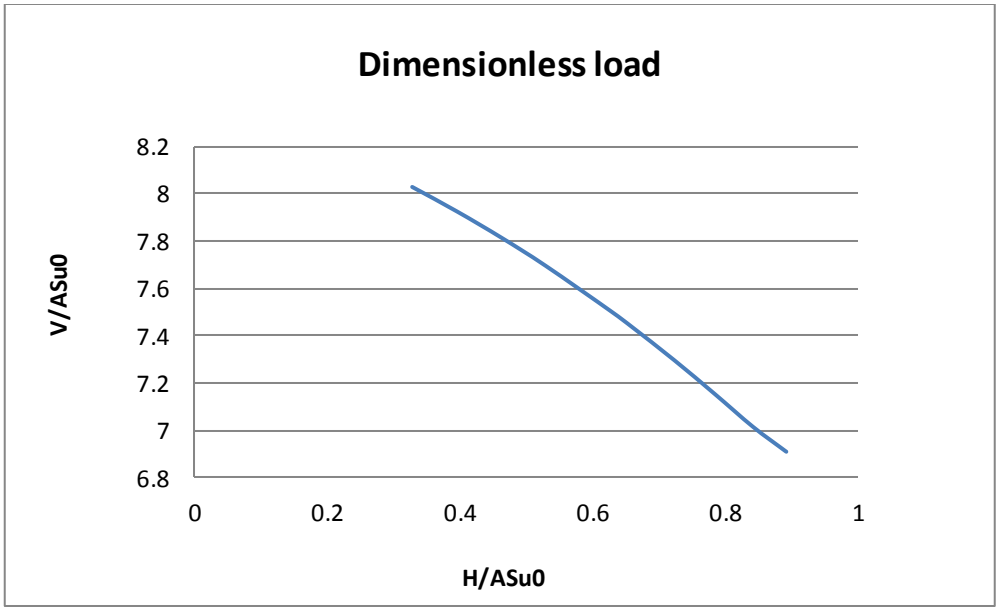

Figure 4.3: Results of Janbu method hand calculations illustrated in V-H dimensionless load space

4.2.2 Vertical and horizontal bearing capacities under different torsions T

When torsion T is included, DNV standard together with Janbu method is used to determine the horizontal bearing capacity under different torsion moments.

Vertical and horizontal bearing capacities of mudmat foundation calculated by Janbu method and DNV standard are shown in Fig.4.4 and Fig.4.5.

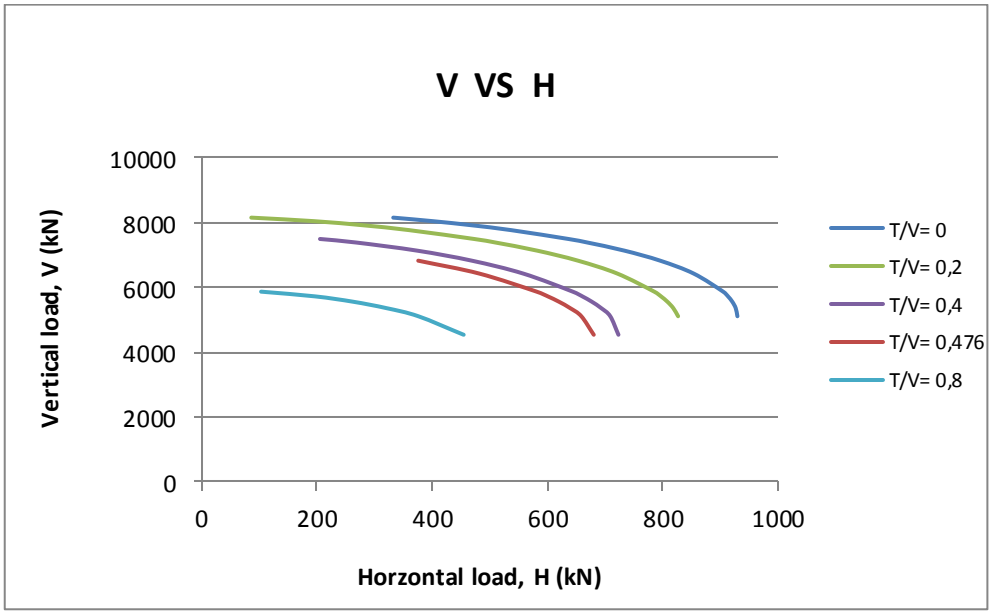

Figure 4.4: Bearing capacities under different torsions in V-H load space

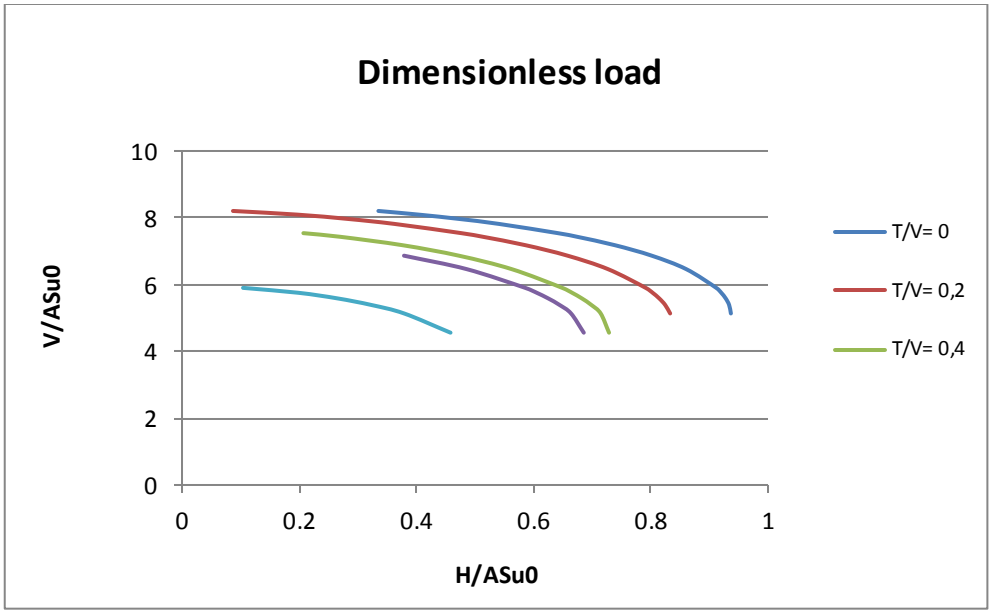

Figure 4.5: Bearing capacities under different torsions in V-H dimensionless load space

4.3 Results of PLAXIS 3D

4.3.1 Failure envelopes in V-T load space

Vertical bearing capacity and ultimate torsion moment determined from PLAXIS 3D can be shown below in Table 4.3 for the example of model 1.

Parameters		unit	Phase #	V	T/V	Mstage	T	V	V/Asuo	T/ABSuo	V/Vult	T/Tult
A=	189	m2	1	10000	0	0,784	0	7840	7,90	0,000	1,000	0,000
B=	9	m2	2	10000	0,2	0,781	1562	7810	7,87	0,175	0,996	0,182
Suo=	5,25	kPa	3	10000	0,4	0,768	3072	7680	7,74	0,344	0,980	0,358
			4	10000	0,8	0,709	5672	7090	7,15	0,635	0,904	0,661
Vult=	7840	kN	5	10000	1,6	0,507	8112	5070	5,11	0,908	0,647	0,946
Tult=	8576	kNm	6	10000	3,2	0,268	8576	2680	2,70	0,960	0,342	1,000
			7	10000	6,4	0,133	8512	1330	1,34	0,953	0,170	0,993
			8	10000	12,8	0,065	8320	650	0,66	0,932	0,083	0,970

Table 4.3: Data analyses for determinations of failure envelopes of Model 1 in V-T load space

Failure envelopes for PLAXIS Model 1 are illustrated in V-T normal load space, dimensionless load space, and normalized load space, respectively. See Fig.4.6 to Fig.4.8.

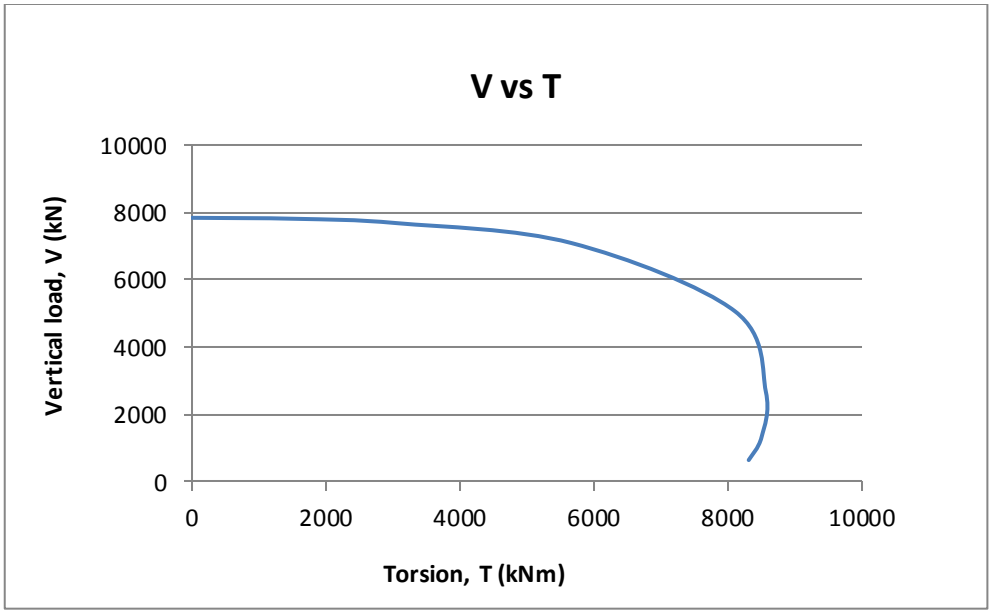

Figure 4.6: Failure envelope of PLAXIS Model 1 in V-T load space

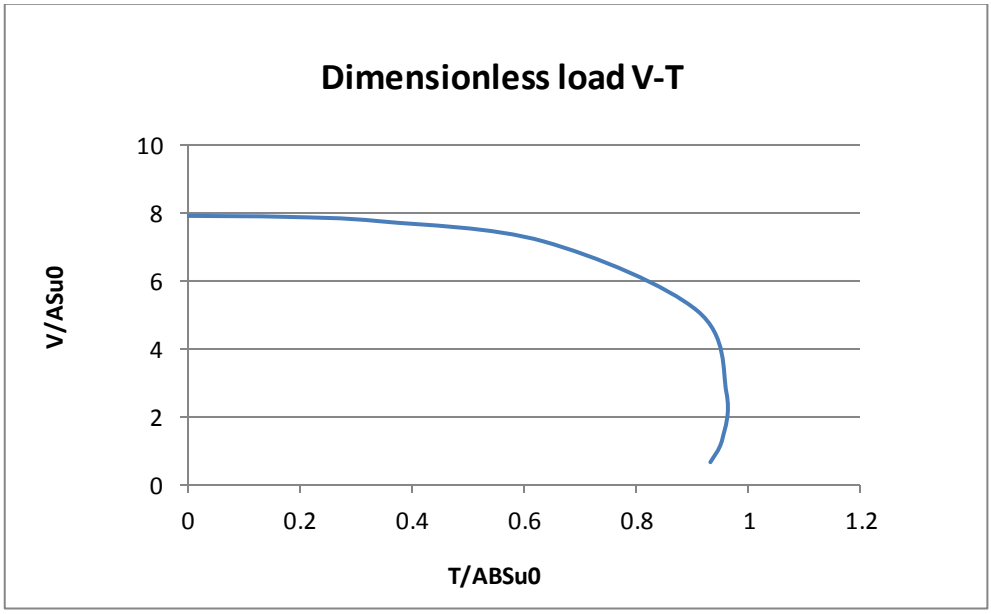

Figure 4.7: Failure envelope of PLAXIS Model 1 in V-T dimensionless load space

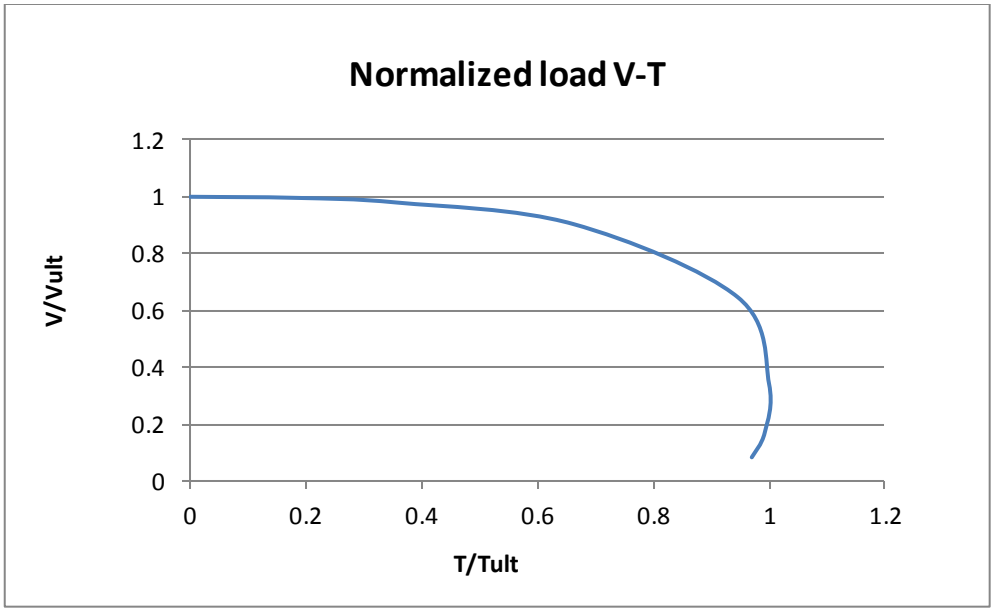

Figure 4.8: Failure envelope of PLAXIS Model 1 in V-T normalized load space

4.3.2 Failure envelopes in H-T load space

Horizontal bearing capacity and ultimate torsion moment determined from PLAXIS 3D can be shown below in Table 4.4 for the example of model 1.

Parameters		unit	Phase #	H	T/H	Mstage	T	H	H/ASuo	T/ABSuo	H/Hult	T/Tult
A=	189	m2	1	2000	0	0,362	0	724	0,73	0,000	1,000	0,000
B=	9	m2	2	2000	0,2	0,362	144,8	724	0,73	0,016	1,000	0,020
Suo=	5,25	kPa	3	2000	0,4	0,362	289,6	724	0,73	0,032	1,000	0,039
Hult=	724	kN	4	2000	0,8	0,362	579,2	724	0,73	0,065	1,000	0,079
Tult=	7372,8	kNm	5	2000	1,6	0,362	1158,4	724	0,73	0,130	1,000	0,157
			6	2000	3,2	0,361	2310,4	722	0,73	0,259	0,997	0,313
			7	2000	6,4	0,345	4416	690	0,70	0,494	0,953	0,599
			8	2000	12,8	0,248	6348,8	496	0,50	0,711	0,685	0,861
			9	2000	25,6	0,14	7168	280	0,28	0,803	0,387	0,972
			10	2000	51,2	0,072	7372,8	144	0,15	0,826	0,199	1,000
			11	2001	102,4	0,036	7372,8	72,036	0,07	0,826	0,099	1,000

Table 4.4: Data analyses for determinations of failure envelopes of Model 1 in H-T load space

Failure envelopes for PLAXIS Model 1 are illustrated in V-T normal load space, dimensionless load space, and normalized load space, respectively. See Fig.4.9 to Fig.4.11.

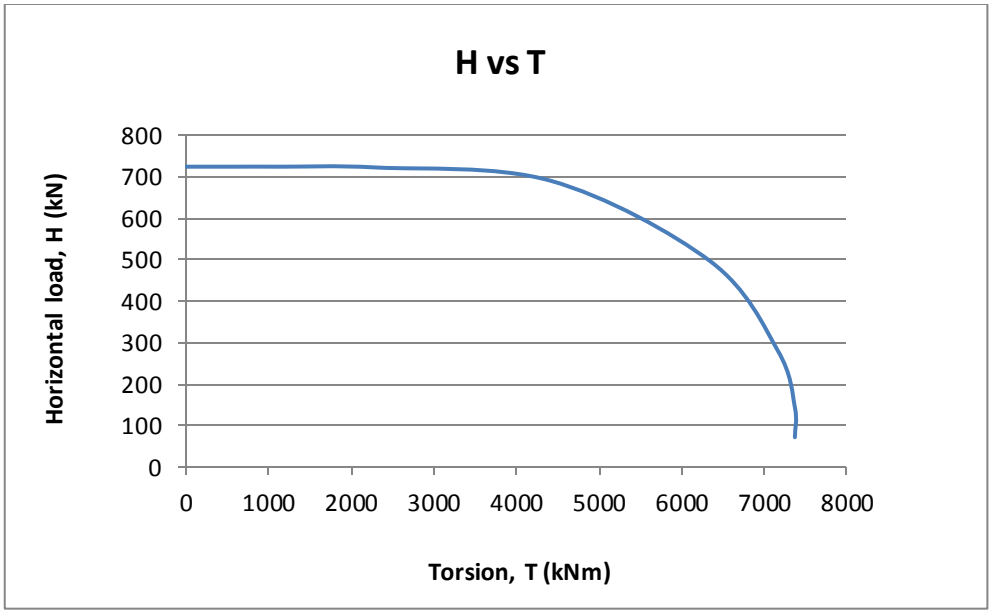

Figure 4.9: Failure envelope of PLAXIS Model 1 in H-T load space

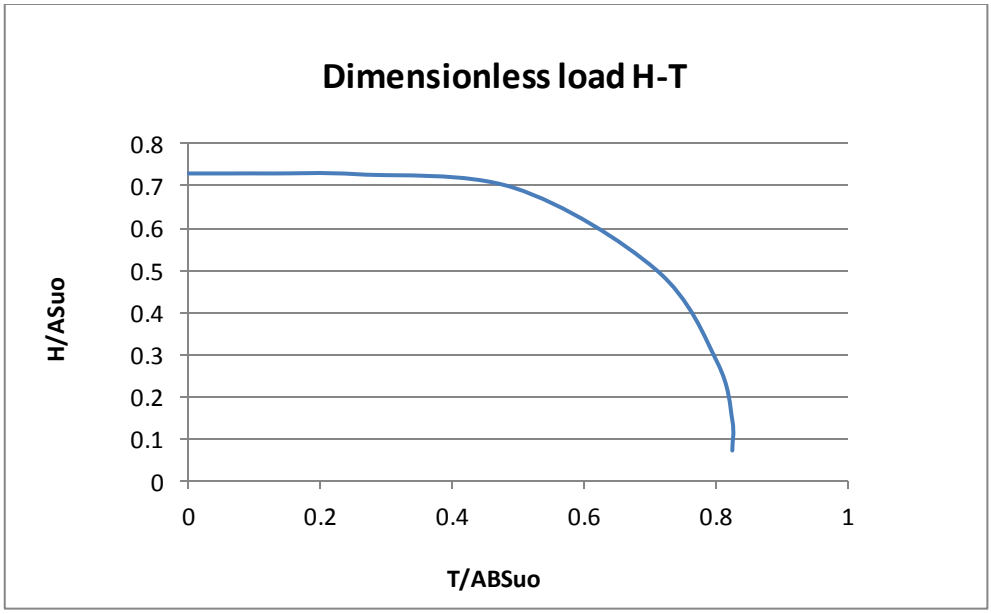

Figure 4.10: Failure envelope of PLAXIS Model 1 in H-T dimensionless load space

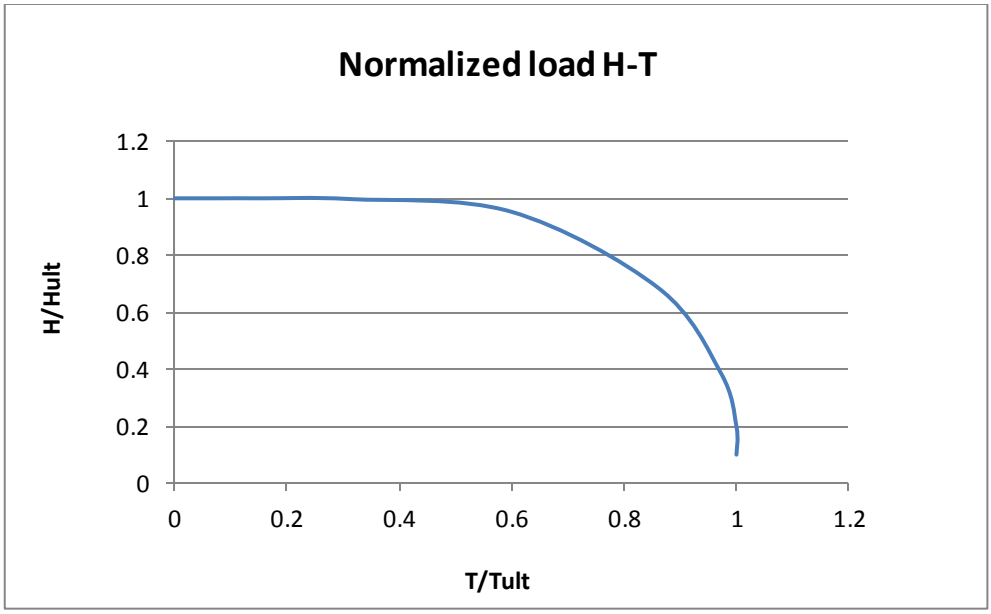

Figure 4.11: Failure envelope of PLAXIS Model 1 in H-T normalized load space

4.3.3 Failure envelopes in V-H load space

Vertical and horizontal bearing capacities determined from PLAXIS 3D can be shown below in Table 4.5 for the example of Model 2.

					T/V=0			T/V=0.2			T/V=0,4			T/V=0,8		
Parameters		unit	V	H/V	Mstage	V	H	Mstage	V	H	Mstage	V	H	Mstage	V	H
A=	189	m2	10000	0	0,746	7460	0	0,743	7430	0	0,73	7300	0	0,672	6720	0
B=	9	m2	10000	0,1	0,646	6460	646	0,642	6420	642	0,629	6290	629	0,58	5800	580
Suo=	5,25	kPa	10000	0,2	0,387	3870	774	0,387	3870	774	0,386	3860	772	0,378	3780	756
Hult=	780	kN	10000	0,4	0,195	1950	780	0,195	1950	780	0,195	1950	780	0,194	1940	776
Vult=	7460	kN	10000	0,8	0,096	960	768	0,096	960	768	0,096	960	768	0,095	950	760
Tult=	14080	kNm	10000	1,6	0,046	460	736	0,046	460	736	0,046	460	736	0,046	460	736

Table 4.5: Data analyses for determinations of failure envelopes of Model 1 in V-H load space

Failure envelopes for PLAXIS Model 1 are illustrated in V-H normal load space, dimensionless load space, and normalized load space, respectively. See Fig.4.12 to Fig.4.14.

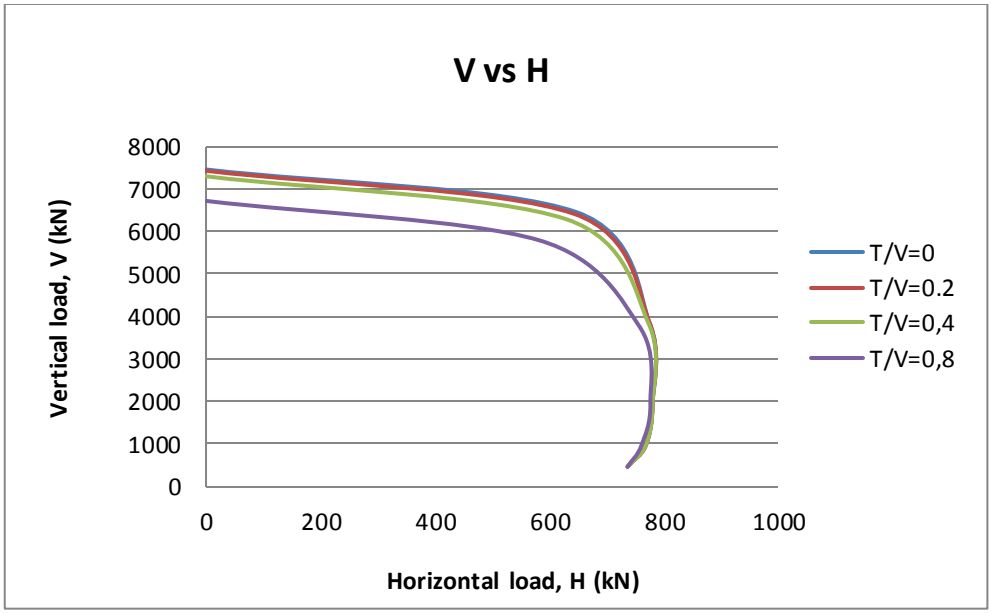

Figure 4.12: Failure envelope of PLAXIS Model 1 in V-H load space

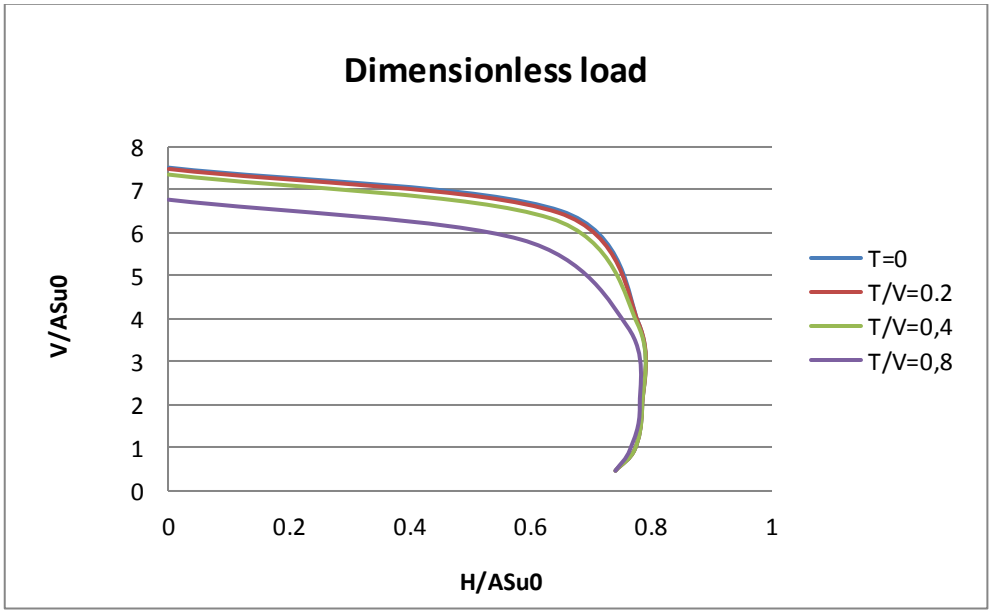

Figure 4.13: Failure envelope of PLAXIS Model 1 in H-T dimensionless load space

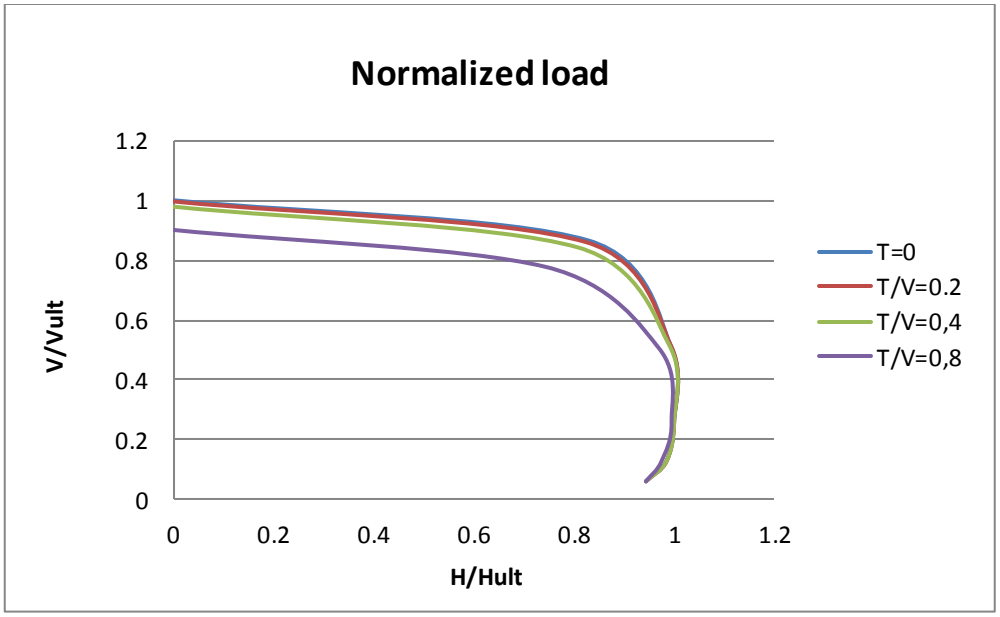

Figure 4.14: Failure envelope of PLAXIS Model 1 in H-T normalized load space

4.4 Comparisons of hand calculations and PLAXIS 3D

4.4.1 Ultimate bearing capacities: V_{ult}, H_{ult}, T_{ult}

The plots of M_{stage} vs displacement(M_{stage} vs u_z) and vertical load vs displacement(V vs u_z) of PLAXIS 3D Model 2 are shown in Fig. 4.15 and Fig.4.16.

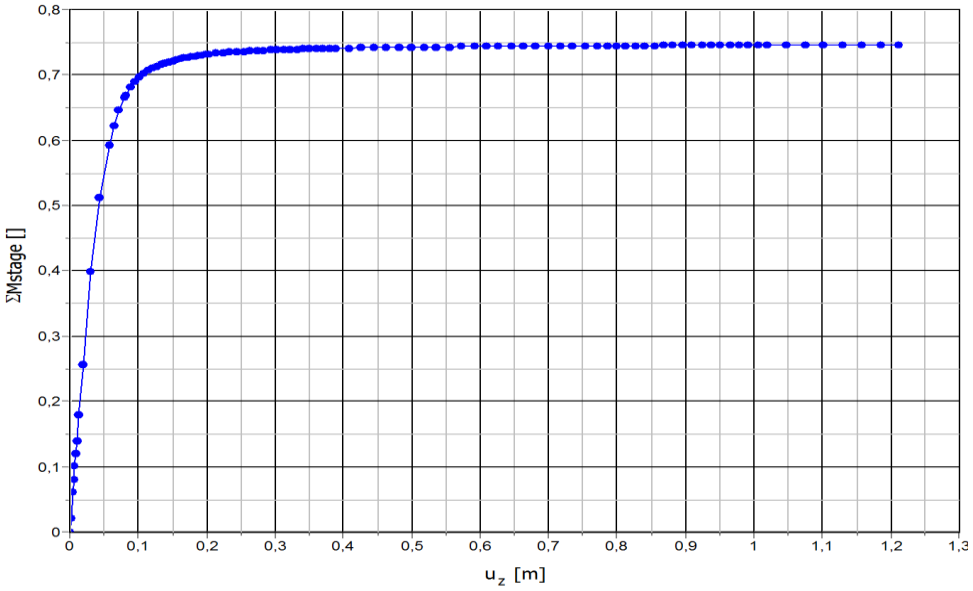

Figure 4.15: Mstage vs vertical displacement, PLAXIS 3D Model 2

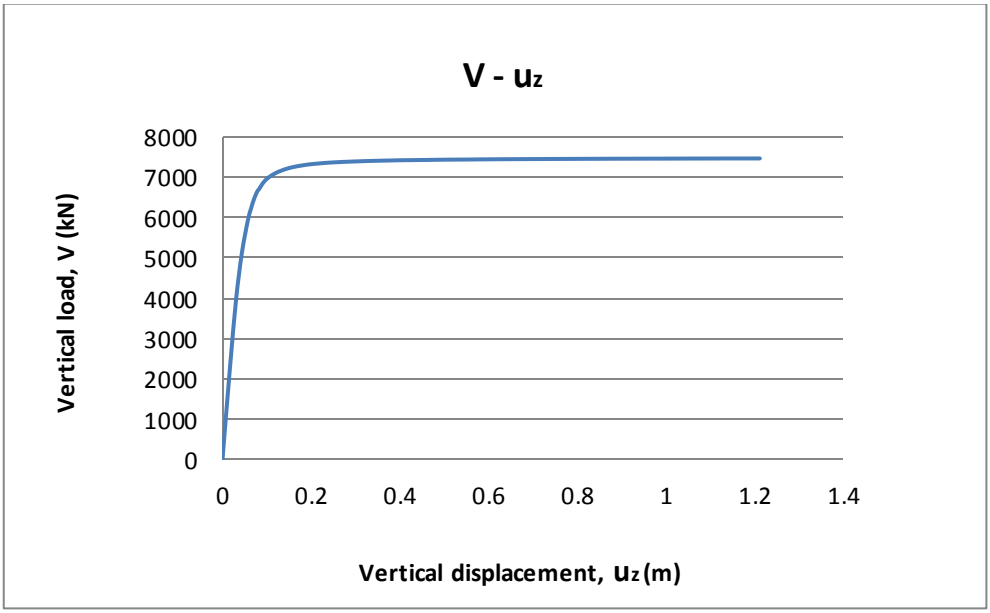

Figure 4.16: Vertical load vs vertical displacement, PLAXIS 3D Model 2

Final results show that: ultimate vertical bearing capacity obtained from Janbu method, Davis & Booker method, as well as finite element method utilizing PLAXIS 3D varies not significantly.

The results are shown in Table 4.2, and plots are illustrated in Fig.4.2.

#	Method		V_{ult} (kN)	H_{ult} (kN)	T_{ult} (kNm)
1	Janbu		7379	670	3515
2	Davis & Booker		8875		3955
3	PLAXIS 3D	Model 1: Medium, no inner skirts	7840	724	7500
4		Model 2: Fine, no inner skirts	7460	670	6890
5		Model 3: Fine, with inner skirts	7410	1014	8430

Table 4.6: Ultimate bearing capacities V_{ult}, H_{ult} and T_{ult} derived from different methods

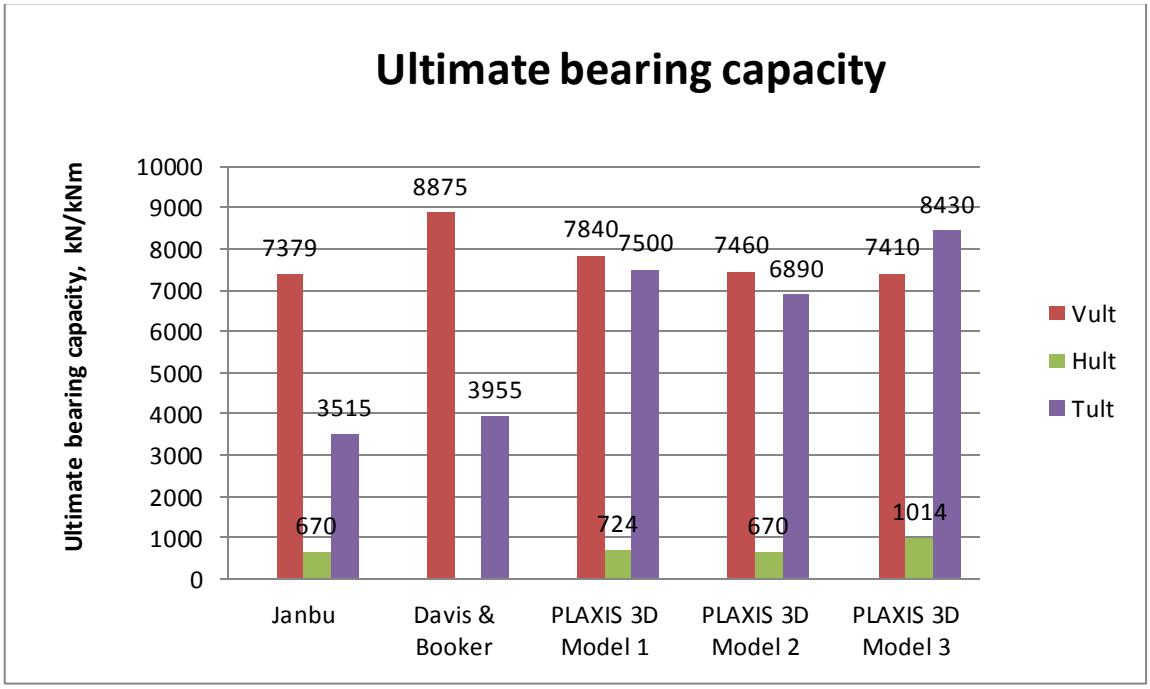

Figure 4.17: Comparison of ultimate bearing capacity Vult, Hult and Tult from different methods

4.4.2 Failure envelopes in V-T load space

Failure envelopes computed by hand calculations and PLAXIS 3D for the foundation subjected to vertical load V and torsion moment T are illustrated in normal load space (V–T), dimensionless load space (V/ASu0 – T/ABSu0) and normalized load space (V/Vult – T/Tult), respectively. See Fig.4.18 to Fig. 4.20.

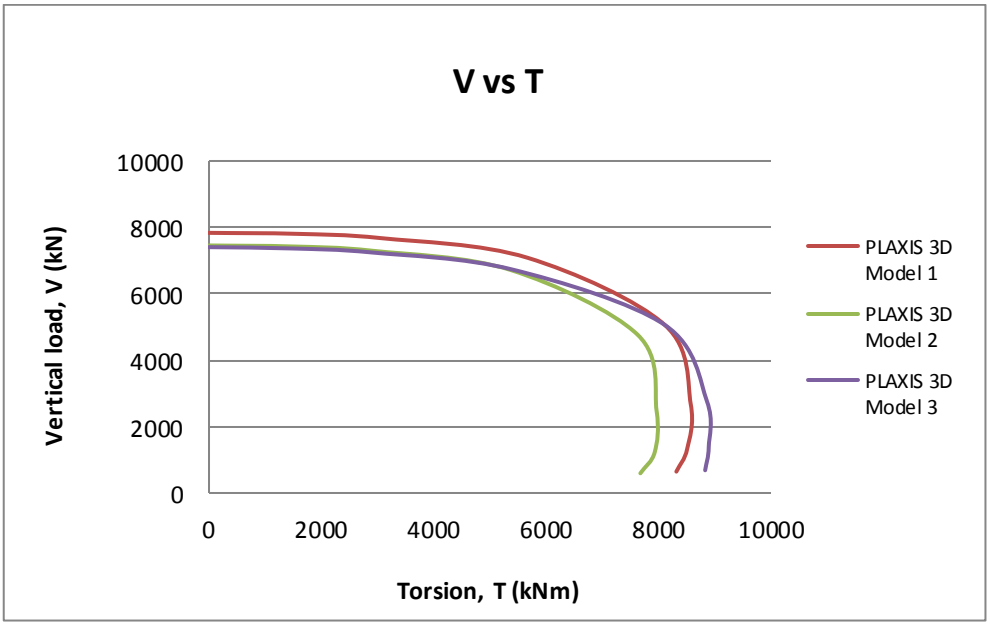

Figure 4.18: Comparison of hand calculation and PLAXIS 3D in V-T normal load space

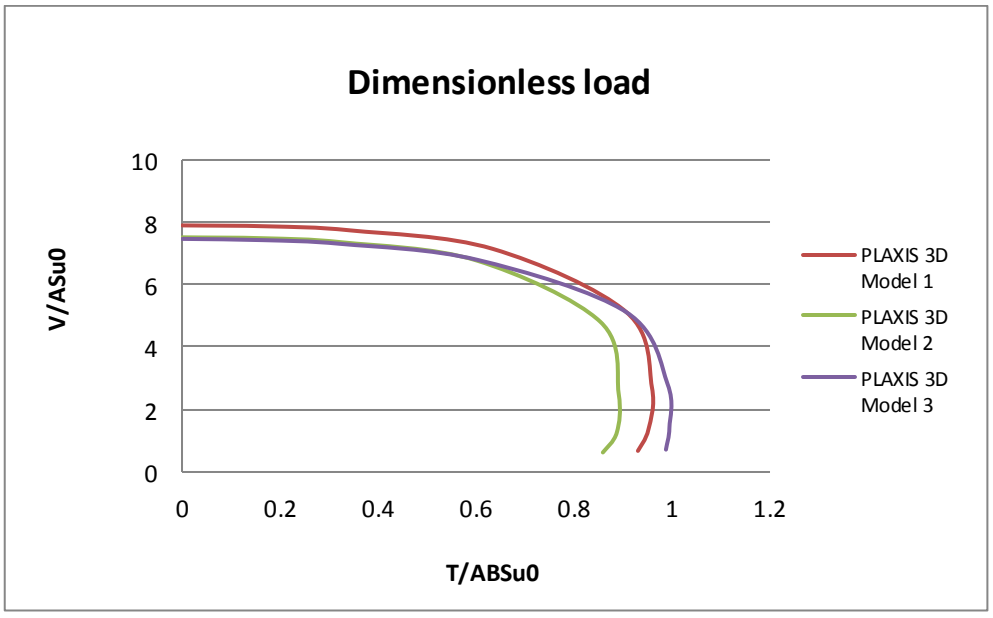

Figure 4.19: Comparison of hand calculation and PLAXIS 3D in V-T dimensionless load space

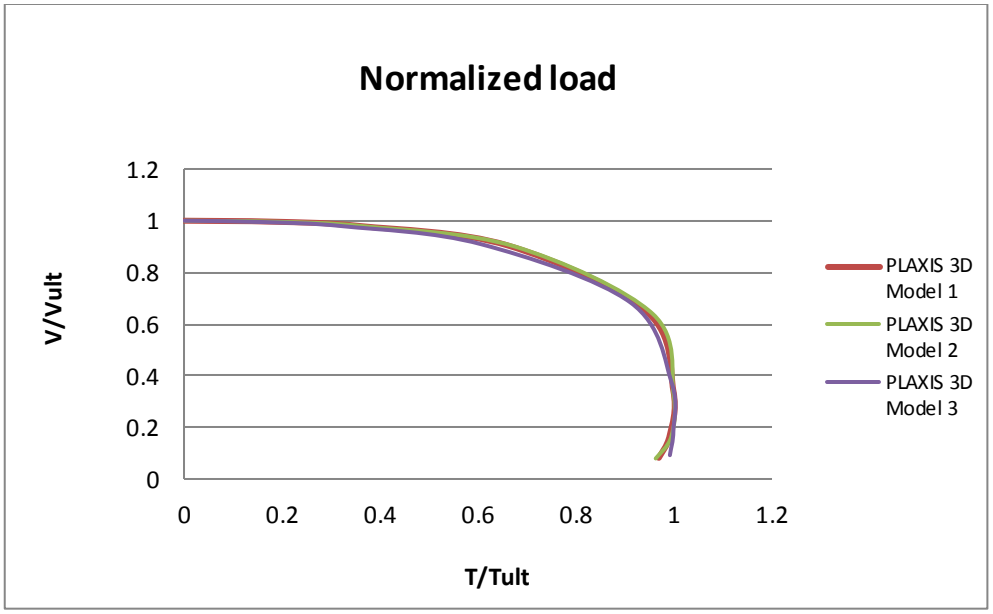

Figure 4.20: Comparison of hand calculation and PLAXIS 3D in V-T normalized load space

4.4.3 Failure envelopes in H-T load space

Failure envelopes obtained from Janbu method and PLAXIS 3D when subjected to horizontal load H and torsion moment T are illustrated in dimensionless load space (H/ASu0 – T/ABSu0) and normalized load space (H/Hult – T/Tult), repectively. See Fig.4.21 to Fig.4.23.

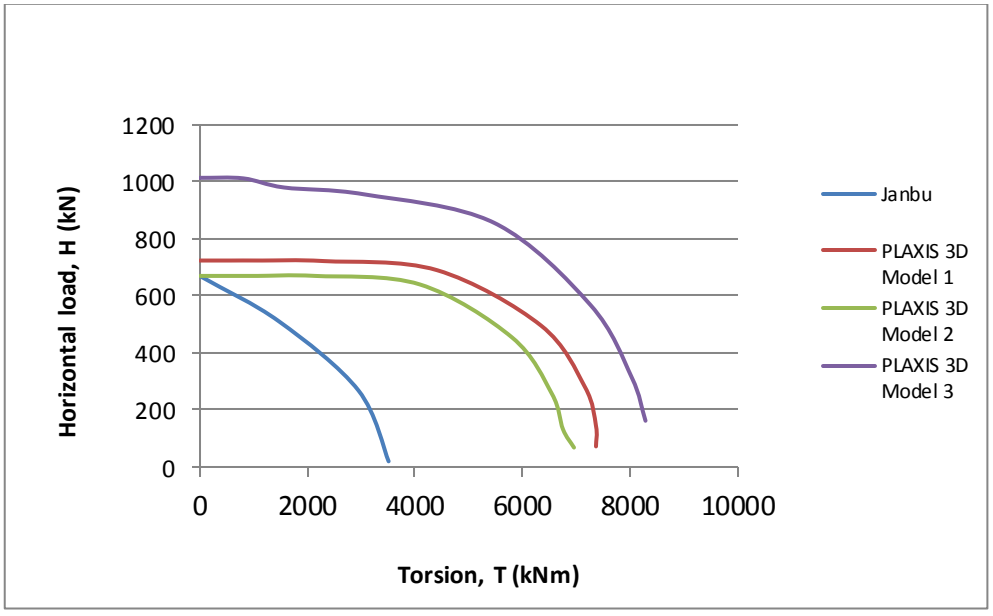

Figure 4.21: Comparison of Janbu and PLAXIS 3D in H-T load space

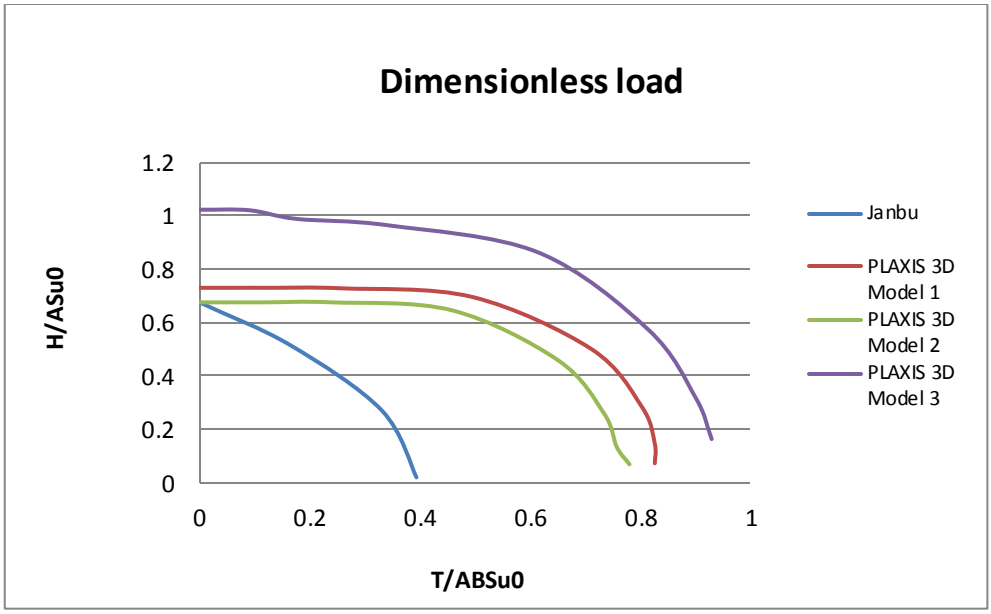

Figure 4.22: Comparison of hand calculation and PLAXIS 3D in H-T dimensionless load space

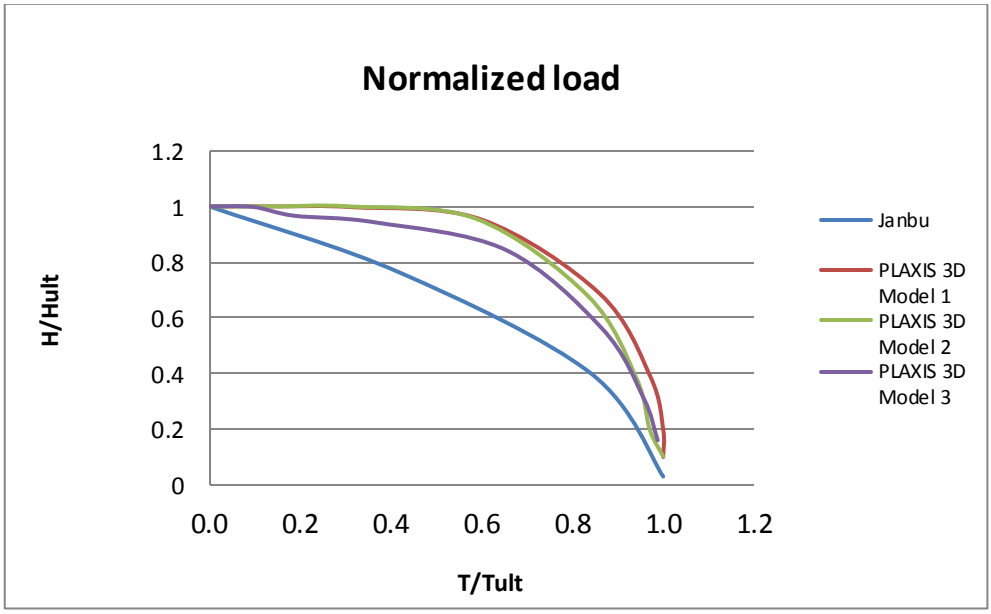

Figure 4.23: Comparison of hand calculation and PLAXIS 3D in H-T normalized load space

4.4.4 Failure envelopes in V-H load space

- Torsion moment T=0

When torsion moment is T=0: failure envelopes determined by Janbu and D&B method captures some of the failure envelopes from finite element results. The results are shown in Table 4.7, and the plot is illustrated in Fig.4.24.

Janbu		PLAXIS 3D					
		Model 1		Model 2		Model 3	
V	H	V	H	V	H	V	H
8146,2	776,4	7840	0	7460	0	7410	0
8036,7	892,4	6810	681	6460	646	6880	688
7909,5	1006,9	4120	824	3870	774	5360	1072
7760,9	1119,0	2080	832	1950	780	2950	1180
7487,2	1280,1	1030	824	960	768	1460	1168
7378,8	1330,8	500	800	460	736	710	1136
7128,2	1425,4						
6818,5	1505,7						
6419,8	1561,2						
5863,2	1566,1						

Table 4.7: Ultimate bearing capacity V_{ult} and H_{ult} derived from different methods

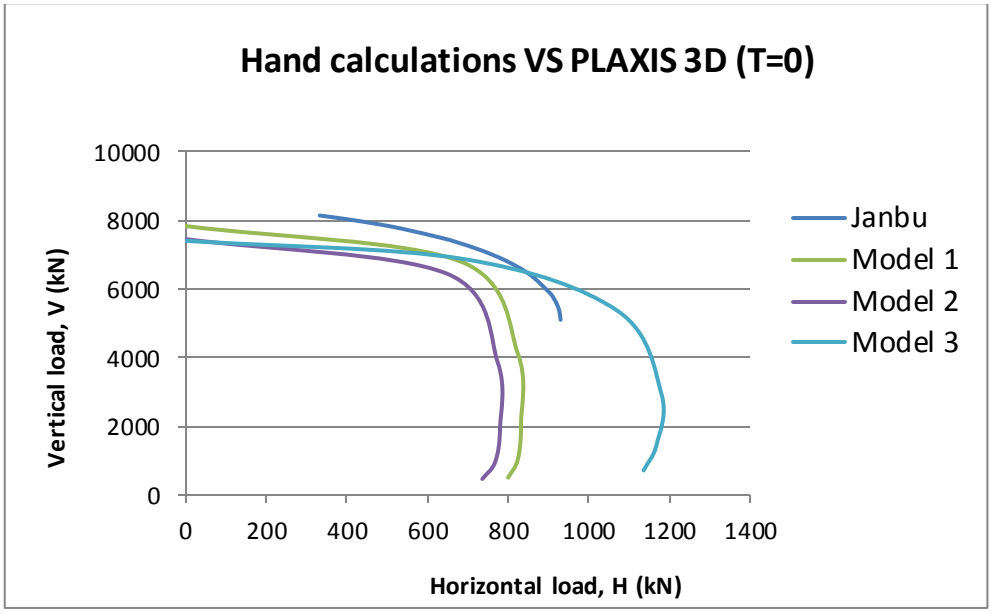

Figure 4.24: Comparison of failure envelopes on V-H space from different methods

- Torsion moment T/V=0, 0.2, 0.4, 0.8

Failure envelopes in the V-H loading space for the foundation subjected to different torsion moments determined by Janbu method and PLAXIS 3D models are shown in Fig.4.25 and Fig.4.26 below for medium meshes model and fine meshes model respectively. It can be observed that the failure envelopes in the V-H loading space are decreasing with the increase of torsion moments.

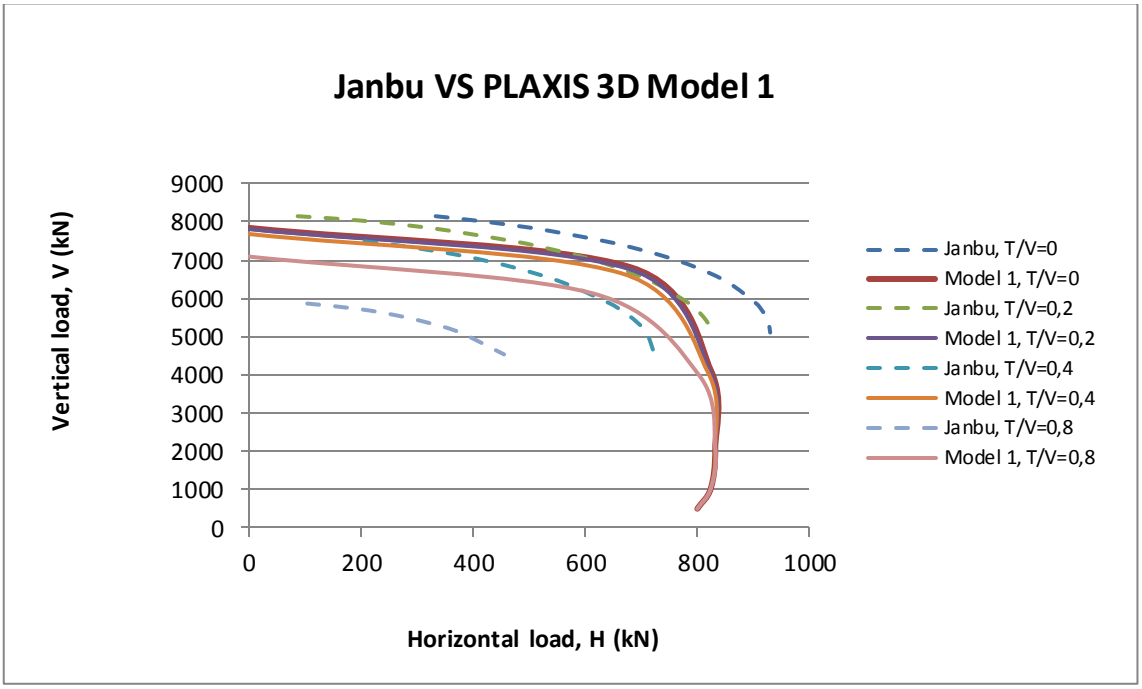

Figure 4.25: Comparison of failure envelopes by Janbu method and PLAXIS 3D Model 1

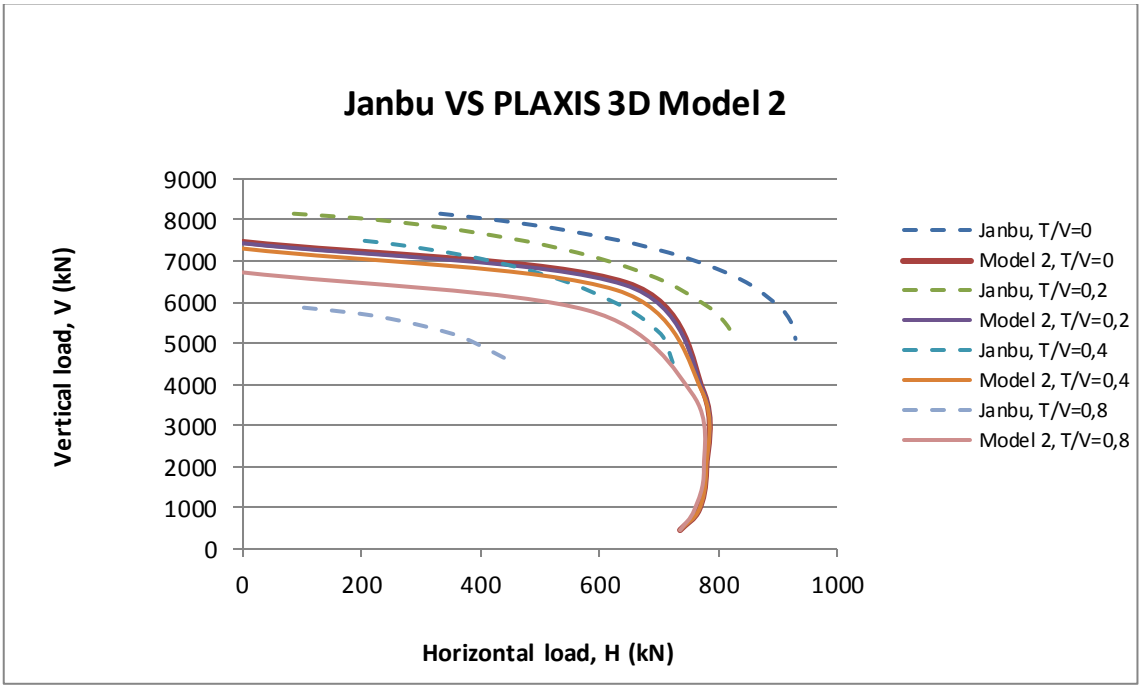

Figure 4.26: Comparison of failure envelopes by Janbu method and PLAXIS 3D Model 2

4.5 Approximating expressions for prediction of ultimate limit states

As shown in previous figures such as Fig.4.22, two-dimensional slices through a three-dimensional envelope illustrate how the foundation capacity varies with interaction of the different load components, and permit direct determination of ultimate limit states under general loading. For routine use it is convenient if the form of the interaction diagram can be defined explicitly. The complex shape of failure envelopes for general loading conditions is not conducive to an interpolating expression, and the dependence of the VHT interaction on foundation geometry and soil strength profile makes the nature of finding an approximating expression all the more challenging.

Approximating expressions to describe VHM failure envelopes for shallow foundations with bonding on the foundation/soil interface have been proposed in the past (e.g. Bransby & Randolph, 1998). A simplifying transformation based on an upper-bound solution from limited plane strain finite element analyses was proposed by Bransby & Randolph(1998), and the expression was derived for a surface strip foundation and a soil with a shear strength profile linearly increasing with depth given by κ=6. See Equation (4.1)

$$f = \left(\frac{V}{V_{ult}}\right)^{2.5} - \left(1 - \frac{H}{H_{ult}}\right)^{\frac{1}{3}}\left(1 - \frac{M^*}{M_{ult}}\right) + \frac{1}{2}\left(\frac{M^*}{M_{ult}}\right)\left(\frac{H}{H_{ult}}\right)^5 = 0 \qquad (4.1)$$

Where, V_{ult}, H_{ult} and M_{ult} are the capacities under pure vertical, horizontal and moment load respectively, and M^* is a modified moment parameter given by the expression:

$$\frac{M^*}{AD\,S_{u0}} = \frac{M}{AD\,S_{u0}} - \frac{L}{D}\frac{H}{AS_{u0}} \qquad (4.2)$$

Where, L is the height above the foundation of the center of rotation of the scoop mechanism governing ultimate moment capacity, M_{ult}.

To describe the VHT failure envelopes for this mudmat foundation, an approximating expression similar to Equation (4.2) is introduced as shown in Equation (4.3).

$$\left(\frac{H}{H_{ult}+110}\right)^a + \left(\frac{V}{V_{ult}}\right)^b + \left(\frac{T}{T_{ult}}\right)^c = 1 \qquad (4.3)$$

Where, V_{ult}, H_{ult} and T_{ult} are the capacities under pure vertical, horizontal and torsion load respectively.

Different trials of the parameters a, b, c were undertaken to find out the most approximating values for Equation (4.3). The method is that: by comparing the V-H plots from PLAXIS Model 1 and from Equation (4.4) shown below, the most approximating values of a, b, and c of the expression is determined.

$$H = (H_{ult} + 110) * \left[1 - \left(\frac{V}{V_{ult}}\right)^b - \left(\frac{\alpha V}{T_{ult}}\right)^c\right]^{\frac{1}{a}} \qquad (4.4)$$

Determinations of parameters a, b and c for the elipse type relation of V-H-T are illustrated below.

- For PLAXIS Model 1

The comparing V-H plots determined from PLAXIS Model 1 and Equation (4.4) by parameters in Table 4.8 are illustrated in Fig.4.27.

a	4	H_{ult}	724 kN
b	5	V_{ult}	7840 kN
c	2.5	T_{ult}	7500 kNm

Table 4.8: Parameters a, b, c and ultimate bearing capacities determined from PLAXIS Model 1

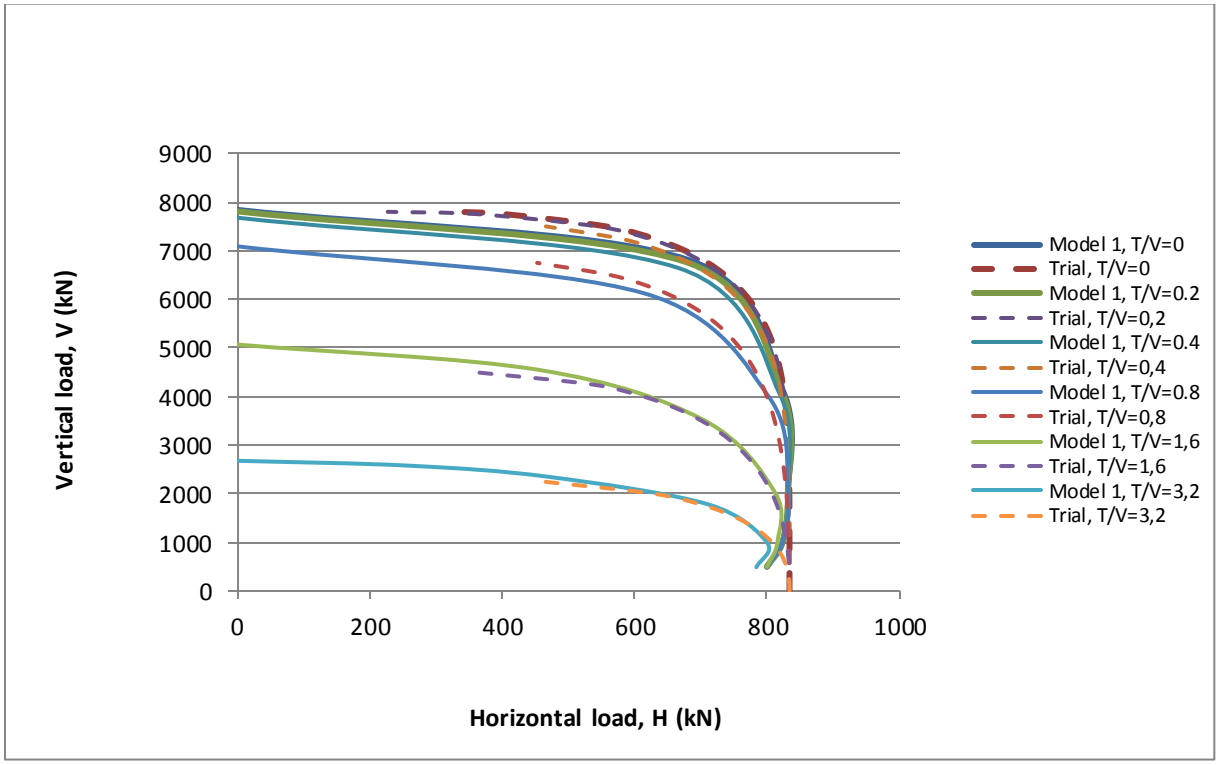

Figure 4.27: Determination of approximating expression by PLAXIS Model 1

- For PLAXIS Model 2

The comparing V-H plots determined from PLAXIS Model 2 and Equation (4.4) by parameters in Table 4.9 are illustrated in Fig.4.28.

a	4	H_{ult}	670 kN
b	5	V_{ult}	7460 kN
c	2.5	T_{ult}	6890 kNm

Table 4.9: Parameters a, b, c and ultimate bearing capacities determined from PLAXIS Model 2

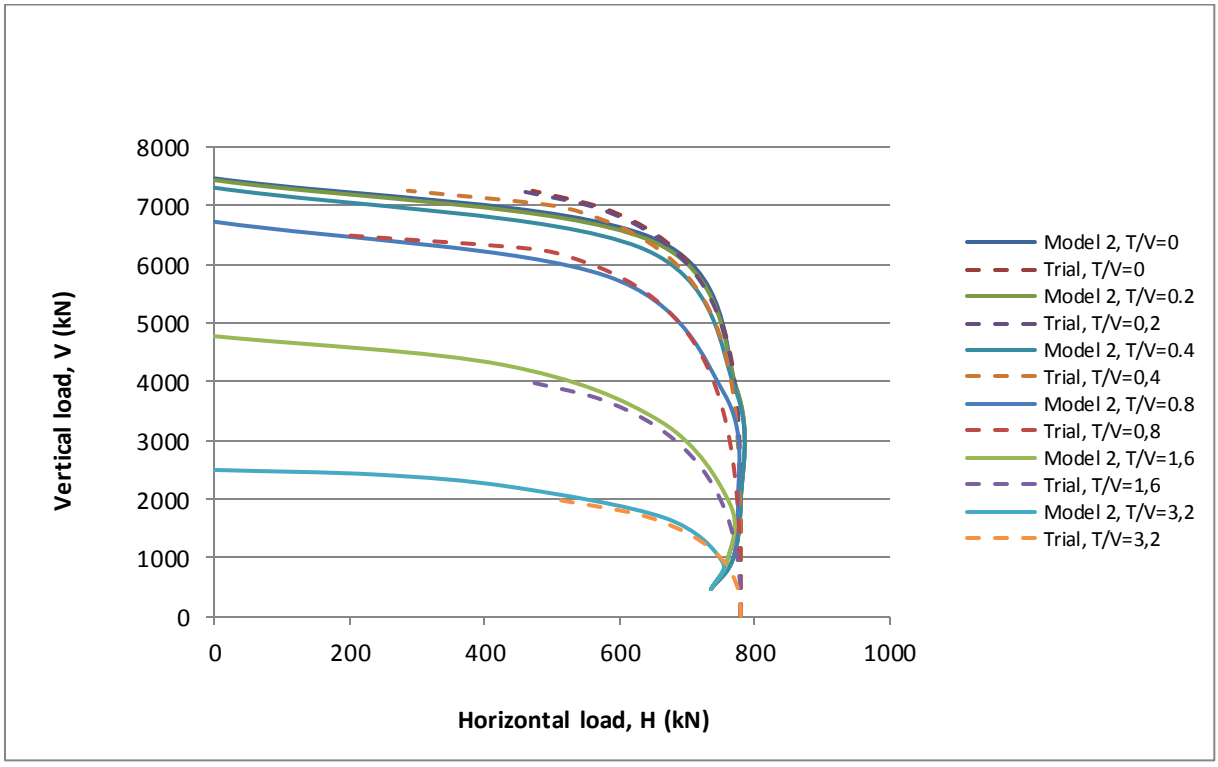

Figure 4.28: Determination of approximating expression by PLAXIS Model 2

Approximating values of parameters a, b and c for Equation (4.3) could be: a=4, b=5, c=2.5. Therefore, an approximating expression for the prediction of ultimate limit states could be:

$$\left(\frac{H}{H_{ult}+110}\right)^4+\left(\frac{V}{V_{ult}}\right)^5+\left(\frac{T}{T_{ult}}\right)^{2.5}=1 \qquad (4.5)$$

Chapter 5 DISCUSSIONS

5.1 Vertical load and failure mechanism

Fig.5.1 illustrated the vertical bearing capacities of mudmat foundation determined from hand calculations and PLAXIS 3D models.

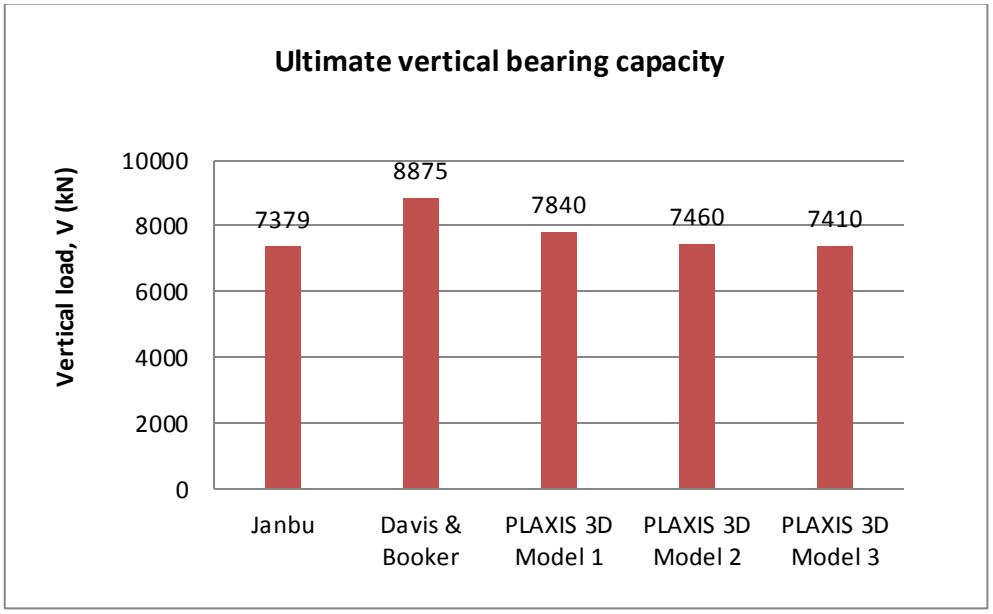

Figure 5.1: Vertical bearing capacities

Some conclusions can be summarized by the following points.

- PLAXIS 3D programs consistently provides higher capacity than Janbu method. Model 1 with medium element networks gives a relatively higher value than Model 2 with fine element networks.
- It may also be noted that Davis & Booker method provides much higher capacity than Janbu method and PLAXIS 3D program.
- The 1*2 inner skirts did not increase the vertical bearing capacity as we expected, in the opposite, the vertical bearing capacity was slightly reduced by 0,7%.

These conclusions remind us that: the user should be aware of the problem, taking into account the finite element program can provide some unonservative result. It is also clear that an even finer element network would have lower capacity. Janbu method basically provides solution for 2 dimensional cutting shape, but taking into account the 3D effect by multiplying the capacity factor with an area factor. However, PLAXIS generated a full 3 dimensional shear failure. This may also be used to explain why the PLAXIS provides higher capacity.

Fig.5.2 to Fig.5.5 illustrate the failure mechanism and stress distribution of the soil surrounding the mudmat foundation skirt tips and baseplate along the length, for Model 2 without inner skirts.

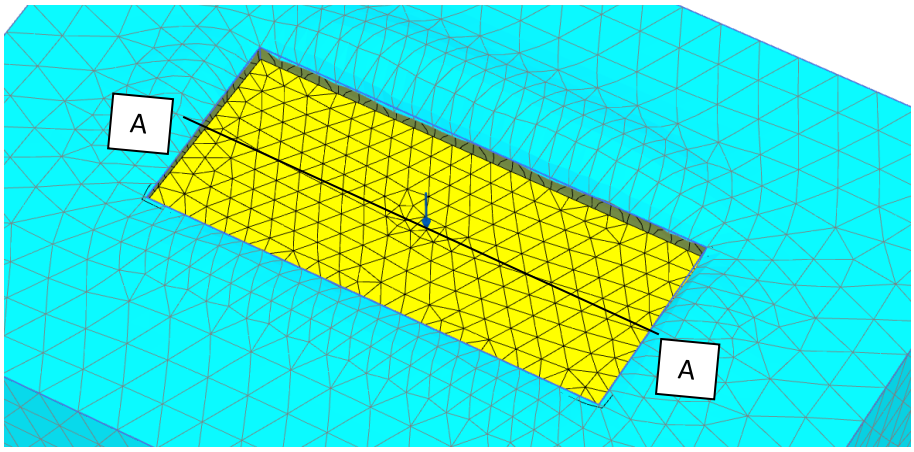

Figure 5.2: Deformed mesh due to ultimate vertical load V_{ult}

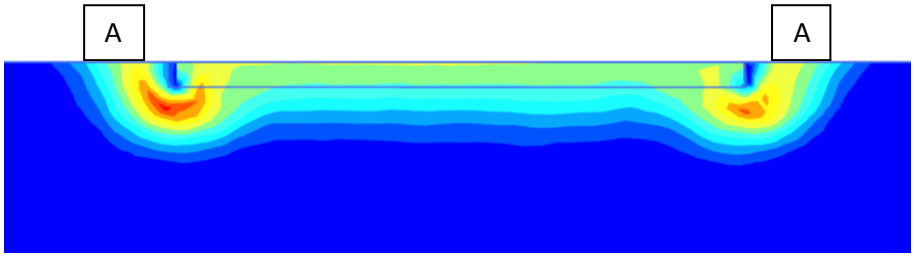

Figure 5.3: Total displacement under V_{ult} illustrated with shadings of A-A cross section

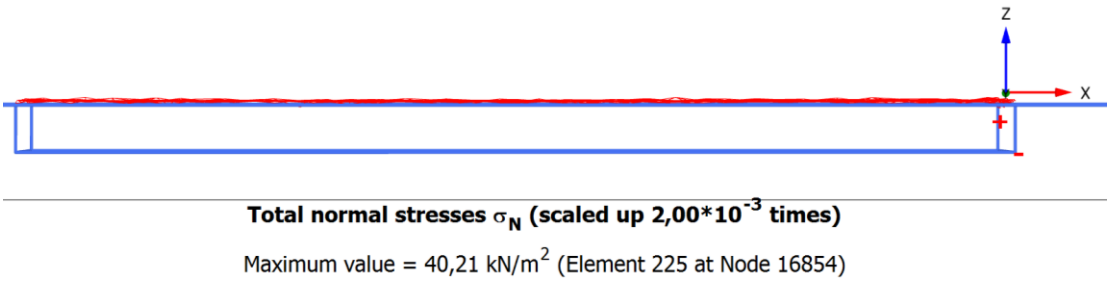

Figure 5.4: Total normal stresses, subjected to pure vertical loading

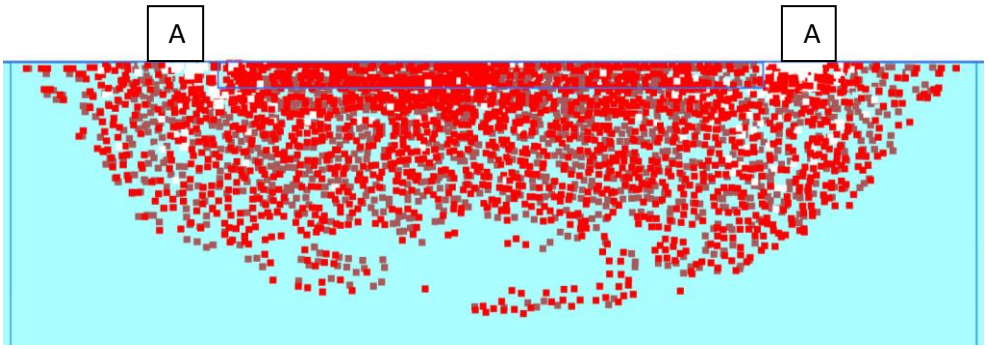

Figure 5.5: Plastic points of A-A cross section in PLAXIS 3D Model 2

5.2 Horizontal load and failure mechanism

Fig.5.6 illustrated the horizontal bearing capacities of mudmat foundation determined from hand calculations and PLAXIS 3D models.

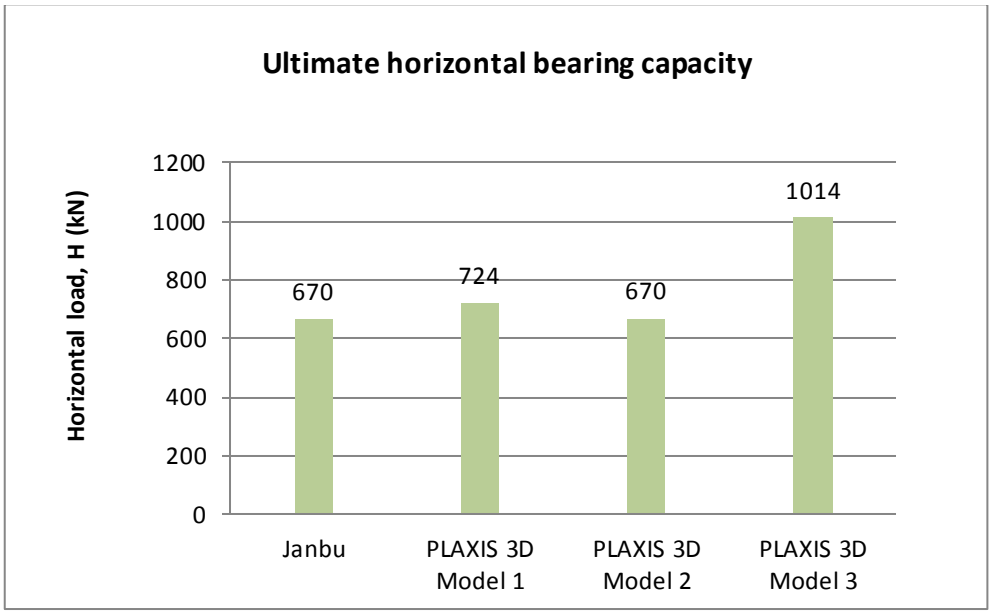

Figure 5.6: Horizontal bearing capacities

Some conclusions can be summarized by the following points.

- Again, PLAXIS 3D analyses with coarse element networks provide higher capacity than the analysis of fine element networks. The explanation for this is shown in Section 5.1.
- The 1*2 inner skirts increase the horizontal bearing capacity significantly by more than 50 percent.
- Comparing with the finite element program PLAXIS 3D, the traditional formulas derived by Janbu method give a slightly lower capacity.

This could be interpreted by that: PLAXIS 3D takes into account all affections, while the other methods give a more conservative result. It is therefore appropriate to create a composite bearing capacity formula that takes into account everything. So the results from PLAXIS 3D can be verified.

Fig.5.7 to Fig.5.10 illustrate the failure mechanism of the soil surrounding the mudmat foundation skirt tips and baseplate along the length, for Model 2 without inner skirts.

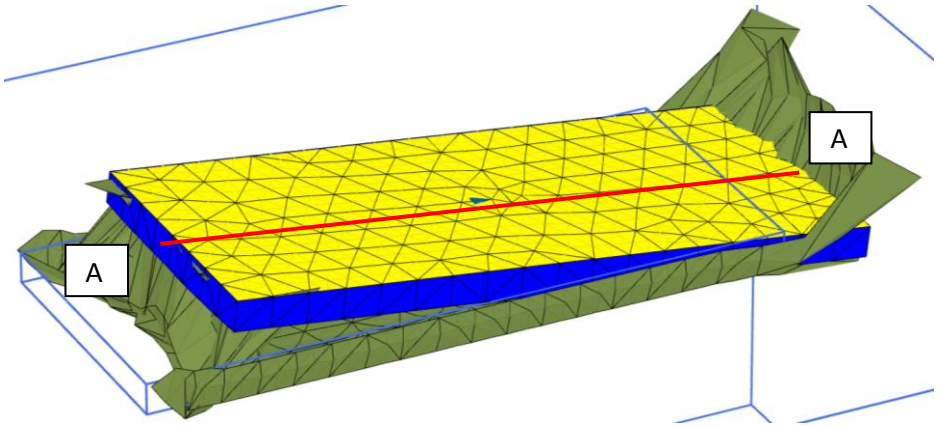

Figure 5.7: Deformed mesh due to ultimate vertical load H_{ult}

Figure 5.8: Total displacement under H_{ult} illustrated with shadings of A-A cross section

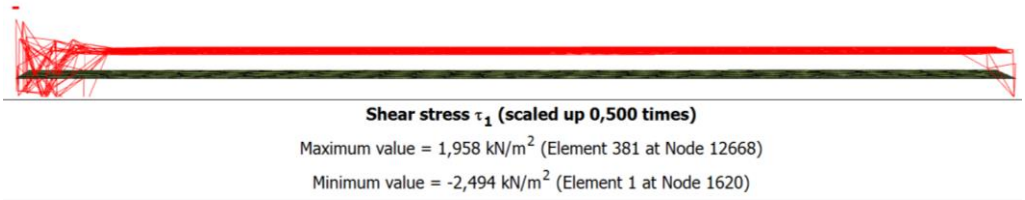

Figure 5.9: Shear stress between base plate and soil compartment

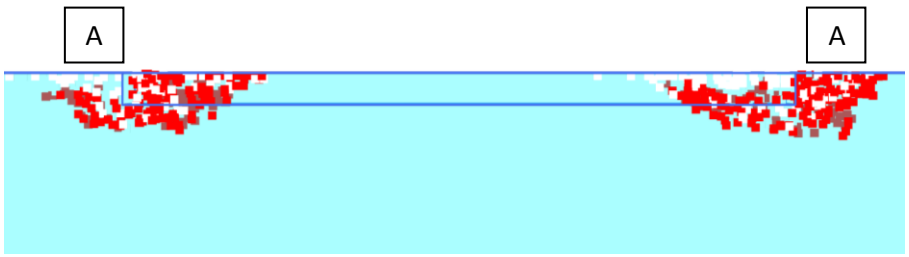

Figure 5.10: Plastic points of A-A cross section in PLAXIS 3D Model 2

5.3 Torsion moment and failure mechanism

The torsional bearing capacity determined from PLAXIS 3D does not correspond well with that from hand calculations. A large difference showed up, which is not as we expected. See Fig.5.11.

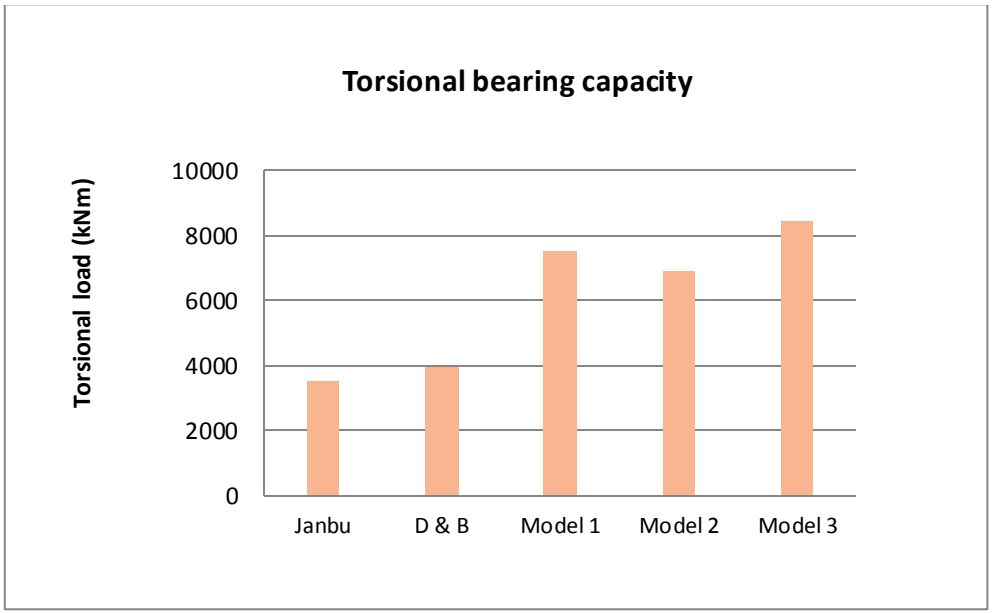

Figure 5.11: Torsional bearing capacities

The reasons could be that:

- Janbu and D&B methods only consider the plain strain, without taking into account the 3D affections, and this may result in very conservative results.
- Besides, there could be some parametric errors in the PLAXIS 3D models, which may result in the results shown above.

The analyses in PLAXIS 3D clearly show that torsion reduces significantly the vertical bearing capacity, but slightly reduces the horizontal bearing capacity. This is illustrated in Fig.5.12 for the comparisons of two capacity curves for load combinations with and without torsion.

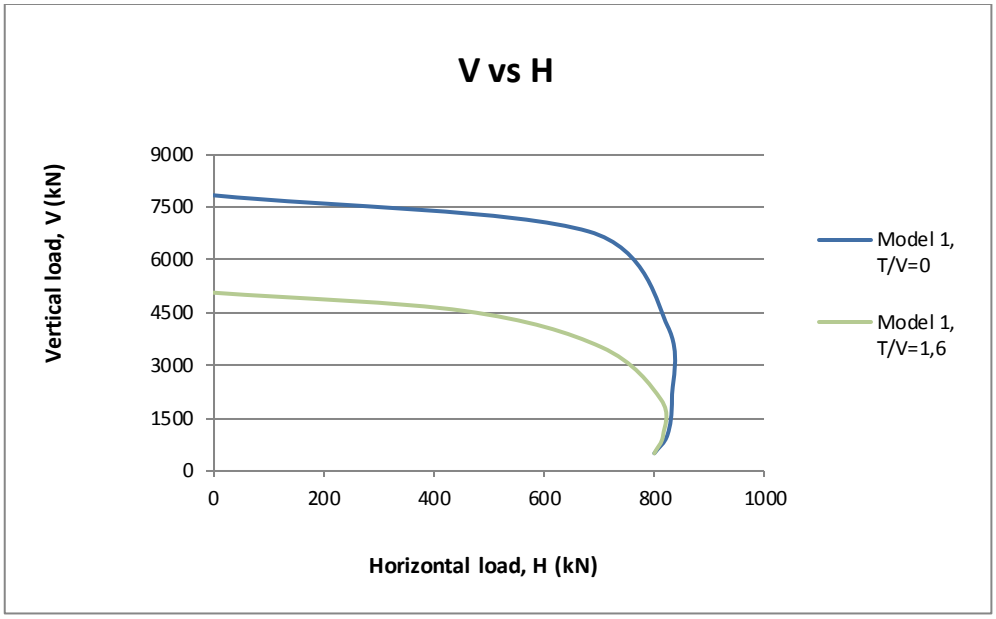

Figure 5.12: V-H capacity curves with and without torsions

The vertical bearing capacity is significantly reduced when the shear stresses due to torsion and horizontal load ($\tau_{tot}=\tau_t+\tau_h$) exceed the shear capacity, this was discussed previously in Chapter 2.

A horizontal cross section at skirt tips (D=1m) from PLAXIS 3D analyses when subjected to pure torsion showed that:

- Soil elements at skirt tips close to the corners are more easily mobilized, thus corner areas of mudmat foundation seems more vulnerable to generate failure surface when subjected to pure torsions;
- Soil elements in the central area of mudmat foundation are not mobilized obviously, which means the torsions do not have large affections in the central areas of mudmat foundation when subjected to pure torsions;

The failure mechanism illustrated by total displacements of horizontal cross section at skirt tips are shown below in Fig.5.13.

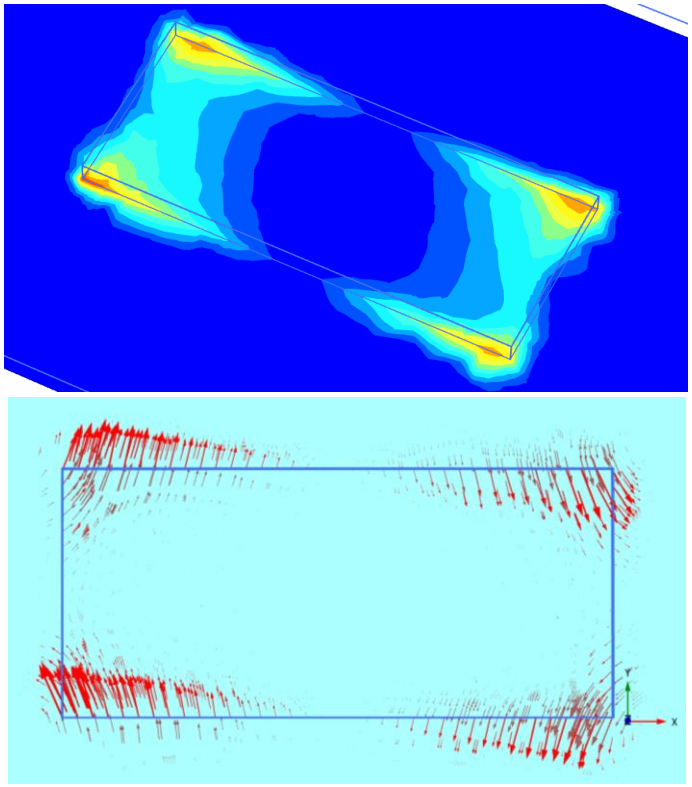

Figure 5.13: Total displacements of horizontal cross section at skirt tips in shadings and arrows

When mudmat foundation is subjected to vertical load and torsion together, with the increase of torsion, failure areas seem to move forward to the corners. This is illustrated by comparisons of figures below.

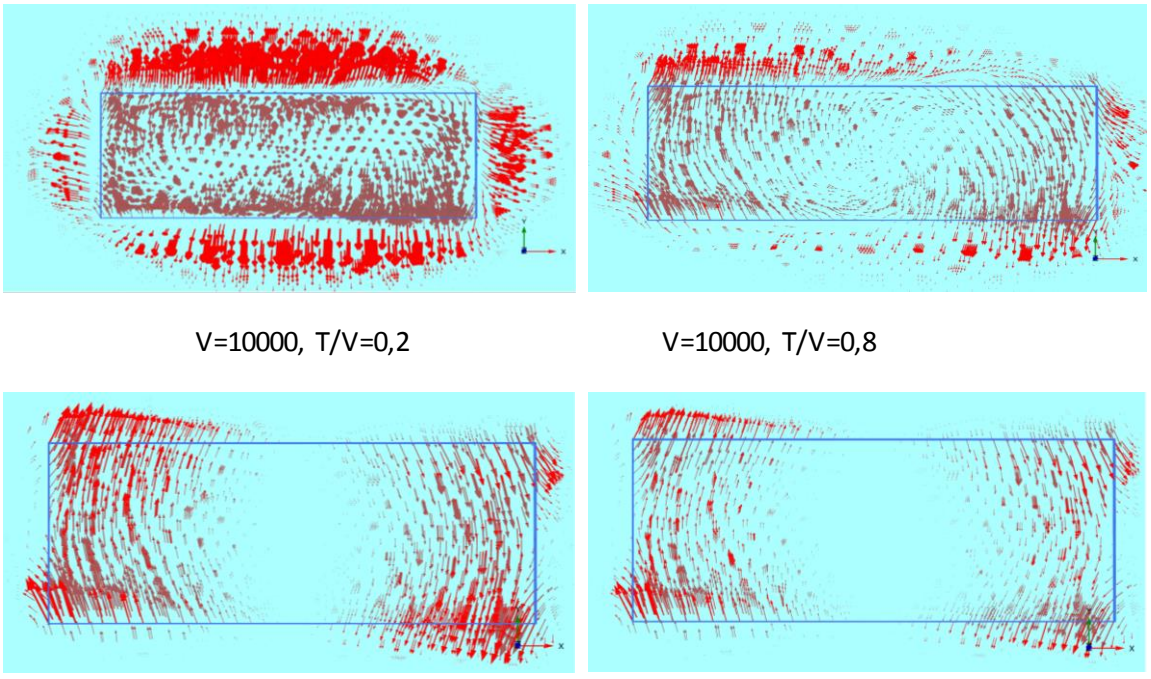

V=10000, T/V=0,2 V=10000, T/V=0,8

V=10000, T/V=3,2 V=10000, T/V=12,8

Figure 5.14: Horizontal cross sections, when subjected to constant V and increasing T

5.4 Inner skirts

Skirted foundations under combined loadings were numerically investigated, Bransby and Randolph (1999), Gourvenec (2003) etc. for clays with undrained constant shear strength S_u and varying shear strength S_u with depth. According to Gourvenec, negative excess pore pressures can develop within the soil plug during undrained uplift (owing to overturning or the buoyancy of a floating structure) that enables mobilization of reverse end bearing (Gourvenec, 2011). These features of mudmat foundations cause classical soil mechanical theories to underestimate the foundation capacities. Thus, the use of explicitly derived failure envelopes(see Chapter 4) would be an attractive alternative for design.

Mudmat foundations are often equipped with both outer and inner skirts, which will penetrate the seabed during installation confining a soil plug. The skirts could enhance additional bearing capacities for mudmat foundation, and this could be interpreted by the suction developed within the skirt when subjected to combined loadings.

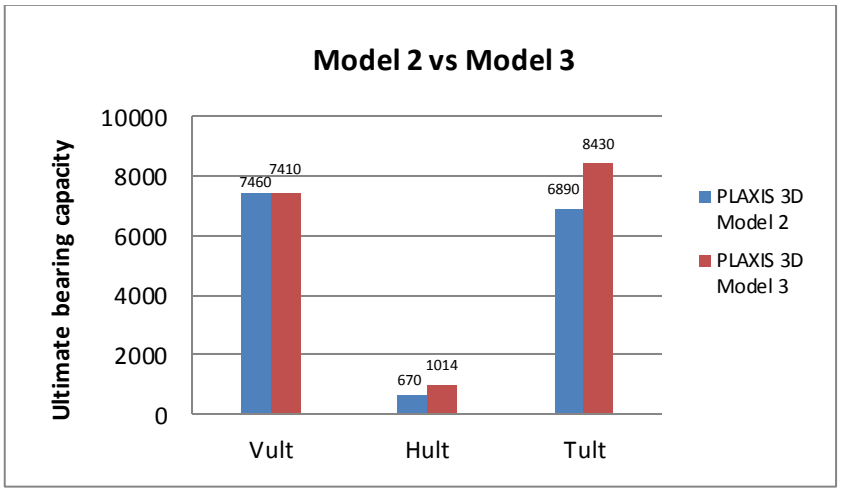

Figure 5.15: Comparisons of bearing capacities for mudmat with and without inner skirts

Some conclusions can be summarized by the following points:

- Vertical bearing capacity was not increased by inner skirts, to the opposite, it was slightly reduced. This may be due to the interface roughness R=0.5.
- Horizontal and torsion bearing capacity were significantly increased, corresponding to an increase of 51% and 22%, respectively.
- Therefore, inner skirts have significant affections on both horizontal and torsion bearing capacities.

The failure mechanism of mudmat foundations with inner skirts subjected pure horizontal loading are illustrated by Fig.5.16 and Fig.5.17.

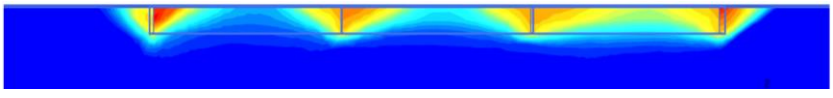

Figure 5.16: Vertical cross section of mudmat with inner skirts

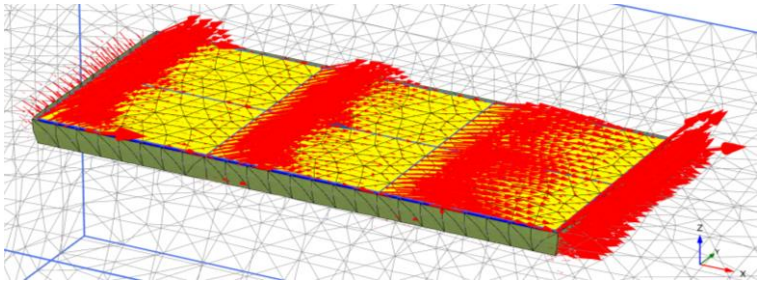

Figure 5.17: Total displacements of mudmat with inner skirts, horizontal loading

When subjected to pure torsion moment, the failure mechanism illustrated by total displacements of horizontal cross section at skirt tips are shown below in Fig.5.17 and Fig.5.18.

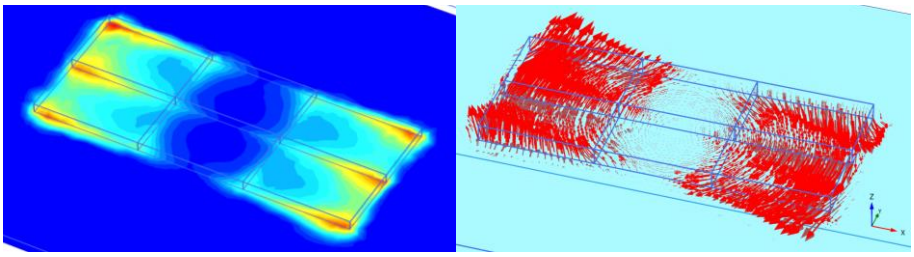

Figure 5.18: Total displacements of horizontal cross section at skirt tips

When mudmat foundation is subjected to horizontal load and torsion together, with the increase of torsion, horizontal displacement gradually becomes negligible while the rotational displacement becomes predominant. When shear stresses due to torsion and horizontal load ($\tau_{tot}=\tau_t+\tau_h$) exceed the shear capacity, total displacement changes slightly. This is illustrated by comparisons in Fig.5.19.

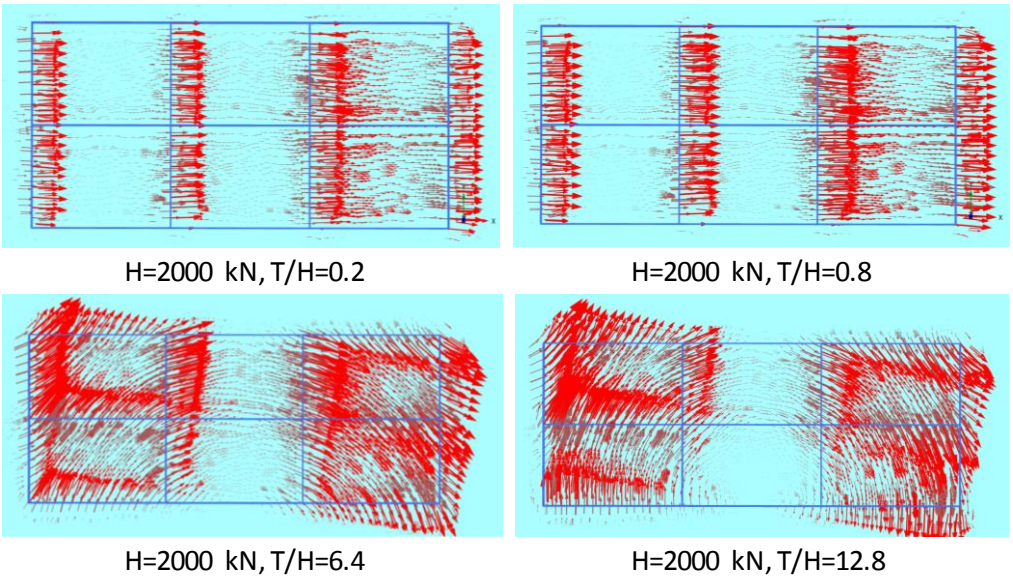

Figure 5.19: Horizontal cross sections, when subjected to constant H and increasing T

5.5 Suitability of simplified method accounting for torsion

Fig.4.25 and Fig.4.26 showed the failure envelopes on V-H space accounting for torsion moments determined from simplified method(Janbu method and DNV standard) and PLAXIS 3D.

By comparing these two plots, some points can be concluded:

- When torsion was relatively small(for example, T/V=0, and T/V=0.2), this simplified method did not give results that correspond well with PLAXIS 3D program. The PLAXIS 3D program gave little more conservative results.

- However, when torsion was relatively large (for example, T/V=0.8), the simplified method gave much more conservative results than PLAXIS 3D program.

- The failure envelopes given by PLAXIS 3D did not show many differences with the increase of torsion moments, i.e. the failure envelopes were very close.

- However, the failure envelopes given by simplified method seemed more divergent than those from PLAXIS 3D for combinations of T/V=0, 0.2, 0.4, and 0.8.

Chapter 6 CONCLUSIONS

This thesis aims at evaluating the bearing capacity of rectangular mudmat foundation subjected to combined loadings including vertical loading, horizontal loading and torsion moments, as well as comparing the results from finite element program PLAXIS 3D and Jan bu method.

Vertical and horizontal bearing capacities of mudmat foundation from finite element program PLAXIS 3D correspond well with the hand calculation results by Janbu method. However, the vertical bearing capacities from PLAXIS 3D are slightly higher than Janbu method, with a difference of 460kN(Model 1) and 80 kN(Model 2), corresponding to a difference of 6% and 1%, respectively. It may have several explanations:

- The results of finite element programs is dependent on network element and element type. Theoretically, the analyses of model with more fine meshes and smaller average element size would generate more accurate results.
- PLAXIS 3D builds a real 3-dimensional model, taking into consideration the 3D affections. However, Janbu method is based on the plane strain.

However, torsional bearing capacity from PLAXIS 3D is almost twice the value determined from hand calculations, which may because of the conservative calculation method or some possible parametric errors in PLAXIS 3D.

By intergrating the FEM analyses package PLAXIS 3D with the Swipe test procedure of loading, the failure envelopes of mudmat foundation and approximating expressions are investigated. Through numerical computations and comparative analyses based on FEM, the two-dimensional failure envelopes of mudmat foundation are established by using proposed method to evaluate the stability of foundation under combined loadings. These results could be utilized to provide vital reference for the design and construction of mudmat foundation.

By comparing the results from PLAXIS 3D with those from simplified method accounting for torsion moments with Janbu method and DNV standard(see Fig.4.25 and Fig.4.26), some points can be concluded:

- When torsion was relatively small(for example, T/V=0, and T/V=0.2), this simplified method did not give results that correspond well with PLAXIS 3D program. The PLAXIS 3D program gave more conservative results.
- However, when torsion was relatively large (for example, T/V=0.8), the simplified method gave much more conservative results than PLAXIS 3D program.

Some man-made errors probably exist in the judgement of limit equilibrium states and ultimate capacities, due to some inaccuracies of FEM analyses.

Chapter 7 REFERENCE

Andersen. (2008). *Deep Water Geotechnical Engineering.* Oslo, Norway: NGI.

Andresen, L. (2004). *Erfaringer med bruk av elementmetoden for dimensjonering av avstivede byggegroper i leire.* NGI.

API. (1993). Recommended Practice for Planning, Designing, and Constructing Fixed Offshore Platforms - Load and Resistance Factor Design. US.

Athanasiu, C. (2006). *Samtale om fundament belastet av torsjonsmoment.* Trondheim.

Davis, B. (1973). *The effect of increasing strength with depth on the bearing capacity of clays.*

Detail Design Inc. (n.d.). Retrieved from http://www.detaildesigninc.com/

DNV. (2010). *Offshore Standard DNV-OS-J101.* Oslo.

DNV, A. G. (2010). *Offshore Standard DNV-OS-J101.* Oslo: DNV.

Emdal, A. G. (2011). *Theoretical Soil Mechanics in TBA4105.*

Firstsubsea. (2012). *Firstsubsea.com*. Retrieved from Firstsubsea.

Gourvenec. (2011). Undrained failure envelope for skirted foundations under general loading.

Gourvenec, S. (2007). *Failure envelopes for offshore shallow foundations under general loading.*

Janbu, N. (2010). *TBA 5100 Theoretical Soil Mechanics.* NTNU.

Mjølhus, G. (2006). *The effect of torsion moment and horizontal load on bearing capacity of foundations.* Trondheim.

PLAXIS. (2012). *Modelling soil-structure interaction: interfaces.*

PLAXIS 2D Reference, 2012. (n.d.).

PLAXIS 3D Reference, 2012. (n.d.).

Tan. (1990). *Centrifuge and theoretical modeling of conical footings on sand.*

Vegvesen, S. (1992). *Håndbok 016, Geoteknikk I vegbygging.* GCS A/S.

Vilod, E. (2009). *Mud mat design for steel jacket on-bottom stability.*

Wu Ke, M. M. (2011). *Study on the failure envelope of suction bucket foundation under torsion shear load.*

Chapter 8 APPENDIX

1. Hand calculations of bearing capacity with Janbu method

The model of mudmat foundation for hand calculations is shown below.

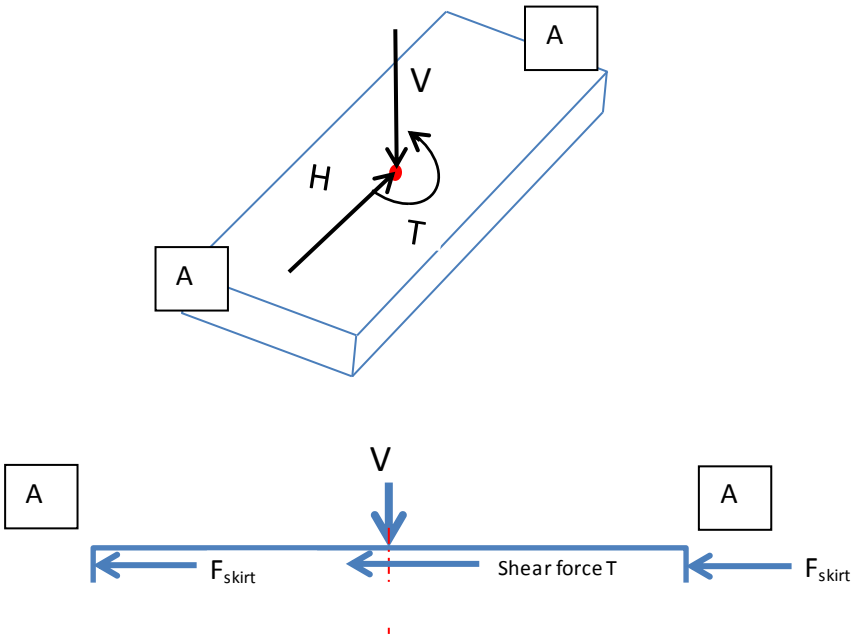

Figure 8.1: Simplified model of mudmat foundation for hand calculations

Find the shear and normal stress acting on both sides of the wall for undrained condition.

γ =15.5kN/m^3, r =0.5, B=9m, D=1m, p=15.5kPa

$$\omega = 0.5 \arcsin(r) = 0.262$$

$$z_r = \frac{B}{2(2-r)} \sin\left(\frac{\pi}{4} - \omega\right) + D = 2.5$$

Mean Su: S_u=2+1.3*D=5.25kPa, q=0

- Vertical bearing capacity:

ω=0.5arcsinr=0.262

N_c=1+π-2ω+cos2ω=4.484

q_v=$N_c S_u$+p=4.484*5.25+15.5=39kPa

V=q_v*A=39.04*189=**7379kN**

- Horizontal bearing capacity:

$p_P = q + \gamma z + \kappa S_u$, $p_A = q + \gamma z - \kappa S_u$, $\kappa = 2\sqrt{1 + \frac{2}{3}r}$ for 0<r<1.

For r =0,5, κ =2.31,

$p_{P,z=0}$ =0+0+2.31*5.25= 12.1kPa

$p_{P,z=1}$ =0+15.5*1+2.31*5.25=27.6kPa

$p_{A,z=0}$ =0+0-2.31*5.25= -12.1kPa

$p_{A,z=1}$ =0+15.5-2.31*5.25= 3.4kPa

Neglect tensile stresses in the calculation as they vanish with the first tension crack.

Depth of zero active earth pressure from the relationship ($p_{A,z=1}$ / $p_{A,z=0}$) = (1-z)/z yields now z= 0.78m. Passive and active earth pressure distribution along the skirt is seen in Fig.11.2.

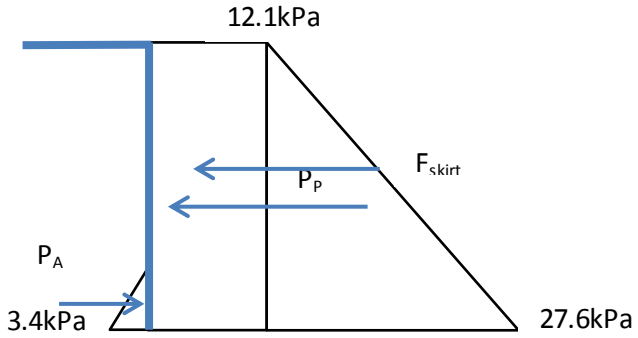

P_P = 0.5*1*(12.1+27.6)=19.85kN/m

P_A =0.5*3.4*(1-0.78)=0.37kN/m

Neglect active earth pressure, since it is close to 0 and is much smaller than passive earth pressure.

Horizontal load capacity of one skirt:

$F_{skirt} = P_P$ *DL = 19.85*1*9=178.65kN

Shear stress under base plate, at tip skirts:

$t_h = rS_{u0}$ =0.5*(2+1.3*1)=1.65kPa

Shear force of base plate:

$T = t_h A$= 1.65*189=312kN

Therefore, the horizontal load capacity can be determined by:

$H = 2F_{skirt} + T$ = 2*178.65+312= **670kN**

2. Hand calculations to determine failure envelopes

- Janbu method, V-H failure envelopes

r	ω	Nc	Zr	Mean Su	p	qv	th	th/qv	$2P_p$	V	H	V/ASu0	H/ASu0
0	0,000	5,142	2,591	5,37	15,5	43,1	0,00	0,00	332,76	8146	333	8,03	0,33
0,1	0,050	5,036	2,589	5,37	15,5	42,5	0,33	0,01	338,99	8037	401	7,93	0,40
0,2	0,101	4,920	2,581	5,36	15,5	41,8	0,66	0,02	344,75	7909	469	7,81	0,46
0,3	0,152	4,791	2,566	5,34	15,5	41,1	0,99	0,02	349,92	7761	537	7,70	0,53
0,45	0,233	4,568	2,522	5,28	15,5	39,6	1,49	0,04	356,19	7487	637	7,50	0,63
0,5	0,262	4,484	2,500	5,25	15,5	39,0	1,65	0,04	357,74	7379	670	7,44	0,66
0,6	0,322	4,298	2,437	5,17	15,5	37,7	1,98	0,05	359,67	7128	734	7,30	0,72
0,7	0,388	4,080	2,341	5,04	15,5	36,1	2,31	0,06	359,36	6818	796	7,15	0,78
0,8	0,464	3,814	2,186	4,84	15,5	34,0	2,64	0,08	355,33	6420	854	7,02	0,84
0,9	0,560	3,458	1,915	4,49	15,5	31,0	2,97	0,10	343,92	5863	905	6,91	0,89
0,92	0,584	3,365	1,833	4,38	15,5	30,3	3,04	0,10	339,93	5718	914	6,90	0,90
0,94	0,611	3,260	1,735	4,26	15,5	29,4	3,10	0,11	334,91	5552	921	6,90	0,91
0,96	0,644	3,135	1,612	4,10	15,5	28,3	3,17	0,11	328,31	5356	927	6,92	0,91
0,98	0,685	2,970	1,441	3,87	15,5	27,0	3,23	0,12	318,8	5104	930	6,97	0,92
1	0,785	2,571	1,000	3,30	15,5	24,0	3,30	0,14	292,87	4533	917	7,27	0,90

- Davis & Booker method, V-T failure envelopes

T	τ	r	ω	F	Nc	ρB/4	Su,z=D	1+0,2B/L	p	additional shear factor	Su,z=D/2	qv	th	$2P_p$	V	T'
0	0	0	0	1,46	5,14	2,925	3,3	1,086	15,5	1,270	2,65	50,40	0,00	234,90	9525	0
1000	0,122	0,037	0,018	1,46	5,10	2,925	3,3	1,086	15,5	1,270	2,65	50,20	0,15	236,06	9488	146
2000	0,243	0,074	0,037	1,46	5,07	2,925	3,3	1,086	15,5	1,270	2,65	50,00	0,31	237,22	9449	292
4000	0,487	0,147	0,074	1,46	4,98	2,925	3,3	1,086	15,5	1,270	2,65	49,57	0,62	239,48	9368	584
8000	0,973	0,295	0,150	1,46	4,80	2,925	3,3	1,086	15,5	1,270	2,65	48,60	1,24	243,86	9185	1168
10000	1,216	0,369	0,189	1,46	4,69	2,925	3,3	1,086	15,5	1,270	2,65	48,05	1,54	245,98	9082	1460
12000	1,460	0,442	0,229	1,46	4,58	2,925	3,3	1,086	15,5	1,270	2,65	47,46	1,85	248,06	8970	1752
13555	1,649	0,500	0,262	1,46	4,48	2,925	3,3	1,086	15,5	1,270	2,65	46,96	2,09	249,65	8876	1978
14000	1,703	0,516	0,271	1,46	4,46	2,925	3,3	1,086	15,5	1,270	2,65	46,81	2,16	250,10	8847	2043
20000	2,433	0,737	0,414	1,46	3,99	2,925	3,3	1,086	15,5	1,270	2,65	44,37	3,09	256,01	8385	2919
24000	2,919	0,885	0,543	1,46	3,52	2,925	3,3	1,086	15,5	1,270	2,65	41,93	3,71	259,78	7924	3503
26000	3,162	0,958	0,641	1,46	3,15	2,925	3,3	1,086	15,5	1,270	2,65	39,96	4,02	261,63	7552	3795
27100	3,296	0,999	0,762	1,46	2,67	2,925	3,3	1,086	15,5	1,270	2,65	37,45	4,19	262,63	7078	3955

- Janbu method and DNV standard, V-H failure envelopes

T/V= 0

r	H'	Nc	V	H	V/ASu0	H/ASu0
0	332,8	5,14	8146,2	332,8	8,210	0,335
0,1	401,4	5,04	8036,7	401,4	8,100	0,404
0,2	469,5	4,92	7909,5	469,5	7,971	0,473
0,3	537,0	4,79	7760,9	537,0	7,822	0,541
0,45	636,9	4,57	7487,2	636,9	7,546	0,642
0,5	669,6	4,48	7378,8	669,6	7,436	0,675
0,6	733,9	4,30	7128,2	733,9	7,184	0,740
0,7	795,9	4,08	6818,5	795,9	6,872	0,802
0,8	854,3	3,81	6419,8	854,3	6,470	0,861
0,9	905,3	3,46	5863,2	905,3	5,909	0,912
0,92	913,7	3,37	5717,6	913,7	5,762	0,921
0,94	921,2	3,26	5551,8	921,2	5,595	0,928
0,96	927,1	3,13	5355,8	927,1	5,398	0,934
0,98	930,0	2,97	5103,9	930,0	5,144	0,937
1	916,6	2,57	4532,9	916,6	4,568	0,924

T/V= 0,2

r	H'	Nc	V	H	V/ASu0	H/ASu0
0	332,8	5,14	8146,2	86,4	8,210	0,087
0,1	401,4	5,04	8036,7	195,5	8,100	0,197
0,2	469,5	4,92	7909,5	281,0	7,971	0,283
0,3	537,0	4,79	7760,9	360,0	7,822	0,363
0,45	636,9	4,57	7487,2	473,2	7,546	0,477
0,5	669,6	4,48	7378,8	510,0	7,436	0,514
0,6	733,9	4,30	7128,2	582,5	7,184	0,587
0,7	795,9	4,08	6818,5	653,3	6,872	0,658
0,8	854,3	3,81	6419,8	721,7	6,470	0,727
0,9	905,3	3,46	5863,2	785,7	5,909	0,792
0,92	913,7	3,37	5717,6	797,4	5,762	0,804
0,94	921,2	3,26	5551,8	808,6	5,595	0,815
0,96	927,1	3,13	5355,8	818,7	5,398	0,825
0,98	930,0	2,97	5103,9	827,1	5,144	0,834
1	916,6	2,57	4532,9	825,7	4,568	0,832

T/V= 0,4

r	H'	Nc	V	H	V/ASu0	H/ASu0
0	332,8	5,14	8146,2	#NUM!	8,210	#NUM!
0,1	401,4	5,04	8036,7	#NUM!	8,100	#NUM!
0,2	469,5	4,92	7909,5	#NUM!	7,971	#NUM!
0,3	537,0	4,79	7760,9	#NUM!	7,822	#NUM!
0,45	636,9	4,57	7487,2	205,6	7,546	0,207
0,5	669,6	4,48	7378,8	268,2	7,436	0,270
0,6	733,9	4,30	7128,2	374,2	7,184	0,377
0,7	795,9	4,08	6818,5	469,1	6,872	0,473
0,8	854,3	3,81	6419,8	558,5	6,470	0,563
0,9	905,3	3,46	5863,2	644,3	5,909	0,649
0,92	913,7	3,37	5717,6	661,0	5,762	0,666
0,94	921,2	3,26	5551,8	677,4	5,595	0,683
0,96	927,1	3,13	5355,8	693,6	5,398	0,699
0,98	930,0	2,97	5103,9	709,4	5,144	0,715
1	916,6	2,57	4532,9	723,6	4,568	0,729

T/V= 0,8

r	H'	Nc	V	H	V/ASu0	H/ASu0
0	332,8	5,14	8146,2	#NUM!	8,210	#NUM!
0,1	401,4	5,04	8036,7	#NUM!	8,100	#NUM!
0,2	469,5	4,92	7909,5	#NUM!	7,971	#NUM!
0,3	537,0	4,79	7760,9	#NUM!	7,822	#NUM!
0,45	636,9	4,57	7487,2	#NUM!	7,546	#NUM!
0,5	669,6	4,48	7378,8	#NUM!	7,436	#NUM!
0,6	733,9	4,30	7128,2	#NUM!	7,184	#NUM!
0,7	795,9	4,08	6818,5	#NUM!	6,872	#NUM!
0,8	854,3	3,81	6419,8	#NUM!	6,470	#NUM!
0,9	905,3	3,46	5863,2	103,4	5,909	0,104
0,92	913,7	3,37	5717,6	197,0	5,762	0,199
0,94	921,2	3,26	5551,8	263,2	5,595	0,265
0,96	927,1	3,13	5355,8	320,7	5,398	0,323
0,98	930,0	2,97	5103,9	376,3	5,144	0,379
1	916,6	2,57	4532,9	455,0	4,568	0,459

3. Data of PLAXIS Models to determine failure envelopes

- V-T failure envelopes from PLAXIS 3D:

Model 1:

V-T

Parameters		unit	Phase #	V	T/V	Mstage	T	V	V/Asuo	T/ABSuo	V/Vult	T/Tult
A=	189	m2	1	10000	0	0,784	0	7840	7,90	0,000	1,000	0,000
B=	9	m2	2	10000	0,2	0,781	1562	7810	7,87	0,175	0,996	0,182
Suo=	5,25	kPa	3	10000	0,4	0,768	3072	7680	7,74	0,344	0,980	0,358
			4	10000	0,8	0,709	5672	7090	7,15	0,635	0,904	0,661
Vult=	7840	kN	5	10000	1,6	0,507	8112	5070	5,11	0,908	0,647	0,946
Tult=	8576	kNm	6	10000	3,2	0,268	8576	2680	2,70	0,960	0,342	1,000
			7	10000	6,4	0,133	8512	1330	1,34	0,953	0,170	0,993
			8	10000	12,8	0,065	8320	650	0,66	0,932	0,083	0,970

Model 2:

V-T

Parameters		unit	Phase #	V	T/V	Mstage	T	V	V/Asuo	T/ABSuo	V/Vult	T/Tult
A=	189	m2	1	10000	0	0,746	0	7460	7,52	0,000	1,000	0,000
B=	9	m2	2	10000	0,2	0,743	1486	7430	7,49	0,166	0,996	0,186
Suo=	5,25	kPa	3	10000	0,4	0,73	2920	7300	7,36	0,327	0,979	0,366
		kN	4	10000	0,8	0,672	5376	6720	6,77	0,602	0,901	0,675
Vult=	7460	kN	5	10000	1,6	0,477	7632	4770	4,81	0,855	0,639	0,958
Tult=	7968	kNm	6	10000	3,2	0,249	7968	2490	2,51	0,892	0,334	1,000
			7	10000	6,4	0,124	7936	1240	1,25	0,889	0,166	0,996
			8	10000	12,8	0,06	7680	600	0,60	0,860	0,080	0,964

Model 3:

V-T

Parameters		unit	Phase #	V	T	Mstage	T	V	V/Asuo	T/ABSuo	V/Vult	T/Tult
A=	189	m2	1	10000	0	0,741	0	7410	7,47	0,000	1,000	0,000
B=	9	m2	2	10000	0,2	0,737	1474	7370	7,43	0,165	0,995	0,166
Suo=	5,25	kPa	3	10000	0,4	0,725	2900	7250	7,31	0,325	0,978	0,326
		kN	4	10000	0,8	0,674	5392	6740	6,79	0,604	0,910	0,606
Vult=	7410	kN	5	10000	1,6	0,507	8112	5070	5,11	0,908	0,684	0,912
Tult=	8896	kNm	6	10000	3,2	0,277	8864	2770	2,79	0,993	0,374	0,996
			7	10000	6,4	0,139	8896	1390	1,40	0,996	0,188	1,000
			8	10000	12,8	0,069	8832	690	0,70	0,989	0,093	0,993

- H-T failure envelopes from PLAXIS 3D:

Model 1:

H-T

Parameters		unit	Phase #	H	T/H	Mstage	T	H	H/ASuo	T/ABSuo	H/Hult	T/Tult
A=	189	m2	1	2000	0	0,362	0	724	0,73	0,000	1,000	0,000
B=	9	m2	2	2000	0,2	0,362	144,8	724	0,73	0,016	1,000	0,020
Suo=	5,25	kPa	3	2000	0,4	0,362	289,6	724	0,73	0,032	1,000	0,039
Hult=	724	kN	4	2000	0,8	0,362	579,2	724	0,73	0,065	1,000	0,079
		kN	5	2000	1,6	0,362	1158,4	724	0,73	0,130	1,000	0,157
Tult=	7372,8	kNm	6	2000	3,2	0,361	2310,4	722	0,73	0,259	0,997	0,313
			7	2000	6,4	0,345	4416	690	0,70	0,494	0,953	0,599
			8	2000	12,8	0,248	6348,8	496	0,50	0,711	0,685	0,861
			9	2000	25,6	0,14	7168	280	0,28	0,803	0,387	0,972
			10	2000	51,2	0,072	7372,8	144	0,15	0,826	0,199	1,000
			11	2001	102,4	0,036	7372,8	72,036	0,07	0,826	0,099	1,000

Model 2:

H-T

Parameters		unit	Phase #	H	T/H	Mstage	T	H	H/Asuo	T/ABSuo	H/Hult	T/Tult
A=	189	m2	1	2000	0	0,335	0	670	0,68	0,000	1,000	0,000
B=	9	m2	2	2000	0,2	0,335	134	670	0,68	0,015	1,000	0,019
Suo=	5,25	kPa	3	2000	0,4	0,335	268	670	0,68	0,030	1,000	0,038
Hult=	670	kN	4	2000	0,8	0,335	536	670	0,68	0,060	1,000	0,077
		kN	5	2000	1,6	0,335	1072	670	0,68	0,120	1,000	0,154
Tult=	6963,2	kNm	6	2000	3,2	0,335	2144	670	0,68	0,240	1,000	0,308
			7	2000	6,4	0,32	4096	640	0,64	0,459	0,955	0,588
			8	2000	12,8	0,227	5811,2	454	0,46	0,651	0,678	0,835
			9	2000	25,6	0,128	6553,6	256	0,26	0,734	0,382	0,941
			10	2000	51,2	0,066	6758,4	132	0,13	0,757	0,197	0,971
			10	2000	102,4	0,034	6963,2	68	0,07	0,780	0,101	1,000

Model 3:

H-T

Parameters		unit	Phase #	H	T/H	Mstage	T	H	H/Asuo	T/ABSuo	H/Hult	T/Tult
A=	189	m2	1	2000	0	0,507	0	1014	1,02	0,00	1,000	0,000
B=	9	m2	2	2000	0,8	0,506	809,6	1012	1,02	0,09	0,998	0,096
Suo=	5,25	kPa	3	2000	1,6	0,49	1568	980	0,99	0,18	0,966	0,187
Hult=	1014	kN	4	2000	3,2	0,478	3059,2	956	0,96	0,34	0,943	0,364
		kN	5	2000	6,4	0,428	5478,4	856	0,86	0,61	0,844	0,652
Tult=	8396,8	kNm	6	2000	12,8	0,284	7270,4	568	0,57	0,81	0,560	0,866
			7	2000	25,6	0,157	8038,4	314	0,32	0,90	0,310	0,957
			8	2000	51,2	0,081	8294,4	162	0,16	0,93	0,160	0,988
			9	2000	102,4	0,041	8396,8	82	0,08	0,94	0,081	1,000

- H-V-T failure envelopes:

Model 1:

Parameters		unit
A=	189	m2
B=	9	m2
Suo=	5,25	kPa
Hult=	800	kN
Vult=	7840	kN

		T/V=0			T/V=0.2			T/V=0,4			T/V=0,8		
V	H/V	Mstage	V	H	Mstage	V	H	Mstage	V	H	Mstage	V	H
10000	0	0,784	7840	0	0,781	7810	0	0,768	7680	0	0,709	7090	0
10000	0,1	0,681	6810	681	0,677	6770	677	0,665	6650	665	0,613	6130	613
10000	0,2	0,412	4120	824	0,411	4110	822	0,409	4090	818	0,401	4010	802
10000	0,4	0,208	2080	832	0,208	2080	832	0,208	2080	832	0,208	2080	832
10000	0,8	0,103	1030	824	0,103	1030	824	0,103	1030	824	0,103	1030	824
10000	1,6	0,05	500	800	0,05	500	800	0,05	500	800	0,05	500	800

	T=0		T/V=0.2		T/V=0,4		T/V=0,8	
	V/Vult	H/Hult	V/Vult	H/Hult	V/Vult	H/Hult	V/Vult	H/Hult
Normalized load	1,000	0,000	0,996	0,000	0,980	0,000	0,904	0,000
	0,869	0,851	0,864	0,846	0,848	0,831	0,782	0,766
	0,526	1,030	0,524	1,028	0,522	1,023	0,511	1,003
	0,265	1,040	0,265	1,040	0,265	1,040	0,265	1,040
	0,131	1,030	0,131	1,030	0,131	1,030	0,131	1,030
	0,064	1,000	0,064	1,000	0,064	1,000	0,064	1,000
	T/V=0		T/V=0.2		T/V=0,4		T/V=0,8	
	V/ASu0	H/ASuo	V/ASu0	H/ASuo	V/ASu0	H/ASuo	V/ASu0	H/ASuo
	7,901	0,000	7,871	0,000	7,740	0,000	7,145	0,000
Dimensionless load	6,863	0,686	6,823	0,682	6,702	0,670	6,178	0,618
	4,152	0,830	4,142	0,828	4,122	0,824	4,041	0,808
	2,096	0,838	2,096	0,838	2,096	0,838	2,096	0,838
	1,038	0,830	1,038	0,830	1,038	0,830	1,038	0,830
	0,504	0,806	0,504	0,806	0,504	0,806	0,504	0,806

Model 2:

Parameters		unit
A=	189	m2
B=	9	m2
Suo=	5,25	kPa
Hult=	780	kN
Vult=	7460	kN

		T/V=0			T/V=0.2			T/V=0,4			T/V=0,8		
V	H/V	Mstage	V	H	Mstage	V	H	Mstage	V	H	Mstage	V	H
10000	0	0,746	7460	0	0,743	7430	0	0,73	7300	0	0,672	6720	0
10000	0,1	0,646	6460	646	0,642	6420	642	0,629	6290	629	0,58	5800	580
10000	0,2	0,387	3870	774	0,387	3870	774	0,386	3860	772	0,378	3780	756
10000	0,4	0,195	1950	780	0,195	1950	780	0,195	1950	780	0,194	1940	776
10000	0,8	0,096	960	768	0,096	960	768	0,096	960	768	0,095	950	760
10000	1,6	0,046	460	736	0,046	460	736	0,046	460	736	0,046	460	736

	T=0		T/V=0.2		T/V=0,4		T/V=0,8	
	V/Vult	H/Hult	V/Vult	H/Hult	V/Vult	H/Hult	V/Vult	H/Hult
Normalized load	1,000	0,000	0,996	0,000	0,979	0,000	0,901	0,000
	0,866	0,828	0,861	0,823	0,843	0,806	0,777	0,744
	0,519	0,992	0,519	0,992	0,517	0,990	0,507	0,969
	0,261	1,000	0,261	1,000	0,261	1,000	0,260	0,995
	0,129	0,985	0,129	0,985	0,129	0,985	0,127	0,974
	0,062	0,944	0,062	0,944	0,062	0,944	0,062	0,944
	T=0		T/V=0.2		T/V=0,4		T/V=0,8	
	V/ASu0	H/ASuo	V/ASu0	H/ASuo	V/ASu0	H/ASuo	V/ASu0	H/ASuo
	7,518	0,000	7,488	0,000	7,357	0,000	6,772	0,000
Dimensionless load	6,510	0,651	6,470	0,647	6,339	0,634	5,845	0,585
	3,900	0,780	3,900	0,780	3,890	0,778	3,810	0,762
	1,965	0,786	1,965	0,786	1,965	0,786	1,955	0,782
	0,967	0,774	0,967	0,774	0,967	0,774	0,957	0,766
	0,464	0,742	0,464	0,742	0,464	0,742	0,464	0,742

Model 3:

Parameters		unit
A=	189	m2
B=	9	m2
S_{uo}=	5,25	kPa
H_{ult}=	1136	kN
V_{ult}=	7410	kN

		T/V=0			T/V=0.2			T/V=0,4			T/V=0,8		
V	H/V	M_{stage}	V	H	M_{stage}	V	H	M_{stage}	V	H	M_{stage}	V	H
10000	0	0,741	7410	0	0,737	7370	0	0,725	7250	0	0,674	6740	0
10000	0,1	0,688	6880	688	0,684	6840	684	0,671	6710	671	0,621	6210	621
10000	0,2	0,536	5360	1072	0,534	5340	1068	0,527	5270	1054	0,498	4980	996
10000	0,4	0,295	2950	1180	0,295	2950	1180	0,293	2930	1172	0,289	2890	1156
10000	0,8	0,146	1460	1168	0,146	1460	1168	0,146	1460	1168	0,146	1460	1168
10000	1,6	0,071	710	1136	0,071	710	1136	0,071	710	1136	0,071	710	1136

	T=0		T/V=0.2		T/V=0,4		T/V=0,8	
	V/V_{ult}	H/H_{ult}	V/V_{ult}	H/H_{ult}	V/V_{ult}	H/H_{ult}	V/V_{ult}	H/H_{ult}
Normalized load	1,000	0,000	0,995	0,000	0,978	0,000	0,910	0,000
	0,928	0,606	0,923	0,602	0,906	0,591	0,838	0,547
	0,723	0,944	0,721	0,940	0,711	0,928	0,672	0,877
	0,398	1,039	0,398	1,039	0,395	1,032	0,390	1,018
	0,197	1,028	0,197	1,028	0,197	1,028	0,197	1,028
	0,096	1,000	0,096	1,000	0,096	1,000	0,096	1,000
	T=0		T/V=0.2		T/V=0,4		T/V=0,8	
	V/AS_{u0}	H/AS_{uo}	V/AS_{u0}	H/AS_{uo}	V/AS_{u0}	H/AS_{uo}	V/AS_{u0}	H/AS_{uo}
	7,468	0,000	7,428	0,000	7,307	0,000	6,793	0,000
Dimensionless load	6,934	0,693	6,893	0,689	6,762	0,676	6,259	0,626
	5,402	1,080	5,382	1,076	5,311	1,062	5,019	1,004
	2,973	1,189	2,973	1,189	2,953	1,181	2,913	1,165
	1,471	1,177	1,471	1,177	1,471	1,177	1,471	1,177
	0,716	1,145	0,716	1,145	0,716	1,145	0,716	1,145